UNIVERSITÄT HOHENHEIM

Faculty of Agricultural Sciences

Institute of Soil Science and Land Evaluation

Assessment of hydrology and dynamics of pesticides in a tropical headwater catchment in Northern Thailand



Cindy Hugenschmidt

FACULTY OF AGRICULTURAL SCIENCES

Institute of Soil Science and Land Evaluation

University of Hohenheim

Field: Biogeophysics

Prof. Dr. Thilo Streck

Assessment of hydrology and dynamics of pesticides in a tropical headwater catchment in Northern Thailand

Dissertation

Submitted in fulfillment of the requirements for the degree

“Doktor der Agrarwissenschaften”

(Dr.sc.agr. / Ph.D. in Agricultural Sciences)

to the

Faculty of Agricultural Sciences

Presented by

Cindy Hugenschmidt

Stuttgart, Germany 2013

This thesis was accepted as a doctoral dissertation in fulfillment of the requirements for the degree “Doktor der Agrarwissenschaften” (Dr.sc.agr. / Ph.D. in Agricultural Sciences) by the Faculty of Agricultural Sciences of the University of Hohenheim on 24.10.2013.

Date of oral examination: 05.11.2013

Examination Committee

Supervisor and Reviewer:	Prof. Dr. Thilo Streck
Co-Reviewer:	Prof. Dr. Stefan Uhlenbrook
	Represented by Prof. Dr. Karl Stahr during the oral exam
Additional Examiner:	Prof. Dr. Georg Cadisch
Head of the Committee:	Prof. Dr. Markus Rodehutscord

Contents

AUTHOR'S COMMENT……

1 GENERAL INTRODUCTION 1

1.1 BACKGROUND 1
1.2 RAINFALL PATTERN IN TROPICAL REGIONS 3
1.3 RUNOFF PROCESSES AND HYDROGRAPH SEPARATION 4
1.4 PESTICIDE DYNAMICS IN STREAM WATER 7
1.5 HYDROLOGICAL TRANSPORT MODELS AND MODEL APPLICATION 9
1.6 THE MAE SA WATERSHED 11

2 OBJECTIVES AND OUTLINE 21

3 PUBLICATION 1 - RAINFALL VARIABILITY IN A TROPICAL, MOUNTAINOUS CATCHMENT IN NORTHERN THAILAND 23

3.1 INTRODUCTION 24
3.2 MATERIAL AND METHODS 27
3.3 RESULTS 31
3.4 DISCUSSION 38
3.5 CONCLUSION 41

4 PUBLICATION 2 - A THREE-COMPONENT HYDROGRAPH SEPARATION BASED ON GEOCHEMICAL TRACERS IN A TROPICAL MOUNTAINOUS HEADWATER CATCHMENT IN NORTHERN THAILAND 43

4.1 INTRODUCTION 44
4.2 MATERIALS AND METHODS 50
4.3 RESULTS 56
4.4 DISCUSSION 65
4.5 SUMMARY AND CONCLUSION 72

5 PUBLICATION 3 - SHORT-TERM DYNAMICS OF PESTICIDE CONCENTRATIONS AND LOADS IN A RIVER OF AN AGRICULTURAL WATERSHED IN THE OUTER TROPICS 75

5.1 INTRODUCTION 76
5.2 MATERIALS AND METHODS 78
5.3 RESULTS 87
5.4 DISCUSSION 101
5.5 SUMMARY AND CONCLUSIONS 106

6 PUBLICATION 4 - SIMULATION OF STREAMFLOW COMPONENTS IN A MOUNTAINOUS CATCHMENT IN NORTHERN THAILAND WITH SWAT, USING THE ANSELM CALIBRATION APPROACH 109

6.1 INTRODUCTION 110
6.2 MATERIAL AND METHODS 115
6.3 RESULTS 121
6.4 DISCUSSION 127
6.5 CONCLUSION AND OUTLOOK 131

7 GENERAL DISCUSSION 133

7.1 RAINFALL ANALYSIS AND ITS IMPORTANCE FOR HYDROLOGICAL ASSESSMENT, PESTICIDE TRANSPORT AND MODELING 133
7.2 CAN KNOWLEDGE OF RUNOFF AND PESTICIDE DYNAMICS IN THE MAE SA WATERSHED BE COMBINED? 136
7.3 HYDROLOGICAL MODELING AS A TOOL FOR TESTING PROCESS ASSUMPTIONS 137

8 FINAL CONCLUSION 141

9 SUMMMARY 145

10 ZUSAMMENFASSUNG 149

11 REFERENCES.. 153

To my family

The world is a thing of utter inordinate complexity and richness and strangeness that is absolutely awesome.

Douglas Adams, London 2001

Author's comment

This is a cumulative dissertation and the journal contributions are the backbone of the thesis. They all follow one purpose: to describe and understand the characteristic of the hydrology of the Mae Sa watershed and the dynamics of pesticides during short-term events. Hence, literature within these journal contributions and the chapters within this thesis is redundant. To avoid repetition, all references are listed at the end of the thesis (Chapter 11).

Rain gauges in Chapter 4, denoted as MSN, MSM, BMK and PNK (Figure 4.1) are identical with Stations R13, R03, R04 and R05 (Figure 3.1), respectively. Rain gauge and station is used interchangeable within the thesis, so is subbasin and subcatchment.

Because flow components are appointed differently in cited literature, the terms used in this thesis (lateral flow, shallow subsurface flow, interflow, preferential flow) are not meant to describe flow processes, but define subsurface water flow, other than groundwater and are used alternately. If the terms imply processes it is explicitly mentioned.

1 General introduction

1.1 Background

Tropical areas cover 36% of the earth´s surface and hold the world´s largest forests and highest species diversity (Bremer, 1999). Half of the tropical landmass is dominated by seasonal climates with distinct wet and dry seasons (Cobley and Steele, 1984). Those unique ecosystems form a home to 40% of the human population (Bremer, 1999) and have undergone dramatic changes during the last decades. The most significant land cover disturbances in those regions can be attributed to forest conversion (FAO, 2006). Driven by a rapid population growth and the resulting demand for food and commodities, considerable alterations are particularly faced in developing countries, where agriculture is a major economic pillar. For Southeast Asia, the agricultural production increased by more than 52% between 1999 and 2009 (FAO, 2010). This is very severe, because the mountainous regions of Southeast Asia harbor an immense wealth of natural resources and biodiversity (Fox and Vogler, 2005)that make this region particularly valuable and extremely vulnerable. In the past decades, socio-economic and environmental developments caused land use intensification throughout Southeast Asia, especially in tropical mountainous regions (e.g. Thailand) (Walsh et al., 2006). Fox and Vogler (2005) give detailed insight into land use changes and their causes in mountainous regions of northern Thailand. In the 1970s, significant conversions have been witnessed due to intense effort of the Thai government to eradicate opium growth. Reforestation projects, prohibition of agriculture in vulnerable areas and the development of national parks decelerated the conversion process of forest area to arable land. Although forest area did not further decrease during 1954-1995, upland agriculture increased from 14% to 20% (Fox et al., 1995). Market access was enhanced by improvement of infrastructure and caused a shift from subsistence agriculture to commercial cash crop production (i.e. Uhlig, 1984; Delang, 2002). Schreinemachers and Sirijinda (2010) monitored land use in the Mae Sa watershed in northern Thailand and showed that bell pepper, cabbage and roses are the main cash crops in the region. Furthermore, most of the crops grown in the area are treated with agrochemicals and approximately 79% of the agricultural area of the Mae Sa watershed is irrigated. Irrigation systems are mainly supplied by stream water, which causes an excessive use of streams during dry season. The highest fractions of agricultural upland sites (52%) are located on slopes with inclinations above 25%, favoring erosion during the monsoon periods. Besides soil erosion, such steep slopes may support a quick transport of agrochemicals to streams via surface runoff and subsurface flow.

In fact, the aforementioned intensification put enormous pressure on natural resources in upland agriculture areas. Soils are degraded (Ziegler et al., 2004) and nutrients are washed off (Schmitter et al., 2011). Furthermore, water bodies may be polluted due to intensive application of agrochemicals. If agricultural crops are cultivated all-year round, the problems mentioned above become even more severe as a higher input of fertilizers is necessary to compensate the low fertility of soils. Moreover, due to irrigation of crops in dry seasons, the pressure on water resources increases in times when stream flow is already low. To secure the yield and to protect crops from pests and diseases, agrochemicals are applied frequently and in large amounts. Overall, these practices put enormous pressure on the natural resources and have serious environmental implications at ecosystem level as well as for the local population (Thirakhupt et al., 2006; Jaipieam et al., 2009; Taneepanichskul et al., 2010). In terms of protection and sustainable management of natural resources, water quality is one of Thailand most critical environmental issues (Panuwet et al., 2012; Kruawal et al., 2004).

Agricultural activities in upland regions must be considered very critically, because those regions are the headwaters of many rivers, not only in Thailand. The largest amount of global runoff (Fekete et al., 2002) and eight out of the ten largest rivers in the world (Latrubesse et al., 2005) originate from tropical headwaters. The Mae Sa River is one of the headwaters of the Ping River, which is a major tributary of the Chao Praya River, the largest river in Thailand. The steep topography and the highly variable nature of monsoonal rainfall create a dynamic system from which sediment (Ziegler et al., 2009), contaminants and solutes are rapidly transported downstream (Delang, 2002).

Despite the extent of the global value of tropical regions, the current pressure it receives and the hydrological importance on global water resources, only few studies (Bonell, 2004; Chapell et al., 2007) investigated the dominant hydrological processes. In order to protect these fragile ecosystems and enhance sustainable water resource management in these regions, a better understanding of the underlying hydrological processes influencing agrochemical transport within tropical mountainous areas is needed.

1.2 Rainfall pattern in tropical regions

The spatio-temporal rainfall variability is particularly important for water resource management, assessment of runoff generation and transport pattern of solutes in a watershed (McGrath et al., 2010; Park et al., 2011). Agrochemical leaching experiments in a catchment in northern Thailand pointed spatio-temporal rainfall pattern as a key variable for losses of contaminants to stream waters (Kahl et al., 2007; Sangchan et al., 2012).

The highest global rainfall amounts are observed in tropical regions and average annual rainfall can easily exceed 2000 mm a^{-1} (GPCC, 2003). The variable nature of rainfall is particularly expressed in inner and outer tropical climates (McGregor and Nieuwolt, 1998), which makes it very difficult to identify trends and to forecast rainfall patterns.

Whereas inner tropics receive rainfall throughout the year, the outer tropics are characterized by distinct wet and dry seasons. The climate of Thailand is dominated by monsoonal regimes (Walker, 2002). The monsoon is driven by the Intertropical Convergence Zone (ITCZ), which crosses the climatic equator around May and November. The northward extension of the ITCZ triggers wind systems that control the Southeast Asian climate (Dykes, 2000). Therefore, Thailand is affected by two major air streams: the northeast and the southwest monsoon. Winds from north and east (northeast monsoon) dominate the period between November and February, when the ITCZ moves southward. During March and April, the ITCZ starts to move northwards, weakening the cold and dry air streams from northeast and causing the first rainfall events (Boochabun et al., 2004). In May, southwest winds from the Indian Ocean deliver humid air and cause heavy rainfall events. Although the monsoon is the driving force behind temporal rainfall distribution, it is reported that rainfall shows large inter-annual changes across East Asia (Park et al., 2011).

Addressing rainfall variability in tropical mountainous regions faces several challenges. Firstly, the monitoring network is often not dense enough to identify spatial patterns, especially not in remote, mountainous regions. The orographic effect on rainfall enhancement is said to be particularly significant in tropical regions (Brujinzeel, 2004). Although the altitudinal increase of rainfall is generally known, only a few studies from tropical regions, report this clear relationship. Mul et al. (2009) monitored large spatial variability of rainfall in a mountainous catchment in Tanzania. Different rainfall amounts within the same elevation bands indicated that the altitudinal increase of rainfall is superimposed by another, unidentified factor. A further study in the Ethiopian highlands used a high-resolution monitoring network to uncover the spatial variability of daily rainfall (Bitew and Gebremichael, 2010). Despite this high resolution, no clear spatial trend of rainfall distribution was identified.

Dykes (2000) reported from a study in Brunei that high intensity rainfall events with a short duration were mainly generated by convection cells, which underlie a topographic influence. He emphasized that there are only few data sets that can be used to assess topographic rainfall enhancement in Southeast Asia. In the Mae Chaem watershed in Northern Thailand (18°06 N, 98°04 E) a clear altitudinal increase of rainfall was identified (Dairaku et al., 2000; Dairaku et al., 2004; Thanapakpawin et al., 2006; Kuraji et al., 2009).

However, the mentioned studies do not deliver a clear and consistent picture, and further investigations on spatio-temporal rainfall variability in tropical regions are necessary to improve the understanding of such environments and the effect on runoff generation and hydrological transport processes.

1.3 Runoff processes and hydrograph separation

Sustainable water resources management requires a profound knowledge of runoff processes and runoff generation within a catchment. Investigations on rainfall-runoff processes, runoff response time and source identification of contributing runoff components are subjects of interest while monitoring catchment hydrology.

Runoff generation has been under focus in hydrological research since decades. In the 1960s, Hewlett and Hibbert (1967) introduced the variable source area (VSA) concept, which has significantly changed runoff generation perceptions in catchment hydrology. Since then, a vast amount of studies on runoff generation was published with the intention to identify sources (i. e., Bazemore et al., 1994; Scanlon et al., 2001), age (i.e., McDonnell, 1990; Peters and Ratcliffe, 1998; Shanley et al., 2002) and processes (i.e., Montgomery et al., 1997; Scherrer and Naef, 2003) of runoff components.

Flow components are distinguished, depending on whether the sources and age of water are of interest or if processes are investigated (Figure 1.1). Surface runoff is the water, which flows on top of the soil and is triggered by three mechanisms: i) infiltration excess (Horton overland flow), ii) saturation excess and iii) return flow. Surface runoff generated by infiltration excess and saturation excess can be considered as water from a specific event, whereas return flow may be water which has been in the catchment prior the event (infiltration and ex-filtration).

Shallow subsurface flow occurs in saturated (phreatic) or unsaturated (vadose) zones of the soil and can be considered as source of interflow. Flow paths, such as lateral flow, macropore flow or preferential flow, are examples for subsurface flow processes. Interflow may occur directly or delayed in the stream, hence, it is impossible to distinguish, if interflow is 'old' (pre-event) or 'new' (event) water. Sourced by ground water that has longer resident times in a catchment than other components, baseflow is considered as 'old' water. Baseflow is also the component that sustains perennial streams during dry spells. In the course of the year and during single events, the contribution, composition and dynamic of the hydrograph is varying. To reveal such behavior, it has been the goal of many studies to identify the contributions of involved components (i.e. end-members) and their sources.

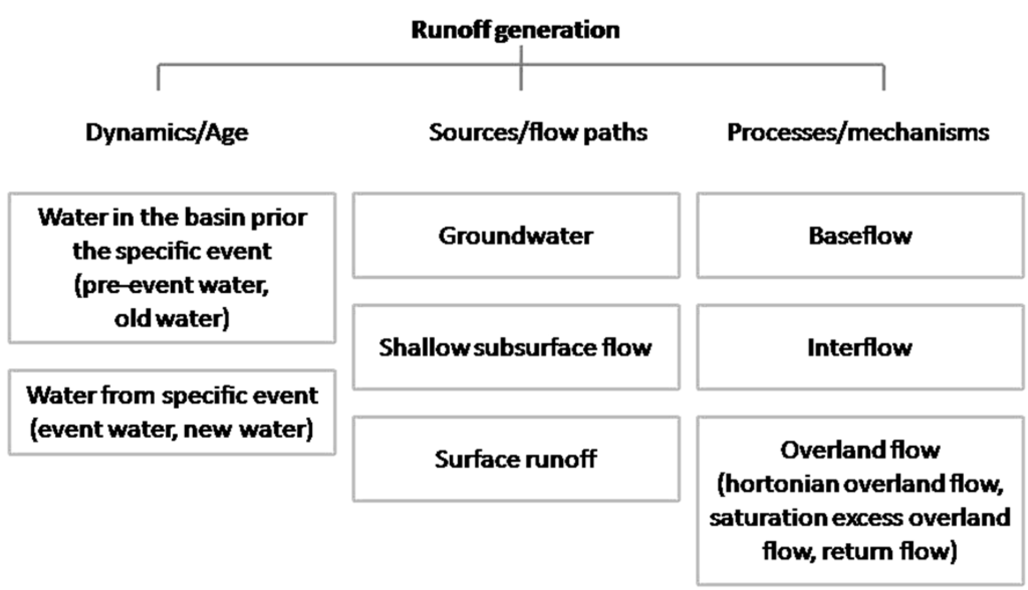

Figure 1.1: Runoff generation and definition of runoff components (modified after Sklash and Farvolden, 1979).

Tracer based hydrograph separation is a common technique to identify and quantify the involved flow components in runoff generation and hence, facilitates the investigation of runoff processes within a catchment. The choice of tracer depends on whether the age of water in the stream is of interest, its source area, or the process it is delivered by. If residence times (new and old water) are under focus, environmental isotopes may be used. Frequently applied isotopes are stable oxygen ($^{18}O/^{16}O$) (Uhlenbrook et al., 2002;

Rodgers et al., 2005), tritium (^3H) (McGlynn et al., 2003) and Radon (^{222}Rn, decay product of ^{238}U) (Kienzler and Naef, 2008). Investigation of geographic sources of flow components is generally based on hydrochemical tracers (e.g. K^+, Mg^{2+}, Na^+, Cl^-) (Wels et al., 1991, Ribolzi et al., 2000; Burns et al., 2001, Ladouche, 2001), but may also be done by isotopes. Several studies on hydrograph separation also use electrical conductivity (Matsubayashi, 1993; Laudon and Slaymaker, 1997) or silica (Wels et al., 1991; Joerin et al., 2002; Uhlenbrook and Hoeg, 2003) to identify flow components.
Sklash and Farvolden (1979) manifested certain rules, which must be followed while performing a hydrograph separation. Some important criteria are that:

i) the isotope content/ion concentration is significantly different in all monitored components,
ii) the isotope content/ion concentration of each component remains stable throughout an event or the alterations during an event can be measured,
iii) isotopes or applied ions are conservative or changes can be monitored.

Most of the studies revealed that old water – or baseflow - dominates storm flow. This finding was initially postulated by Sklash and Farvolden (1979) and has been consolidated by many other investigations (e.g. Peters and Ratcliffe, 1998; Uhlenbrook and Hoeg, 2003). However, most of these studies have been carried out in temperate regions (Giertz et al., 2006). Runoff generation and dominant hydrological processes in tropical regions are not yet fully understood or adequately analyzed (Montanari et al., 2008). Bonell (1993) supposed that climatic and environmental conditions in tropical regions may lead to other dominant processes in runoff generation. Tropical headwaters are known for a rapid and flashy rainfall-runoff response (i.e. Bonell and Gilmour, 1978; Godsey et al., 2004), which may suggest larger fractions of new water, i.e. surface runoff or interflow.
Studies from a small Amazonian watershed revealed the importance of overland flow for storm flow generation (Elsenbeer and Lack, 1996). Follow-up investigations in the same region indicated that near-surface flow paths are important contributors to runoff generation (Elsenbeer and Vertessy, 2000). Chaves et al. (2008) showed that groundwater and shallow soil water only delivered 43% of the annual discharge in a basin in southwestern Brazil. Goller et al. (2005) found that two out of three storm events in a tropical mountainous rain forest in Ecuador were mainly driven by event water. Results from a Malaysian study site support the conclusions presented by Chaves et al. (2008):

shallow groundwater and subsurface flow paths are important during storm flow (Negishi et al., 2007). All named studies were carried out in catchments that receive annual rainfall amounts above 2000 mm and lack longer rainless periods. Although a considerable amount of runoff generation studies has been conducted in the inner tropics, the outer tropics with distinct wet and dry seasons are less addressed within hydrological process studies. Especially Southeast Asia suffers from a general lack of data (Chuan, 2003) and particularly steep and tropical headwater catchments are hardly investigated in terms of hydrological processes (Dykes and Thornes, 2000; Chappel, 2010).

Runoff generation studies from regions where the dry period delivers no rainfall are rare. For Thailand, only a few studies are known, and the known ones did not particularly focus on runoff generation. Ziegler et al. (2000) conducted experiments on overland flow generation under disturbed conditions. Horton overland flow was observed shortly after artificial rainfall on initially dry soils. Less compacted agricultural areas required a higher amount of rainfall to produce overland flow due to their higher infiltration rates. Studies on pesticide transport in northern Thailand also included investigations on runoff patterns and pointed interflow as a major pathway for pesticide losses to streams (Kahl et al. 2007; Kahl et al., 2008).

1.4 Pesticide dynamics in stream water

Thailand exports agricultural products, which account to only 9% of the gross domestic production (GDP) and 19% of the export value (Panuwet et al., 2012). Without chemical crop protection, 50% of crop yields are estimated to be lost due to pests and diseases (Oerke and Dehne, 2004). While producing agricultural products, 40% of the Thai workforce and land surface are needed. The majority of the 40% workforce is contributed by rural Thai people, which are heavily dependent on agriculture as their main income source.

Hence, the use of pesticides has significantly increased across the country. Nowadays, Thailand ranks third out of 15 Asian countries with regard to pesticide use per unit area (Walter-Echols and Yongfan, 2005). This poses severe risks for environment, wildlife and humans, as pollutants may enter the water bodies. The transport of pesticides to stream waters and its fate in streams is highly depending on the hydrological processes within a catchment and on the physico-chemical properties of the compound.

The majority of studies on losses of pesticides focuses on flow paths (transport pathway) and was carried out in temperate regions (e.g., Kreuger, 1998; Riise et al., 2004; Müller et al., 2006; Ulrich et al., 2012). Reichenberger et al. (2002) emphasized the lack of studies on pesticide fate in tropical regions. While surface runoff has been identified as the major transport pathway in many temperate study areas (Wauchope, 1978; Müller et al., 2002; Schriever et al., 2007), subsurface flow or interflow is said to be of minor importance, but also contributes to losses of agrochemicals to surface waters (Kladivko et al., 1991).

Most available studies on pesticide dynamics in Southeast Asian regions are carried out with focus on paddy rice. Bouwmann et al. (2002) monitored losses of nitrate and pesticides from rice fields to the stream to assess the potential pollution of a shallow groundwater aquifer on Luzon Island, Philippines. Although they surveyed the sites from 1998-2000, the average annual mean pesticide concentrations did not exceed the WHO limits for single (0.1 $\mu g\ L^{-1}$) or multiple (0.5 $\mu g\ L^{-1}$) pesticides in the monitored groundwater wells. Nevertheless, several seasonal peaks were monitored, indicating a transfer of pesticides from the paddy rice field to the shallow aquifer. Elfman et al. (2011) showed that several pesticides applied in a rice cultivation system on Leyte, Philippines, ended up in the stream. Amongst others, cypermethrin was analyzed, and 24% of the samples exceeded limits of the Swedish Chemicals Agency (0.0002 $\mu g\ L^{-1}$). A study from northern Vietnam reported pesticide losses from rice paddies to groundwater and surface water after application (Lamers et al., 2011). All applied pesticides occurred in the stream and were detected in varying magnitudes in groundwater wells.

For Thailand, there are also some reports on the environmental fate of pesticides. Aiemsupasit (2005) detected several pesticide residues in rivers across Thailand. Organophosphates reached concentrations of up to 5.47 $\mu g\ L^{-1}$. Kruawal et al. (2005) detected atrazine (0.058-0.086 $\mu g\ L^{-1}$) in the Chao Praya, the largest River in Thailand. Although organochlorines (OC) phased out during the 1970s, they are still found in the environment (Siriwong et al., 2008). Siriwong et al. (2008) found OCs in water, sediment and aquatic organisms in central Thailand. The OC residues in the monitored plankton community ranged between 0.01 and 3.65 $ng\ g^{-1}$ within a one year monitoring period.

In the present study area, the Mae Sa watershed in Northern Thailand, studies on transport of pesticides to the stream water (Ciglasch et al., 2005; Kahl et al., 2007; Kahl et al., 2008) were carried out. Whereas Ciglasch et al. (2005) focused on vertical movement of water and pesticides, Kahl et al. (2007) extended the experiment to lateral transport along the hillslope towards the stream. They identified lateral preferential flow as major contributor of pesticides to the stream.

Despite the intensive use of pesticides in Thailand, none of the studies traced the course of pesticides on the catchment scale. Additionally, the in-stream dynamics of pesticides during single events within a river system have not yet been investigated.

1.5 Hydrological transport models and model application

Hydrological models are frequently applied tools, if, for instance, water resources have to be managed, predictions have to be made or processes need to be transferred between different scales (Beven, 2002). There is a suite of watershed models existing, which were globally tested and applied (Singh and Frevert, 2006). All these models have different strengths and restrictions, which become more or less relevant, depending on the research question. Hence, the modeler should know the capabilities of the model well, before he/she applies it within a study. During model application it is not only important to simulate water balance, but for example, also water quality. As solute transport is highly connected with flow paths and runoff dynamics within a watershed, the applied model should have a strong hydrological component. Additionally, it would be favorable that the model is able to split up the simulated discharge in single runoff components and allows to simulate on continuous time steps.

Despite the vast amount of watershed models, there are only few watershed scale models, which allow to implement detailed land management operations and to simulate transport pattern of contaminants and solutes. The Hydrology Simulation Program-FORTRAN (HSPF), (Johanson et al., 1984; Bicknell et al., 1993) was one of the early generation models that allowed the user to assess water quality. Nutrient and pesticide management could be incorporated in the modeling process. An additional example for a model, which has been further developed during the years, is given by the Areal Nonpoint Source Watershed Environment Response Simulation (ANSWERS) (Beasley et al., 1980). ANSWERS focuses on water quality assessment on watershed scale for single events. It was advanced to ANSWERS-Continuous (Bouraoui and Dillaha, 1996; Bouraoui and Dillaha, 2000) and enabled process simulations not only for single events. The Agricultural Nonpoint Source Pollution Model (AGNPS, Young et al., 1987) is also a watershed scale model, which allows to simulate nitrogen and phosphorus pattern. It was upgraded to AnnAGNPS (Annualized Agricultural Nonpoint Source Model) by Bingner and Theurer (2001). Within this upgrade, the transport of pesticides and the definition of agricultural management were added. The Soil and Water Assessment Tool (SWAT, Arnold et al., 1998) has been developed to assist in the prediction and assessment of water management, sediment and transport of agrochemicals in large, agricultural watersheds or river basins. The model includes a sound data base with several crop parameters and physico-chemical properties of agrochemicals. Furthermore, detailed land management operations can be scheduled, which enhances the incorporation of monitored data on land management.

All mentioned models allow a continuous simulation and are helpful for studies on long-term effects on water resources due to management practices. The SWAT model convinces with the enormous amount of global applications and its large user community (Gassman et al., 2007). The application range suggests that the model is suitable for many distinct regions. Additionally, the model is under constant development and several updates were released during the last year. Neitsch et al. (2002) developed the module for contaminant transport of pesticides, which is nowadays a helpful tool in agricultural areas. The pesticide module allows the user to simulate the fate and transport of pesticide with specified physico-chemical parameters (e.g. solubility, degradation, half-life and partitioning coefficient) in stream. Recently, SWAT is able to operate on hourly time steps (Neitsch et al., 2002), which is of great benefit while focusing on in-stream losses of agrochemicals within watersheds during events. Borah and Bera (2004) recommended the SWAT model as a useful tool for long-term continuous hydrological simulations and assessment of the impact of management practices at the watershed scale. Because of the named advantages, SWAT was chosen as the model to be tested within this study.

Although the SWAT model has frequently been applied in temperate regions (i.e. Kannan et al., 2007; Larose et al., 2007; Boithias et al.,2011) tropical regions still lack documented simulations. Particularly for very steep headwater regions (e.g. Abbaspour et al., 2007) in the tropics, applications of the SWAT model are rare. Ndomba et al. (2008) performed a SWAT simulation in a tropical catchment in Tanzania. A further study from tropical Africa was reported by Setegn et al. (2010) who investigated a large-scale watershed in Ethiopia. Tripathi et al. (2003) used SWAT to perform simulations to develop watershed management schemes in an East Indian, monsoon driven, small-scale study area. For the mountainous regions of Thailand, SWAT model applications are very contemplative. Kuntiyawichai et al. (2011) performed SWAT simulations with regard to

flood management options in the Yang River basin. Another SWAT project in north eastern Thailand was carried out in a subbasin of the Chi River (Reungsang et al., 2010).
The lack of application in catchments with characteristics as given by the Mae Sa watershed highly motivates a SWAT model application in such an environment as represented by the Mae Sa watershed.

1.6 The Mae Sa watershed

The Mae Sa watershed (MSW) is located in the mountainous region of northern Thailand (18°47′ N, 98°59′ E), 35 km northwest of the province capital Chiang Mai (Figure 1.2), and lies within the summer-humid outer tropics (Weischet, 1991). It represents a part of the 30% of Thailand`s area that is covered with steep slopes (TDIC, 1986) and is also an excellent example for an area, in which agricultural activities have grown more important during the last decades. The area is inhabited by ethnic minorities of Northern Thai and Hmong, whose main source of income is based on agricultural production (Schreinmachers et al., 2008). The production system has changed entirely during the last decades, with a remarkable alteration in crop varieties. Where rice has occupied around 70% of the arable land in 1974 (Irwin, 1976), it is almost vanished nowadays and has been substituted by annual crops, flowers and litchi orchards, mainly (Schreinemachers and Sirijinda, 2008; Schreinemachers and Sirijinda, 2010). As a part of the northern highlands, the Mae Sa river is supposed to contribute to a constant supply of major river systems, such as the Ping river and the Chao Praya river (Delang, 2002).
The MSW has a total area of 77 km² and includes two defined subbasins (Figure 1.2). The upper part of the catchment (Headwater) area covers 28 km² of the watershed, the Mae Sa Noi subbasin has a share of 7 km². Sharp reliefs, steep slopes (36% on average) and narrow, V-shaped valleys create a unique landscape. Elevation stretches from around 300 m.a.s.l. (meter above sea level) to 1600 m.a.s.l.

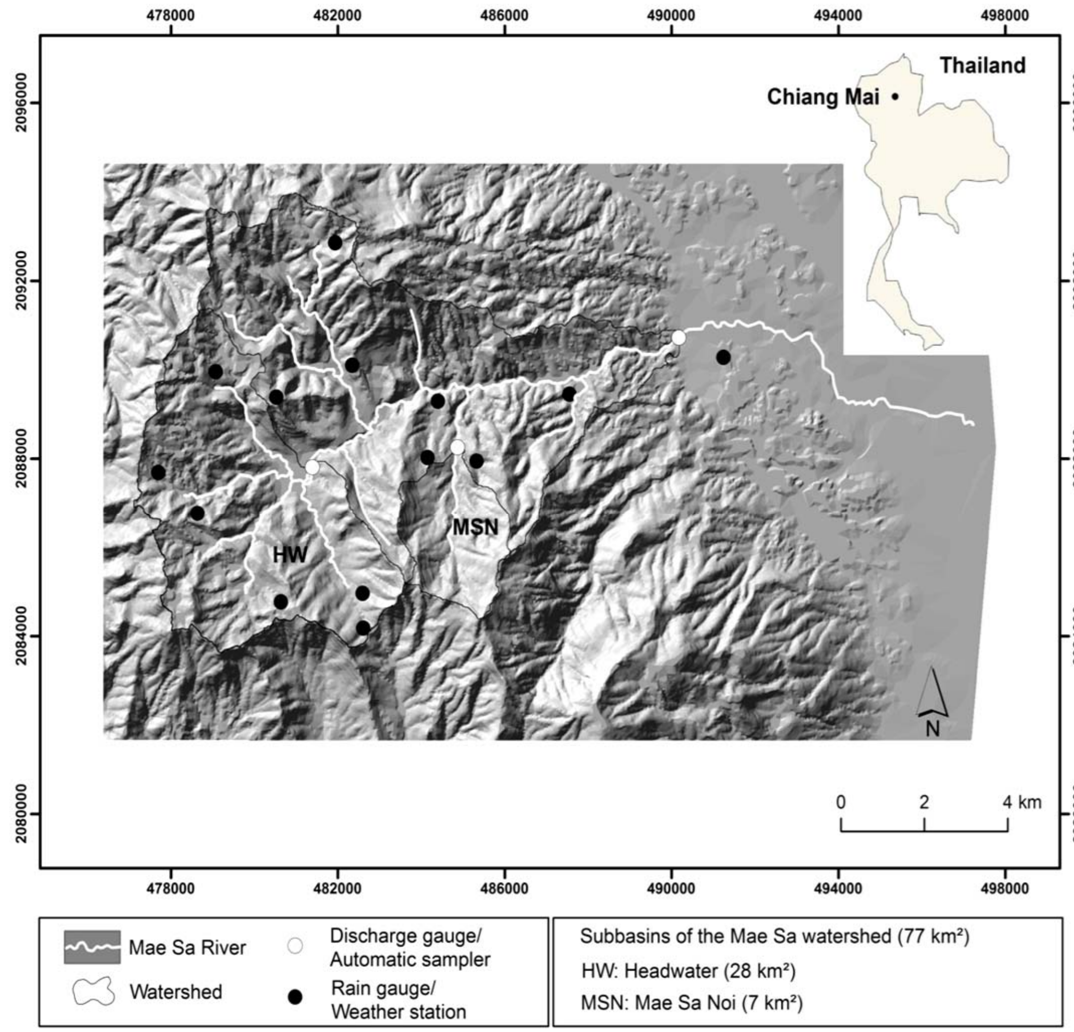

Figure 1.2: The Mae Sa watershed with the Headwater area (HW), Mae Sa Noi subbasin (MSN) and river network. Monitoring devices are also depicted.

The main natural vegetation type in the watershed is secondary forest (e.g. *Ficus altissima*, *Tectona grandis, Pinus spp.),* which covers about 76% of the watershed. The remaining 24% are other types of land use, of which agricultural areas hold the majority (Figure 1.3). Main agricultural products are vegetables (e.g. bell pepper, salad, cabbage) and tree crops, such as *Mangifera indica* or *Litchi sinensis*.

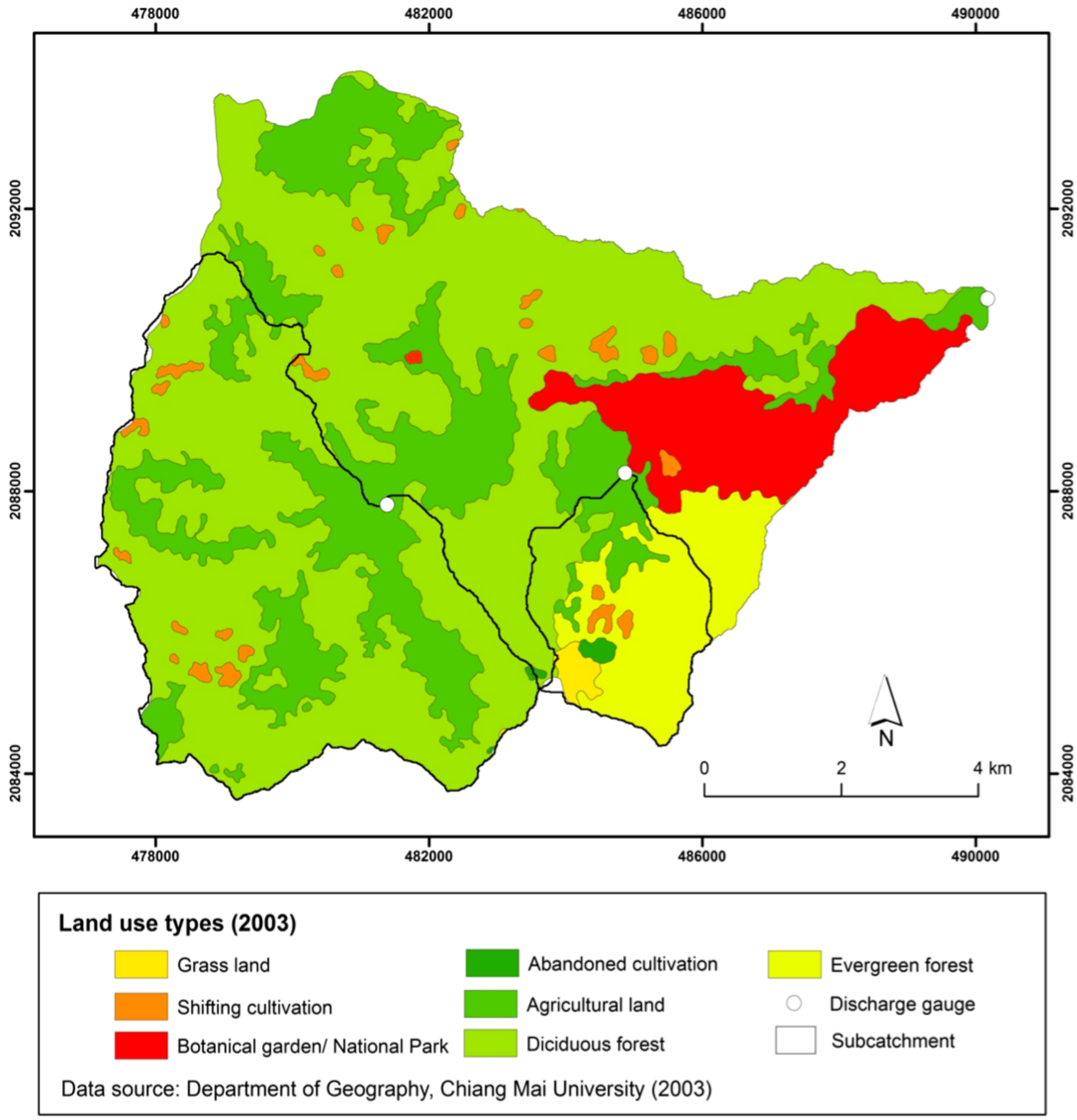

Figure 1.3: Land use in the Mae Sa watershed. Land use details were kindly contributed by the Department of Geography, Chiang Mai University.

Schuler (2008) identified and classified the soil types of the Mae Sa watershed. Acrisols and Cambisols turned out to be predominant soil types (Figure 1.4). Additional soil types are Leptosols, Gleysols, Regosols and Fluvisols. The upper boundaries of Acrisols are around 1300 m.a.s.l., Cambisols are found along the highest parts of the watershed and at very steep slopes. Cambisols are mostly covered by forests, as they are not suitable for agricultural use.

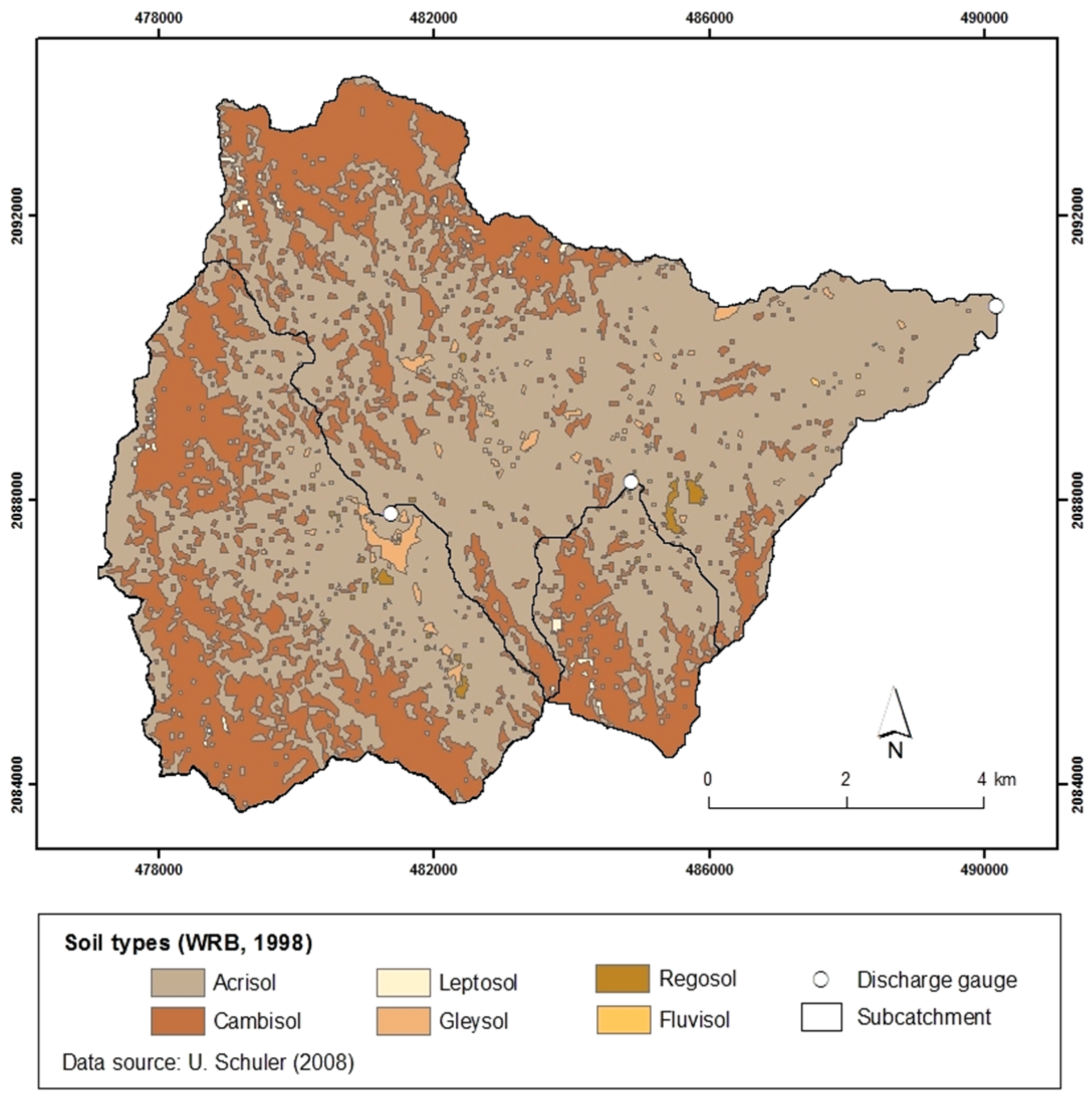

Figure 1.4: Soils in the Mae Sa watershed. Soil data were monitored by U. Schuler (2008).

Agriculture is mainly done on Acrisols, but fertilizers have to be applied because the soils have a very low fertility. A general decrease in hydraulic conductivity and an increase of the bulk density with depth were identified in both Acrisols and Cambisols. Kahl et al. (2007) observed macropores with diameters between 1-10 cm mainly at depths of 60-90 cm in the subbasin Mae Sa Noi. Such macropores can result from animal burrows (i.e. termites) and decrease with depth.

The monitoring network of the Mae Sa watershed includes 14 rain gauges (Figure 1.2), of which two are combined with weather stations. Besides rainfall, the weather stations monitored solar radiation, relative humidity, air temperature and wind speed. The rain gauges cover all altitudinal ranges within the catchment to guarantee a representative observation. Discharge is measured at three stations, Headwater, Mae Sa Noi and at the outlet of the catchment (Figure 1.2, Figure 1.5).

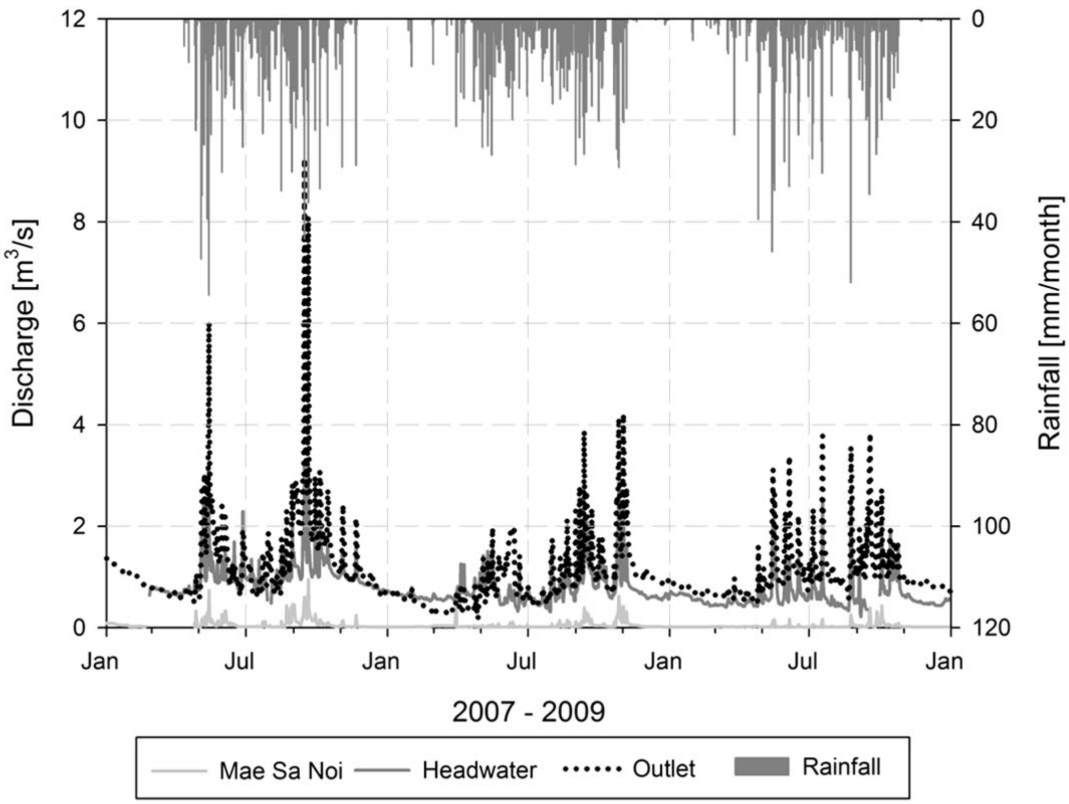

Figure 1.5: Discharge and rainfall at the stations Headwater (HW, 28 km²), Mae Sa Noi (MSN, 7 km²) and Outlet (OL, 77 km²) during the monitored period. Data from A. Ziegler were used to fill gaps and to compare the times series (A. Ziegler, personal communication, 2011).

All gauges are equipped with ultrasonic sensors, which record the water level. Through the establishment of a stage-discharge relationship at each monitoring location these water levels were later on converted to discharges. Alongside the ultrasonic sensors, automatic water samplers were operated at each gauging station to collect water samples for pesticide analytics.

Rainfall in the Mae Sa watershed is dominated by the monsoon and occurs with a bimodal distribution (Figure 1.5). The average is given with 1200 mm a^{-1} between 2003-2009 (data from weather station Mae Sa Noi). Annual totals were 1299 mm (April – December 2007), 1352 mm (January-December 2008) and 1281 mm (January – December 2009). The largest amount of the annual rainfall is received during the rainy season, which lasts from around April to October. During the peak of the rainy season rainfall can exceed 70 mm d^{-1} (79.4 mm; recorded on 15 September 2007). Cumulated rainfall (Figure 1.6) was highest in 2007 and 2009 received lowest annual average rainfall.

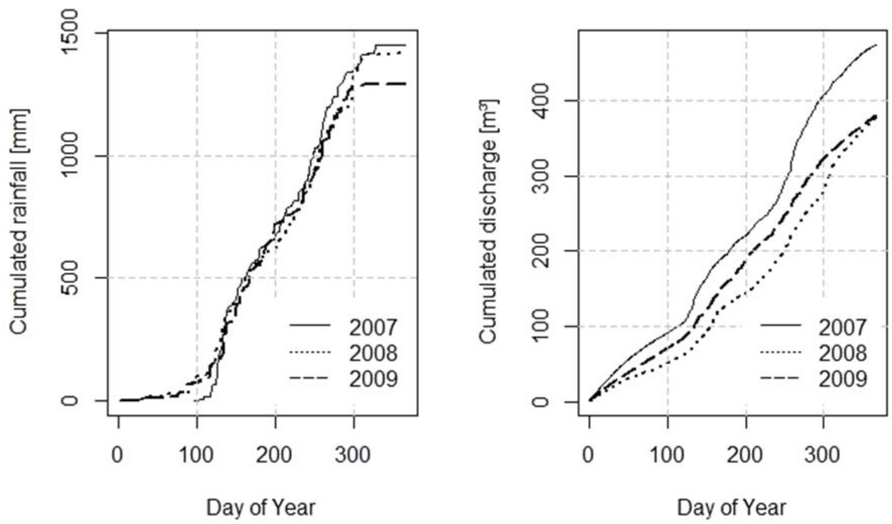

Figure 1.6: Cumulated rainfall (left) and cumulated discharge in the Mae Sa watershed for 2007, 2008 and 2009.

The years 2008 and 2009 show a steady increase of rainfall during the rainy season. In 2007, the bimodal distribution of rainfall maxima within the rainy season is more pronounced. Here, a fast summation of rainfall over a short time indicates an intense rainy season. The frequency distribution of daily rainfall (Figure 1.7) reveals the differences between the years 2007, 2008 and 2009. Whereas 2007 daily rainfall amounts exceeded 40 mm d^{-1}, maximum daily amounts of 2008 and 2009 are around 28 mm d^{-1}.

The main river segment of the Mae Sa stretches over 13 km and has an annual average discharge of 1.1 $m^3 s^{-1}$ (14.2 L s^{-1} km^{-2}; data records from 2007-2009). The stream water travel time from the headwater gauge to the Outlet (10 km) reaches up to four hours, depending on the magnitude of the event. The discharge is highly variable throughout the year and may reach up to 39.2 $m^3 s^{-1}$ (509 L $s^{-1}km^{-2}$, September 15, 2007). Lowest flow volumes (0.4 $m^3 s^{-1}$ or 5 L s^{-1} km^{-2}, April 10, 2008) were mostly observed prior to the wet season. The frequency of daily average discharge (Figure 1.7) shows that the runoff behavior of the Mae Sa river is dominated by rather small volumes and only 2007 exceeds the daily average discharge of 5 $m^3 s^{-1}$. The differences in runoff behavior can also be seen in Figure 1.7 and in the recession behavior, depicted in Figure 1.8.

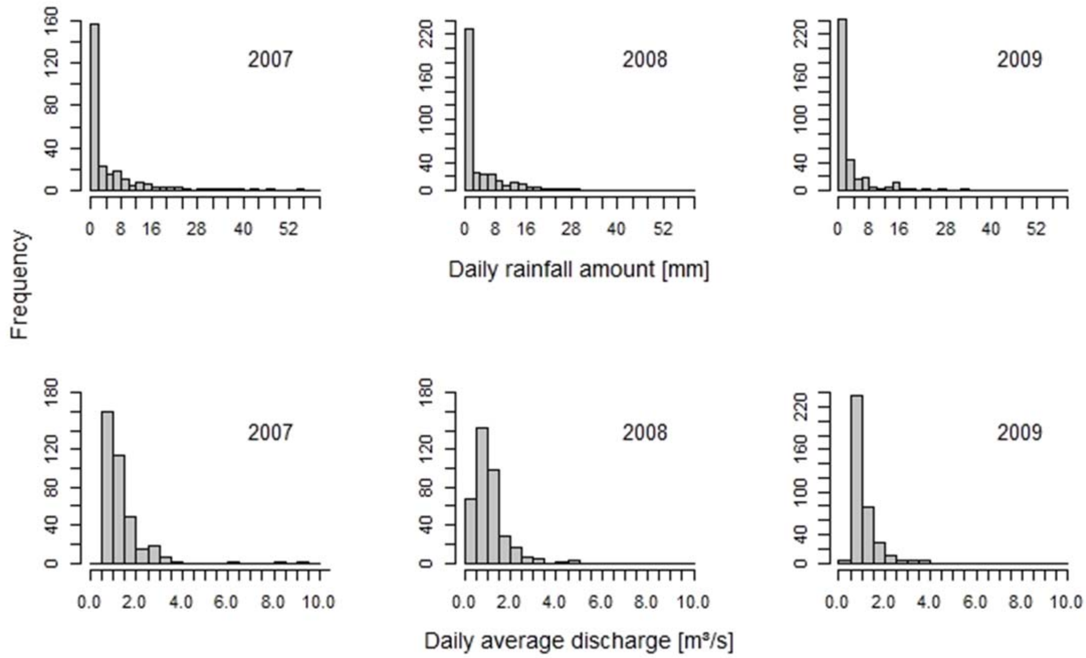

Figure 1.7: Frequency of daily rainfall amount (upper row) and daily average discharge (lower row) in the Mae Sa watershed for 2007, 2008 and 2009.

Lowest flow volumes, runoff coefficients, mean annual runoff and further hydrological characteristics are listed in Table 1.1. The highest runoff contribution was measured at the Headwater, which also had the largest runoff coefficient.

Table 1.1: Overview of hydrological measures of the Mae Sa watershed during 2007-2009 (based on data collected within the presented study).

	Headwater (HW: 28 km²)	**Mae Sa Noi (MSN: 7 km²)**	**Outlet (OL: 77 km²)**
Share of the watershed [%]	36	9	100
Mean annual runoff [m³/s]	0.8	0.05	1.10
Mean annual runoff [mm]	704	218	445
Mean annual runoff contribution [l/s/km²]	28.2	6.5	14.1
Areal average annual rainfall [mm]*	1336	1317	1387
Runoff coefficient [-]	0.53	0.17	0.32

*Based on rainfall records obtained within this study from 2007 – 2009; areal annual rainfall is represented by a simple mean of the stations (n) covered by the subcatchment area: HW: n=7, MSN: n=2, OL: n=14).

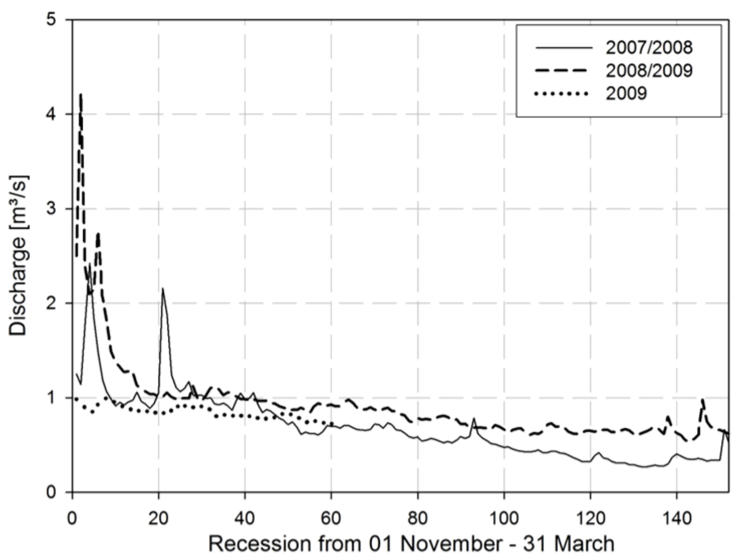

Figure 1.8: Recession limb from 1 November until 31 March, monitored at the Outlet.

For the Mae Sa watershed, evapotranspiration rates of 2-4 mm d^{-1} are estimated. Relative humidity ranges between 40 and 90%, average annual temperature is 21°C. Solar radiation decreases during the rainy season, and shows maxima in January and March/April. The monthly averages from 2003 through 2009 are shown in Figure 1.9.

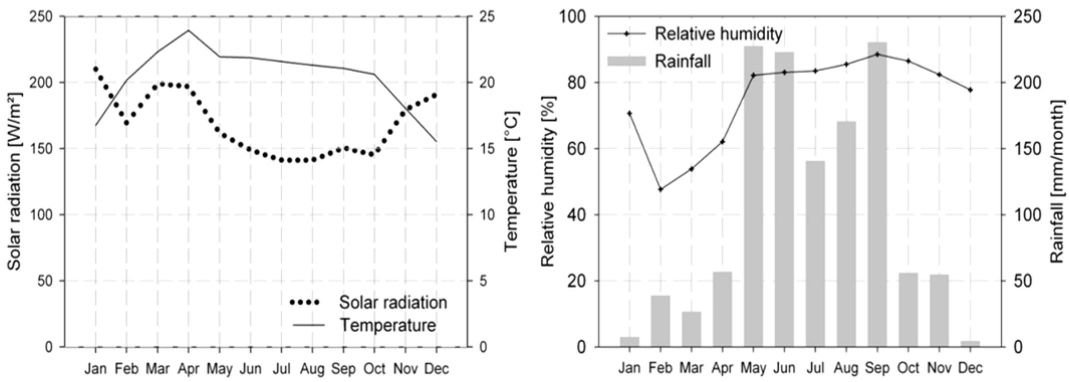

Figure 1.9: Climate characteristics of the Mae Sa watershed. Solar radiation, temperature and rel. humidity are shown in monthly average, rainfall is given in totals per month (data monitored at the weather station of SFB 564, Subproject B2, 2003 - 2009).

Because of its representative character in terms of agricultural development in rural mountainous regions of Southeast Asia, the Mae Sa watershed was object of several research studies in the frame of a special research collaboration (SFB 564: Sustainable development of rural mountainous regions in Southeast Asia). Within the present study, earlier investigations on pesticide dynamics by Ciglasch et al. (2005, 2006) and Kahl et al. (2007, 2009, 2010) are of particular interest. However, hydrology and pesticide dynamics on the catchment scale have not yet been investigated.

2 Objectives and outline

The tropical mountainous headwater catchment in Southeast Asia belongs to a region for which hydrological research papers are rare. Little is known about basic hydrological processes and transport pattern of agrochemicals in such environments. Available publications do not exactly cover the knowledge gaps that are faced in the study area.

While investigating the transport of pesticides in a watershed, hydrological processes become relevant and need to be investigated in advance. Runoff generation is particularly crucial, because pesticide dynamics are strongly related to runoff behavior and the transport of solutes is connected with flow paths. Furthermore, rainfall distribution plays a major role in the transport of pesticides and becomes even more important on catchment scale. In order to improve the model input and decrease uncertainties caused by input data (Beven, 2002), spatial trend in rainfall data need to be identified. As there are only few applications of the SWAT model in steep, tropical mountainous regions, its suitability for such environments firstly needs to be tested. Only then it can be clarified, if the model is able to reproduce the hydrological components; a prerequisite for simulating the fate of pesticides within a catchment. In order to deliver the groundwork for future model applications, this work aimed to

i) investigate the spatio-temporal variability of rainfall in the Mae Sa catchment,

ii) reveal runoff generation in a subcatchment of the Mae Sa watershed and identify the dominant flow components for runoff generation during storm flow,

iii) monitor pesticide dynamics in stream during single runoff events and compare the behavior of several compounds at different scales in the watershed,

iv) assess the suitability of the SWAT model to reproduce rainfall-runoff relations in a tropical, mountainous environment.

In Chapter 3, the spatio-temporal variability of rainfall in the Mae Sa watershed is described, and mean rainfall amounts of each stations (rain gauge) are compared. An ANOVA was applied to compare the station means for several time indices and the necessary amount of stations that need to be operated to maintain the total annual mean was tested. Generalised Additive Mixed Models (GAMMs) with a log link function and Gamma distribution were applied to identify significant effects on rainfall for different time indices. Besides the temporal variability topographic factors, such as elevation, aspect and slope were used to explain the spatial variability. The dominant runoff generating processes were investigated in the Mae Sa Noi subbasin from 2007-2009 (Chapter 4). A tracer-based hydrograph separation was applied to four events to divide the storm flow into fractions of stream flow, surface runoff and shallow subsurface flow. Data on major ion concentrations in the aforementioned fractions were used to obtain further information on flow paths in the catchment.

The third objective was reached by monitoring three rainfall-runoff events and the specific concentration of pesticides in the discharge (Chapter 5). The focus was on dynamics of specific compounds, and whether they were repetitive or changeable on different scales.

The knowledge and information obtained within the prior objectives were used to achieve the final task of this thesis, which is described in Chapter 6. The hydrological processes within the Mae Sa watershed were simulated with the SWAT model. The intention was to test the applicability of the model for such tropical, mountainousregion with monsoonal climate, and also to check, whether the model is able to reproduce the flow partitioning (Chapter 3) reliably. Those results are of particular interest for further studies on the fate of pesticides.

The results from the listed objectives are discussed and linked in an overall discussion (Chapter 7). A final conclusion will close this thesis in Chapter 8.

3 Publication 1 - Rainfall variability in a tropical, mountainous catchment in northern Thailand

C. Hugenschmidt[1], A. Fichtner[2], J. Ingwersen[1], W. Sangchan[1], Y. Sukvanachaikul[3], S. Uhlenbrook[4,5], T. Streck[1]

[1]Institute of Soil Science and Land Evaluation, Biogeophysics (310d), University of Hohenheim, 70953 Stuttgart, Germany. [2]Institute for the Conservation of Natural Resources, Department of Landscape Ecology, University of Kiel, Germany. [3]Dept. of Civil Engineering, Faculty of Engineering, Chiang Mai University, 50200 Chiang Mai, Thailand. [4]UNESCO-IHE Institute of Water Education, PO Box 2601 DA Delft, The Netherlands. [5]Section of Water Resources, Delft University of Technology, PO Box 5048, 2600 GA Delft, The Netherlands.

Journal of Hydrology
(submitted)

Abstract

Assessing the spatio-temporal distribution of rainfall on catchment scale is a frequent problem in hydrological applications. Rainfall variability has a particularly severe impact on solute transport. The problem is even more severe within mountainous areas in the tropics, because orography and climatic conditions increase the variability while data sets are rare.

We collected rainfall data from a tropical headwater catchment in northern Thailand and analyzed them with regard to their spatio-temporal distribution and the station characteristics. Rainfall records were obtained from 14 rain gauges, spread over 77 km² and covering an elevation range from 325 to 1540 m.a.s.l. We used Analysis of Variance (ANOVA) to compare rainfall means between stations at different intervals (daily, two-day, weekly and monthly) and tested the sensitivity of the total annual mean to a random reduction of the stations for each year. Generalized Additive Mixed Models (GAMMs) were applied to analyze the temporal and spatial distribution of rainfall. The ANOVA revealed no significant difference between the station means. This was supported by earlier data analysis, where a test on the effect of station on rainfall distribution resulted non-significantly from zero. To maintain the total annual mean within the 10% limit, at least 9 stations should be operated within the Mae Sa watershed. During the three years of monitoring, rainfall followed a bimodal distribution with peaks in the beginning and at the end of the rainy season. Regarding the spatial distribution of rainfall, slope was the only statistically significant factor. Elevation showed only a weak and non-significant relation with rainfall amounts. Our findings suggest influences of additional variables, such as wind direction and wind speed, which were not monitored within this study. For future applications, we propose to apply simplified meteorological models to produce average wind fields which can then be used for co-regionalization.

3.1 Introduction

Rainfall is known to be highly variable in space and time. Due to the complexity of rainfall generation, it is difficult to predict, particularly in tropical regions. This impedes hydrological applications, such as water resources management and hydrological modeling, where it is necessary to estimate the rainfall-runoff relations as precisely as possible (Bardossy et al., 2008). Because rainfall is the main input of hydrological models (Beven, 2002), uncertainties in records or in spatial interpolation produce uncertain and imprecise model results. Next to water quantity issues, rainfall has also a large impact on solute transport in catchments (i.e. McGrath et al., 2010). Rainfall variability is seen as a key factor of in-stream physicochemical processes affecting surface water quality (Park et al., 2011). This has been shown in several studies, in particular with agrochemicals (e.g. Flury, 1996; Kahl et al., 2007; Sangchan et al., 2012).

It is well recognized that rainfall is particularly difficult to forecast in mountainous regions (Bruijnzeel, 2004; Wulfmeyer et al., 2011). Rainfall variability is high and it becomes even higher when the mountains are located in the outer tropics, with their distinct changes between dry and rainy seasons. Vegetation (e.g., rain forests, Hoyos and Webster, 2007) and the formation of cyclones may further influence rainfall generation and its spatio-temporal distribution.

Buytaert et al. (2006) monitored rainfall distribution in a tropical highly elevated area (3500 to 4100 m.a.s.l.) in the Andes, south Ecuador. The 12 rain gauges were spread over a catchment of 650 km², which results in a network density of about 54 km² per rain gauge. They found an increase of rainfall from West to East within the study catchment, but correlations between rainfall and topographical factors, such as aspect, slope and altitude, were weak. They suggested that the orographical factors are important on the catchment level only, but not on regional scale, because of regional fluctuations in average rainfall. A study in the South Pare Mountains, Tanzania (Mul et al., 2009), based on 14 stations distributed across 300 km² and an elevation range from 600 – 2000 m.a.s.l., revealed that the spatial variability of rainfall can be large, even in areas with the same altitude. The authors were not able to explain the variability of rainfall by orography only, but did not come up with further influences on rainfall enhancement. Similar observations were reported from a study in the Himalaya region: same elevation ranges received different rainfall totals (Singh et al., 1995). The authors found that the rainfall was a function of the orientation (aspect) of the elevation ranges. Their findings suggest that particularly in mountainous monsoon areas factors other than elevation must be considered to explain spatial rainfall distribution.

A high-resolution plot-scale experiment on spatial variability of daily rainfall in the tropical humid Ethiopian highlands was conducted by Bitew and Gebremichael (2010). With a range of elevation from 3050 m.a.s.l. to 3276 m.a.s.l. and a distribution of 22 rain gauges (bulk collectors) over 36 km² the network density was very high. Nevertheless, the authors could not find a clear trend in the daily rainfall within the monitored area.

There are only a few studies on rainfall distributions in South-East Asia. Typical characteristics, such as high intense rainfall events of short duration, were observed by Dykes (2000) in Brunei. They remarked that rainfall was normally caused by convection cells and that topography influences rainfall pattern considerably. Extrapolating rainfall beyond a few kilometers may therefore result in unreliable estimates of areal rainfall. Some authors emphasize the lack of data sets from tropical environments that target at the effect of altitude or orography on rainfall distribution (Dykes, 2000; Singh, 2006). Wilk and Andersson (2000) state that mountainous basins generally suffer from poor assessment of spatial distribution of rainfall and that typically the density of rain gauges becomes less with increasing elevation.

Thanapakpawin et al. (2006) investigated the rainfall distribution in the Mae Chaem watershed in North-West Thailand (18°06 N, 98°04 E). This watershed is close to our study watershed. Based on a network of 7 rain gauges covering an elevation range of 200 – 1400 m.a.s.l. and an area of 3858 km², they found that rainfall increased by 0.5 mm per meter of altitude. A 10-years data set based on 18 rain gauges in the same watershed delivered a clear dependency of rainfall amount and rainfall duration on elevation, but rainfall intensity could not be related to it (Kuraji et al., 2009). Earlier studies by Dairaku et al. (2000) and Dairaku et al. (2004) evaluated the data from 12 rain gauges in the same study area over a period of 6 months (June to November 1998) within an elevation range from 282 to 1585 m.a.s.l. The authors observed a close relation between rainfall and altitude. Amount and duration of rainfall were correlated, but, again, rainfall intensity appeared to be independent from altitude. There was no relationship between orography and rainfall. Singh and Kumar (1997) conjectured that other factors blur the impact of elevation on rainfall totals, particularly in monsoon areas.

In North Thailand and also in greater Southeast Asia rainfall occurs seasonally with a distinct dry and rainy season. Rainfall shows large inter-annual changes (Park et al., 2011). The rainy season is normally split into two high peak periods (Campling et al., 2001). This has been monitored for a long time in North Thailand, where the bimodal distribution is caused by the south-west monsoon, resulting in rainfall periods from May to September (Walker, 2002). A bimodal distribution with rainfall peaks around May and November was observed in Malaysia as well (Noguchi et al., 1996).

Despite these studies on rainfall variability from South-East Asia, there is still a lack of knowledge on spatial patterns, especially in mountainous regions. Typically, the network density was rather low, which hampers the identification of spatial trends. With a network density of about one rain gauge per 5 km² and a temporal resolution of 10 minutes, we collected data at high spatio-temporal resolution in a remote area. The study was embedded in a project dealing with the transport of agrochemicals in a tropical headwater catchment in North Thailand. Earlier studies in the catchment revealed that rainfall variability is a key factor of losses and transport of solutes (Kahl et al., 2007; Sangchan et al., 2012).

The objectives of this paper are i) to evaluate to which extent a dense monitoring network is required for reasonable rainfall monitoring, ii) to investigate spatio-temporal distribution of rainfall in a mountainous area in the outer tropics and iii) to relate it to the dominant orographic factors.

3.2 Material and methods

3.2.1 Study site

The study has been carried out in the Mae Sa watershed, which is located in the mountainous region of North Thailand, some 35 km north-west of Chiang Mai (18° 47′ N, 98° 59′ E). The Mae Sa River is a tributary of the Ping River, one of the major rivers of Thailand, which is of high importance for water supply. The Mae Sa watershed has a total area of 77 km². Its elevation ranges between 325 m.a.s.l. and 1540 m.a.s.l. The orography is very heterogeneous. The watershed is characterized by narrow and steep valleys with a sharp relief (Figure 3.1). The average slope is 36%. Although the catchment is under intense agricultural use, the major vegetation is forest, which covers almost 80% of the area. The climate of the region is controlled by the northward movement of the Intertropical Convergence Zone (ITCZ), which drives the south-west monsoon (Walker, 2002). The monsoon controls the seasonality with a distinct wet and dry season. The average temperature is 21°C, and annual rainfall is on average 1200 mm per year.

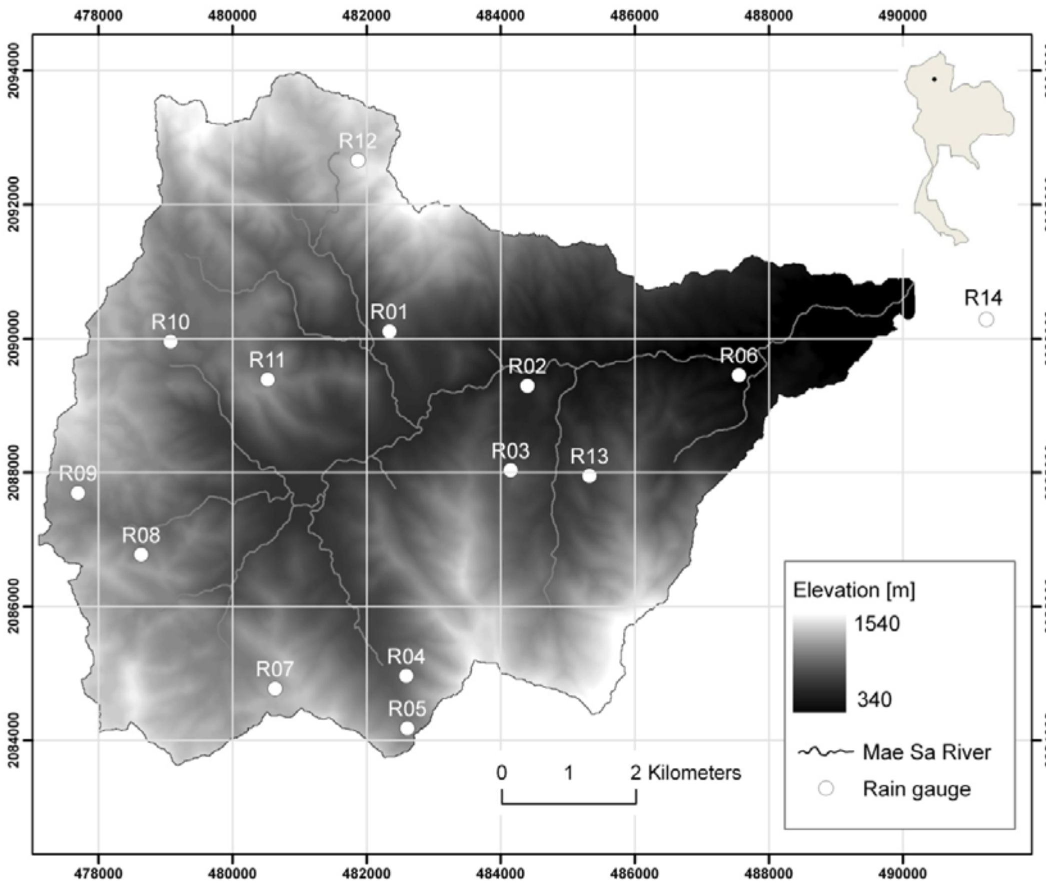

Figure 3.1: Distribution of the rain gauges R01-R14 in the Mae Sa Watershed, Northern Thailand. Further details on rain gauges are given in Table 3.1

3.2.2 Rain gauge network

The rain gauge network consisted of 14 locations (R01 – R14, Figure 3.1) within or in direct vicinity of the watershed. The stations were distributed among different elevation bands (Figure 3.1, Table 3.1). Each rain gauge was equipped with an automatic tipping bucket including an integrated data logger (Fischer Company, Germany). The surface area of the rain gauges was 200 cm². Each tipping volume equals 4 cm³, equivalent to 0.2 mm per tip. The logging interval was set to 10 minutes.

Table 3.1: Characteristics of the rain gauges in the Mae Sa Watershed.

Rain gauge	Elevation (m.a.s.l.)	Slope (%)	Aspect (°N)	Annual Mean (mm/d)	SD[1] (mm/d)	Min (mm/d)	Max (mm/d)	n (d)[2]
R01	804	20.20	233	3.79	8.15	0.00	58.00	926
R02	667	11.90	8	4.34	8.96	0.00	79.40	926
R03	904	13.90	41	4.59	9.16	0.00	60.40	906
R04	854	16.70	286	5.33	10.32	0.00	72.40	959
R05	1000	9.40	19	4.89	9.58	0.00	63.40	1002
R06	542	6.80	48	3.89	8.14	0.00	47.80	708
R07	1056	13.50	318	4.31	8.91	0.00	76.40	888
R08	961	12.70	14	4.16	9.06	0.00	68.20	987
R09	1182	7.00	160	3.43	7.49	0.00	63.60	915
R10	1135	6.90	129	3.67	8.61	0.00	56.00	797
R11	997	15.80	10	4.09	8.62	0.00	67.00	991
R12	1197	12.40	295	4.06	8.66	0.00	70.40	1002
R13	805	10.60	286	3.91	9.06	0.00	59.20	956
R14	345	1.40	340	3.38	7.03	0.00	58.00	480

[1]Standard deviation, [2]Number of data records

A weather station (R13, Figure 3.1) was set up in 2003 and was also included in the monitoring. 12 additional rain gauges and another weather station (R14, Figure 3.1) were installed in April 2007. Hence, rainfall data were recorded at 14 stations from April 2007 till December 2009. Considering the catchment size of 77 km², each rain gauge covers, on average, an area of about 5 km². This is a very high resolution for an automatic rain gauge network and is normally not found in watersheds other than experimental study sites.

3.2.3 Data analysis

Differences in rainfall between stations (rain gauge) were analyzed with one-way ANOVA (Analysis of Variance), followed by pair wise comparisons (Tukey's test).

Models were fitted for varying temporal rainfall resolutions (daily, 2-days, weekly and monthly). Autocorrelations between sequential station samples were taken into account using an autoregressive correlation structure for the residuals of the order 1 (AR-1): cor (ε_s, ε_{s-k}) = ρ^k, where ε_s is the residual error at time s, k is the time lag (in days), ρ is the correlation parameter to be estimated. This structure represents a decline in temporal correlation for increasing lags, or number of days between the observations (Pinheiro and Bates, 2004). Prior to analysis, rainfall data were log+1 transformed to stabilize the variance.

To determine how many rain gauges are needed in the catchment in order to reliably measure the total annual mean, the variation of the total annual mean with regard to the number of rain gauges was analyzed. Within this study we defined a deviation of below 5% or 10%, repectively, from the "true" mean as acceptable. The "true" mean (*tTAM)* was calculated from the data of all (*n*=14) stations. The analysis was twofold. To test the impact of a single station on the total annual mean, one station was removed and the mean (modified total annual mean, *mTAM*) was recomputed from the data of the remaining stations (*n*=13). In total, we recomputed the annual mean about 13 times. Further, we estimated the number of stations needed to obtain a mean, which deviates less or more 5% or 10% from the "true" mean. For this, we randomly removed stations, one by one and without replacement, from the set and calculated the total mean from the data of remaining stations. The procedure was terminated as soon as the deviation (*DEV*) from the "true" mean was larger than 5% and 10%, respectively. The procedure was performed about five times. The deviation (*DEV in %*) of the modified total annual mean (*mTAM*) from *tTAM* is computed as follows:

$$DEV = \left(1 - \frac{|mTAM - tTAM|}{tTAM}\right) \cdot 100 \qquad (Eq.\ 3.1)$$

We applied generalised additive mixed models (GAMMs) with a log link function and gamma distributions to assess the effects of topographical variables on rainfall pattern. Because rainfall measurements are typically skewed and heteroscedastic continuous data, the gamma distribution was preferred to avoid the biases associated with logarithmic transformations, while the log link ensures positive values for the fitted response variable (McCullagh and Nelder, 1989). Smooth functions were constructed as thin plate regression splines, with optimal amount of smoothing determined by cross-validation

(Wood, 2006). Similarly to the ANOVA, GAMMs were fitted with an AR-1 correlation structure. Rainfall was used as response variable at varying temporal resolutions (daily, weekly and monthly). Location, seasonal (time of the year) and orographic effects (aspect, elevation and slope) were taken as predictors. The resulting GAMMs have the form:

$$\text{Rainfall}_s \sim \text{Gamma}$$
$$(\text{Rainfall}_s + 0.01) = \exp(\alpha + f_1\,(\text{Time}) + f_2\,(\text{Aspect}) + f_3\,(\text{Elevation}) + f_4\,(\text{Slope}));$$

where Rainfall_s is the rainfall at day_s, week_s or month_s, α is the intercept in logarithmic space, f_1 is a smoothing function for the day of the year. The functions $f_{2,3,4}$ are smoothers for orographic effects. As the model includes a log-transformation, rainfall records with the value zero were set to 0.01.

Models were fitted for each investigation year separately, since initial comparisons of rainfall means indicated no significant long-term effect (see below). Model selection (backward procedure) was based on the Akaike Information Criterion (AIC). The model with the lowest AIC value was preferred (Zuur et al., 2009).

To evaluate the spatial relationships between rain gauges we calculated Spearman's rank correlation coefficients. GAMMs were fitted using the *mgcv* library in R, version 2.10.1 (R Development Core Team, 2009).

3.3 Results

The daily rainfall measured at the 14 stations during the monitoring period (2007-2009) is shown in Figure 3.2. The maximum daily value was recorded on 15 September 2007 (79.4 mm d^{-1}) (Table 3.1), followed by that on 24 August 2009 (76.4 mm d^{-1}). In 2008, the fourth highest daily rainfall was measured (23 April 2008, 70.4 mm d^{-1}). Station R04 received the highest mean daily rainfall in all years. While in 2009 rainfall during January and April was almost null, the preceding year (2008) had remarkable rain events in the early rainy season. The peaks during 2008 were lower than in 2007 and 2009 and rainfall was rather uniformly distributed (Figure 3.2).

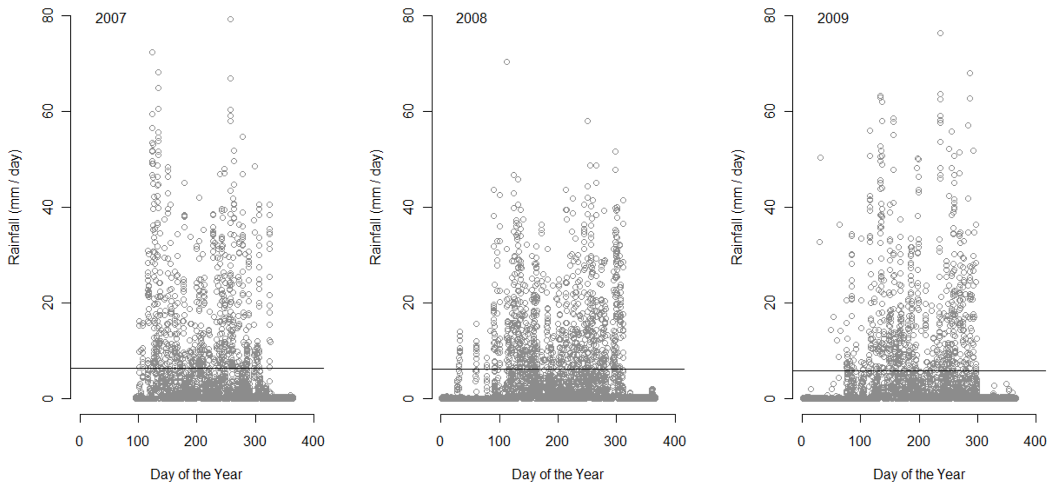

Figure 3.2: Annual distribution of daily rainfall in the Mae Sa Watershed. The black horizontal lines indicate the grand means during the rainy seasons (April-October):6.4 mm d^{-1} (2007), 6.1 mm d^{-1} (2008), 5.8 mm d^{-1} (2009).

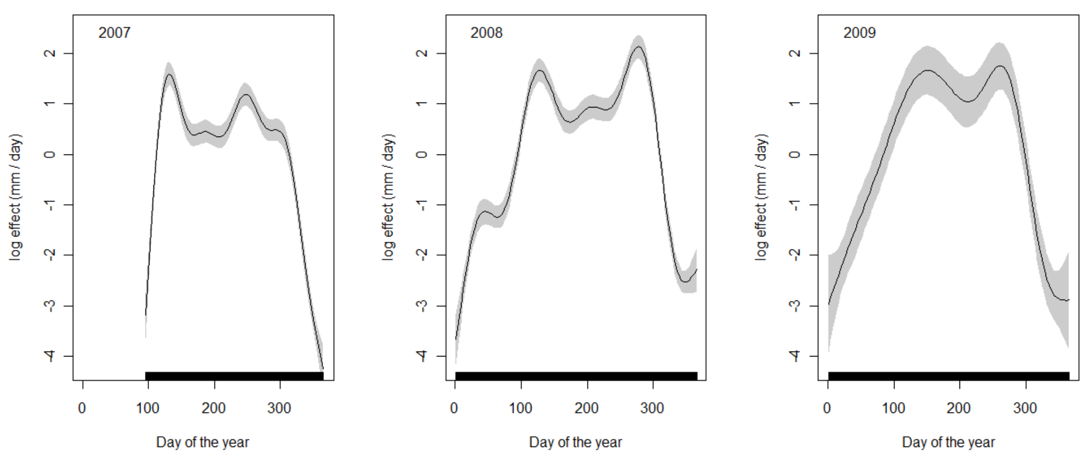

Figure 3.3: Partial effects of temporal variation on the daily rainfall distribution. Grey areas indicate the 95% confidence intervals; the Y-axis represents the contribution of the smoother to the fitted values in mm d^{-1} (logarithmic scale)

There were also differences in the extent of the dry spell from June to August. It was mostly expressed in the year 2007 and 2008, but not in 2009 (Figure 3.3). Nevertheless, daily rainfall means during the rainy season did not significantly differ between the years ($F = 2.12$, $P = 0.12$). Yearly means of daily rainfall during the rainy seasons ranged from 6.4 mm d^{-1} (2007) and 6.1 mm d^{-1} (2008) to 5.8 mm d^{-1} (2009) (Figure 3.2).

ANOVA indicated no significant station effect on each on the temporal rainfall indices tested (Table 3.2). Additional time indices were checked, but no different results could be obtained. Also, preliminary data analysis showed that station (or the location of the rain gauge in the catchment) has no significant effect on rainfall.

Table 3.2: Results of the ANOVA (Tukey HSD Test) including all stations and different time indices.

Time indices	F-value	P-value
daily	1.474	0.118
2 days	0.796	0.665
weekly	0.297	0.993
monthly	0.153	1.000

The true annual means (*tTAM*) for the monitored years were 5.32 mm d^{-1} (2007), 3.88 mm d^{-1} (2008) and 3.30 mm d^{-1} (2009). Station R02 was the only station the removal of which caused the mean of the remaining stations to deviate from the mean of all (14) stations by >5% or >10% in all three years. The mean after removing R02 was 4.61 mm d^{-1} (2007), 3.67 mm d^{-1} (2008) and 3.82 mm d^{-1} (2009), respectively. Hence, in 2008 the deviation was >5% (-0.21 mm), whereas in 2007 (-0.71 mm) and 2009 (+0.52 mm) it was even >10%. The deviation after the removal of other stations ranged from 0.02% (2009, station R11 removed) to 30.13% (2009, station R01 removed). The simulated reduction of stations brought up a similar picture: there hardly was a repetitive pattern in the data set. For the year 2007, the reduction did not result in exceedance of the 10% limit, at all. While computing the modified total annual mean with only two stations, a deviation of maximum 8.7% (4.86 mm d^{-1}) was identified. In 2008, the effect of the random reduction of stations on the total annual mean was highest. While reducing two stations only, the *mTAM* passed the 10% limit in three out of five trial runs. The remaining two runs ended in a crossing of the 10% threshold after the reduction of 6 and 8 stations. Three out of five runs in 2009 resulted in an exceedance of the 5% limit after the exclusion of four randomly chosen stations.

The GAMMs indicated that the intra-annual variations were a stronger predictor for daily rainfall distribution than the orographic variables (Table 3.3). Daily rainfall showed a typical bimodal distribution with peaks at the beginning and the end of the rainfall season (Figure 3.2). Intra-annual variations were slightly different between the three monitored years (Figure 3.3).

In 2007, early season rainfall (April/May) was higher than values recorded in the later part of the rainy season (September/October) and rainfall occurred with higher temporal variability (Table 3.3). In 2008, an opposite trend was observed. Here, the highest amount of rainfall was measured in October, while the rainfall in the early season (April/May) was lower. In contrast, differences between the two peaks almost declined in 2009. This is expressed in the decrease of randomness in rainfall generation and increase of temporal autocorrelation (ρ), respectively (Table 3.3).

Table 3.3: Results from a generalized mixed models (GAMM) analysis predicting variation in rainfall indices (daily, weekly, monthly) by temporal and topographical effects. Significant effects (P > 0.05) are highlighted in bold. ρ denotes the estimated autocorrelation coefficient.

		Daily			Weekly (7 days)			Monthly (30 days)		
Year	Predictor variables	*F*	*P*	*ρ*	*F*	*P*	*ρ*	*F*	*P*	*ρ*
2007	Time	139.17	**<0.001**		111.60	**<0.001**		261.53	**<0.001**	
	Elevation	0.01	0.99		1.73	0.19		0.01	0.92	
	Slope	7.27	**<0.01**		2.32	**<0.05**		19.06	**<0.001**	
	Aspect	0.01	0.94		0.80	0.37		2.29	0.13	
				0.05			0.01			0.01
2008	Time	157.95	**<0.001**		106.20	**<0.001**		184.49	**<0.001**	
	Elevation	0.13	0.72		0.10	0.76		0.10	0.75	
	Slope	5.40	**<0.05**		1.98	**<0.05**		6.03	**<0.05**	
	Aspect	0.34	0.56		0.80	0.37		0.08	0.77	
				0.20			0.15			0.28
2009	Time	39.46	**<0.001**		44.62	**<0.001**		38.44	**<0.001**	
	Elevation	1.84	0.18		0.48	0.49		1.78	0.18	
	Slope	3.85	**<0.05**		3.83	**<0.05**		3.3	0.07	
	Aspect	2.60	0.11		1.45	0.23		2.48	0.11	
				0.38			0.05			0.56

Slope is the only orographic variable with a significant ($P > 0.05$) effect on rainfall. The effects of aspect and elevation were not significant (Table 3.3). Slope was positively related to daily rainfall with the greatest effect in 2009 (Figure 3.4).

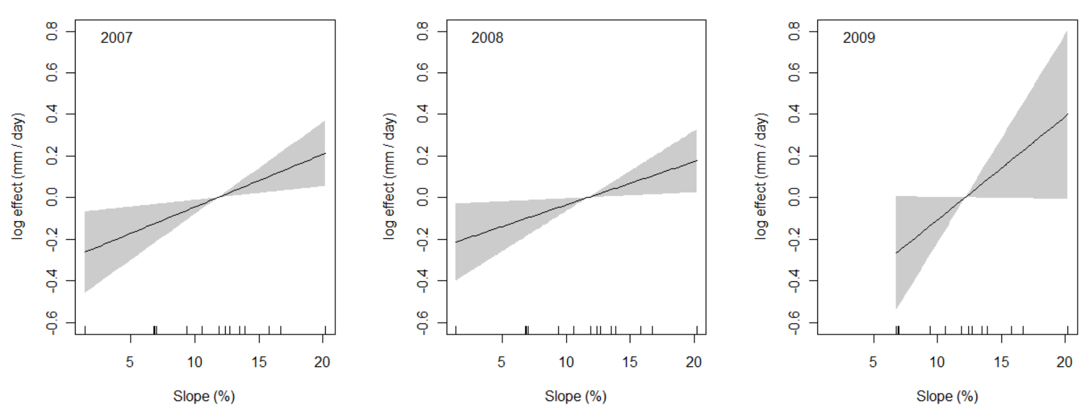

Figure 3.4: Partial effects of slope on the daily rainfall. Grey areas indicate the 95% confidence intervals; the Y-axis represents the contribution of the smoother to the fitted values in mm d^{-1} (logarithmic scale).

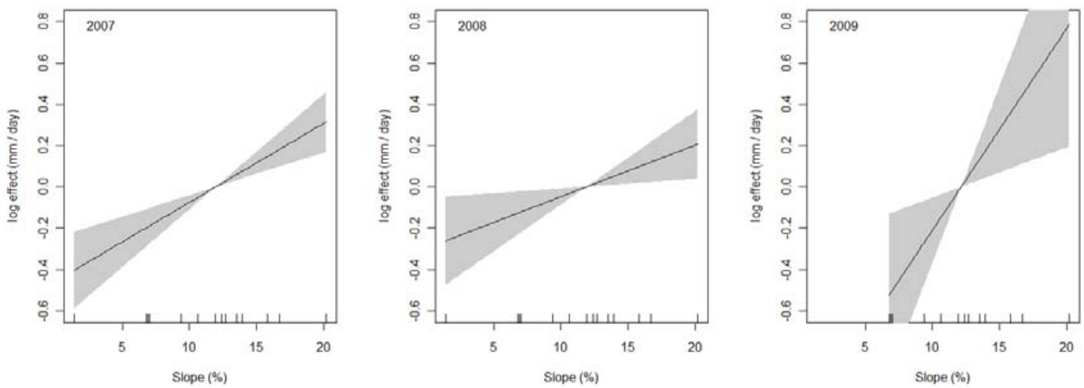

Figure 3.5: Partial effects of slope on the monthly sum of rainfall. Grey areas indicate the 95% confidence intervals; the Y-axis represents the contribution of the smoother to the fitted values in mm d^{-1} (logarithmic scale).

Daily rainfall (in 2009) on very steep slopes (25%) was almost twice as high compared to values found on moderate slopes (7%). This trend was consistent over all time indices tested, such as the 7-day sum of rainfall and the 30-day sum of rainfall (Figure 3.5).

Although the GAMMs revealed elevation as a non-significant factor ($0.18 \leq P \geq 0.99$, Table 3.3), a linear regression indicated a partial relation between altitude and daily mean rainfall. In fact, the altitudinal effect is restricted to elevations above 1000 m: the amount of rainfall of stations above this elevation (n = 5) are related to elevation by a coefficient of determination of $R^2 = 0.67$. Other than expected, daily rainfall decreases by 0.79 mm per 100 m. Below 1000 m.a.s.l. (n = 9) R^2 is only 0.27, while daily rainfall decreases by 0.14 mm per 100 m.

Table 3.4 presents the matrix of Spearman's rank correlation coefficients of daily rainfall between the stations. There is no persistent pattern of a decline in *r* with increasing distance.

Very good correlations were found between R03 - R13 (*r* = 0.9), R04 – R05 (*r*= 0.94) and R09 – R08 (*r*= 0.94) (Table 3.4). These stations are close to each other. Although R06 and R14 are also very close to each other, *r* is only 0.59. R14 and R09 are the stations with the largest separation, yet they result in r = 0.59.

.

Table 3.4: Spearman Rank Correlation of the rain gauges in the Mae Sa watershed (bold font indicates the largest and smallest correlations).

	R01	R02	R03	R04	R05	R06	R07	R08	R09	R10	R11	R12	R13	R14
R01	1	0.74	0.72	0.73	0.72	0.65	0.68	0.62	0.66	0.65	0.78	0.74	0.71	**0.54**
R02		1	0.9	0.85	0.84	0.78	0.78	0.76	0.78	0.8	0.87	0.85	0.88	0.68
R03			1	0.88	0.89	0.82	0.8	0.76	0.83	0.81	0.9	0.87	0.9	0.63
R04				1	**0.94**	0.78	0.87	0.78	0.79	0.81	0.88	0.85	0.86	0.66
R05					1	0.77	0.86	0.77	0.83	0.83	0.87	0.88	0.86	0.68
R06						1	0.68	0.63	0.69	0.68	0.79	0.77	0.78	0.59
R07							1	0.77	0.76	0.77	0.8	0.77	0.8	0.57
R08								1	0.81	0.79	0.79	0.77	0.78	0.56
R09									1	0.85	0.82	0.82	0.82	0.59
R10										1	0.86	0.85	0.82	0.59
R11											1	0.9	0.85	0.63
R12												1	0.85	0.66
R13													1	0.64
R14														1

3.4 Discussion

The rainfall distribution during the rainy season was clearly bimodal. This finding is in good agreement with other studies from the same region (Noguchi et al., 1996; Walker, 2002). The rainfall pattern is dominated by the movement of the ITCZ, which crosses the climatic equator around May and November, causing the monsoon cycle. The south-west monsoon initiates higher rainfall during April and May (Dykes, 2000; Walker, 2002) and lasts until September and October, when the air moves back towards the equator (northeast monsoon). The drier spell between rainfall peaks in a season (June/July) was emphasized by Walker (2002) and was identified in the analyzed data set, too. Our findings are also congruent with those of Kuraji et al. (2009), who identified the same temporal dynamics between 1999 and 2007 in the Mae Chaem watershed, which is located near the Mae Sa watershed. Whereas the bimodal distribution is stable, time and magnitude of the maximum rainfall vary.

As indicated by ANOVA, varying stations did not significantly differ in rainfall, no matter which temporal index had been selected. This supports results from a preliminary analysis, in which we tested the effect of location on rainfall amount and the effect of station on rainfall amount. To assign location, the stations were clustered according to wind direction and monsoon directions (northeast and southwest) and were defined by their coordinates. Similarly, there was no significant location effect (results not shown here). In contrast to our findings, Bitew and Gebremichael (2010) figured that daily rainfall amount between neighboring stations in a smaller catchment (36 km²) can significantly differ from each other. Their setup comprised 22 stations, giving a network density of 1.6 km² per station and fluctuations of daily rainfall of stations between 10 and 35 mm were reported. However, they did not monitor rainfall on long term, and only compared daily values from a short monitoring period, which hampers a direct comparison between both studies.

The similarity of the stations is also indicated by the tests that were run to identify the necessary amount of station to maintain the true annual mean (*tTAM*) within the catchment. During the tests, in which one station was left out per iteration, only R02 resulted in a modified mean leading to an exceedance of the of 5% and 10% limit for all three years. This legitimizes the second approach, where stations were randomly removed per iteration. There, also no repetitive behavior of any station was identified, emphasizing their similarity. As an extreme example, the 10% limit was crossed after removing 8 stations during 2008. Hence, at least 9 stations should be operated to stay within the 10% limit for all years. Location effects can be excluded as cause for different sensitivities during the years, because the stations were at fixed positions during the whole measurement. Temporal distribution of rainfall may cause an increased sensitivity to the reduction of stations, on the other side. An example is given during 2008. For that year, a reduction of the stations by two would already have caused a modified mean outside the 5% limit. Here, the true annual mean (3.88 mm d^{-1}) would be over- or underestimated by 0.26 mm or 0.28 mm, respectively. The maximum range of the upper and lower deviation boundary is given with 1.06 mm for the 10% limit in 2007. The remaining ranges vary between 0.33 and 0.78 mm. While one could probably deal with some 0.28 mm below the true annual mean during further investigations (i. e., modeling), over- or underestimation of the annual mean around 1.0 mm may have considerable effects on future data processing. Many authors have focused on the effect of rainfall uncertainties with regard to hydrological modeling (i. e. McMillan et al., 2012; McMillan et al., 2011; Gabelani et al., 2007) and often, rainfall input is identified as the major source of uncertainties with regard to rainfall-runoff modeling (e. g. Syed et al., 2003). Such model applications may serve as a supportive tool on testing the means and the effects of their over- or underestimation within the Mae Sa catchment.

We found a significant effect of slope on rainfall amount ($P > 0.05$), whereas the effects of elevation and aspect were statistically not significant (Table 3.3). The amount of rainfall increased with increasing slope, which holds true for all time indices. A slight relationship between amount of rainfall and altitude, which however was not significant, could be shown for the stations above and below 1000 m.a.s.l. In contrast, the Mae Chaem watershed (282 – 1585 m.a.s.l.), showed a strong correlation between altitude and the amount of rainfall (e. g. Dairaku, 2000; Dairaku, 2004; Thanapakpawin, 2006; Kuraji, 2009), but slope was not considered in the analysis. These authors derived their results from networks ranging from a resolution of 200 km² (Kuraji et al., 2009) to 550 km² per rain gauge (Thanapakpawin et al., 2006). Although the spatial resolution of the monitoring network in the Mae Sa watershed is higher (5 km² per rain gauge) and the rain gauges were distributed over several elevation bands, rainfall variation could not be related with elevation. Our data suggest that the impact of elevation on rainfall is blurred by the effect of other factors, i.e. slope, wind direction and wind speed. As in our study, investigations in a mountainous research site in Tanzania revealed a high variation of rainfall, even within the same elevation bands (Mul et al., 2009). There, Mul et al. (2009)

were not able to explain rainfall variability by elevation and the impact of slope or aspect on rainfall distribution were not considered. Similar findings were reported by Bitew and Gebremichael (2010) on a smaller scale. Although rainfall distribution was monitored with a network density of 1.6 km² per rain gauge, no clear trend between rainfall and elevation or other variables could be revealed. Based on monitoring data from two weather stations in a small study area in Brunei, Dykes (2000) emphasized the local influence of topographic effects on convection cells. In the Mae Sa watershed, rainfall and its spatial variability may also be influenced by the geometry of the narrow valleys (Figure 3.1).

Whereas statistically significant results are one side of the story, physical interpretation and explanation is the other one. The available data set does so far not allow a final explanation for the rainfall pattern. Regarding this issue, Blocken et al. (2006) allude to wind-driven-rain (WDR) effects, which are caused by micro-scale topography due to locally perturbed wind patterns. WDR becomes very important in heterogeneous terrain and on the micro-scale. As the Mae Sa Watershed is heterogeneous with regard to orography and topography, such WDR may be of importance within the catchment. According to Blocken et al. (2006) the geometry of the topographic feature, the position on the topography, wind speed and wind direction are factors that may influence micro-scale variations in rainfall distribution. Transferred to the present study site, it is assumed that convection cells are forced to locally rise along the hillslope, triggering rainfall on a small scale where no further uplift is possible. Where the slopes are very steep, convection cells may become encaged along the valleys, which is not necessarily along the ridges of the watershed. This phenomenon has been observed by the authors several times during the monitoring period.

Reports from a south Indian study site (Wilk and Andersson, 2000) showed that either slope or elevation dominated the rainfall pattern, depending on the direction of the monsoon (northeast or southwest). With about 4100 km² their study area was much larger than the Mae Sa watershed (77 km²) and a direct transfer of the finding is difficult. However, we investigated the effect of monsoon direction on rainfall pattern in an earlier stage of the data analysis but could not produce significant results. Although Wilk and Andersson (2000) were able to identify a pattern for clustered rain gauges, they emphasized the existence of complex rainfall pattern in their study catchment, because a correlation between the rainfall stations was not found. This again, is similar to the findings in the Mae Sa watershed. The results of the Spearman's rank correlation (Table

3.4) reassure the implications from an earlier stage of data analysis. There, regression kriging was applied to predict spatial pattern in the data set, but no variogram fitting was possible and the approach was not further followed. Singh et al. (1995) also faced the phenomenon of different rainfall amounts along a single elevation band from a study area in the ranges of the Himalaya. They figured that the orientation of the ranges explains the variations of rainfall amount along same elevation bands. The effect of aspect on rainfall was tested in the Mae Sa watershed, but it was not significant.

Data analysis and field observations speak for a combination of factors that affect rainfall in the Mae Sa watershed. As pinpointed by several authors (e.g., Blocken et al., 2006; Singh et al. 2006), next to orographical factors rainfall is most likely to be controlled by meteorological factors such as wind direction and wind speed. These, however, are too costly to measure and therefore non-suitable covariates for predicting rainfall distribution in a catchment. Probably the best alternative would be to run a simplified meteorological model to produce an average wind field. Simulated wind direction and wind speed could then be used as covariates in the regionalization of rainfall.

3.5 Conclusion

We analyzed data from a network of fourteen rain gauges in a 77 km^2 tropical mountainous catchment. Although the magnitude of rainfall peaks varied over the three years of our study, the temporal dynamics was always similar. Higher rainfall peaks were recorded in the beginning and at the end of the rainy season with a period of lower rainfall in between. While testing the necessary amount of stations to maintain within a 5% and 10% deviation interval of the total annual mean, a random reduction of the stations to up to nine remaining stations seemed to be acceptable for the Mae Sa catchment. This is considered as an extreme example, because further reduction may result in critical over- or underestimation of the annual mean and corrupt further analysis, such as simulations of water balance or else. The only terrain attribute affecting the distribution of rainfall was slope, but not elevation and aspect. We assume that relationships are blurred by meteorological variables, such as wind direction and wind speed. Those variables and their spatial distribution are not easily measured and therefore not suited as covariates for regionalization. Valuable alternatives could be modeling average wind fields with a simplified meteorological model, or testing the data set in a meteorological or hydrological model. This, however, was beyond the scope of our work and will be left for future studies.

Acknowledgements

We would like to thank Dr. Mario Hasler for his support during the analysis and Ittipon Sodsaard and Mai Tanarumgruang for their assistance during the data collection in the field. This research was funded by Deutsche Forschungsgemeinschaft (DFG) as a part of the Collaborative Research Programme SFB 564: Sustainable Land Use and Rural Development in Mountainous Regions of Southeast Asia.

4 Publication 2 - A three-component hydrograph separation based on geochemical tracers in a tropical mountainous headwater catchment in northern Thailand

C. Hugenschmidt[1], J. Ingwersen[1], W. Sangchan[1], Y. Sukvanachaikul[2], A. Duffner[1], S. Uhlenbrook[3,4], T. Streck[1]

[1]Institute of Soil Science and Land Evaluation, Biogeophysics (310d), University of Hohenheim, 70953 Stuttgart, Germany. [2]Dept. of Civil Engineering, Faculty of Engineering, Chiang Mai University, 50200 Chiang Mai, Thailand. [3]UNESCO-IHE Institute of Water Education, PO Box 2601 DA Delft, The Netherlands. [4]Section of Water Resources, Delft University of Technology, PO Box 5048, 2600 GA Delft, The Netherlands.

Hydrology and Earth System Science
(submitted)

Abstract

Land use change in the mountainous parts of northern Thailand is reflected by an increased application of agrochemicals which may be lost to surface and ground water. Due to the close relation between flow paths and the transport of contaminants within a hydrological system it is necessary to recognize and understand the dominant hydrological processes. So far, the vast majority of studies on runoff generation have been carried out in temperate regions. Tropical regions suffer from a general lack of data and little is known about runoff generation processes. To fill this knowledge gap, a three-component hydrograph separation based on geochemical tracers was carried out in a steep, remote and monsoon-dominated study site (7 km²) in northern Thailand. Silica and EC were identified as useful tracers and were applied to calculate the fractions of groundwater (similar to pre-event water), shallow subsurface flow and surface runoff on stormflow. K^+ was found to be a useful indicator for surface runoff dynamics and Ca^{2+} revealed some insight on groundwater behavior. Nevertheless, neither of both measures was applicable for the quantification of runoff components. Cl^- and further parameters (e.g. Na^+, K^+, and Mg^{2+}) were neither helpful for flow path identification, nor were the concentrations distinguishable among the components.

Groundwater contributed the largest fractions to stormflow (62% - 80%) throughout all events, followed by shallow subsurface flow (17% - 36%) and surface runoff (2% - 13%). Our results give important insights into the dynamics of the runoff processes in the study area and may be used to assess the transport pattern of contaminants (i.e., agrochemicals) in the area.

4.1 Introduction

Land use in the mountainous regions in northern Thailand has been intensifying during the last decades. Land use systems have changed in many regions from subsistence to market-oriented production. In the Mae Sa Watershed, a study area close to Chiang Mai, Chiang Mai Province, remarkable changes have been observed. The proportion of annual cash crops increased from 8% to 39% between 1974 and 2006, whereas rain fed rice production declined from 21% to 0.5% within the same time period (Schreinemachers and Sirijinda, 2008; Irwin 1976). Intensification of cropping system is accompanied by a higher input of agrochemicals to increase and secure yields. As a consequence, these agrochemicals may leach to groundwater aquifers and surface water contaminating the environment. According to Kruawal et al. (2004) water pollution is one of Thailand´s most critical environmental issues. Because the transport of agrochemicals within a hydrological system strongly depends on the dominant hydrological processes (i. e. Müller et al., 2006), it is important to understand the hydrology of the underlying system.

Studies on runoff generation during stormflow events have been the subject of many research approaches within the last decades. The dominance of groundwater as a main contributor to stormflow generation in a temperate study area was initially postulated by Sklash and Farvolden (1979) and has been further consolidated by subsequent studies (e.g. Peters and Ratcliffe, 1998; Hoeg et al., 2000, Uhlenbrook and Hoeg, 2003). Whereas studies on runoff generation processes in temperate regions are plentiful, Giertz et al. (2006) imply a lack of studies within tropical regions. Chuan (2003) also remarks a general lack of data on runoff generation processes within tropical regions, which applies especially for Southeast Asia.

While runoff generation processes are investigated under tropical conditions some alterations are expected due to different characteristics of rainfall (Bonell, 1993). Tropical rainfall patterns not only deviate from temperate ones, there is also a strong variability within the tropical belt. The amount of rainfall in the inner tropics may easily be double the amount received in the outer tropics (Table 4.1). Also, the seasonality of rainfall varies among the outer and inner tropics: Inner tropics receive rainfall throughout the whole year and outer tropics are characterized by distinct wet and dry seasons. Furthermore, differences of texture, mineralogy and structure between soils from temperate and tropical regions have been demonstrated by Hodnett and Tomasella (2002), which may affect runoff generation due to alteration in hydraulic soil conductivity. Schuler (2008) showed that the predominant soils in a mountainous area in Northern Thailand are Acrisols and Cambisols, which are characterized by a sharp decline of hydraulic conductivity with increasing depth. This influences infiltration and percolation, hence, the formation of subsurface flow components.

Although several studies have been carried out within tropical research sites (i.e. Elsenbeer and Lack, 1996; Elsenbeer, 2001; Dykes and Thornes, 2000; Goller et al., 2005), a comparison is difficult because of strong variations in spatial and temporal distribution of rainfall among the reported studies. To facilitate a comparison of those studies, they are grouped according to rainfall pattern, which is comparable to a separation into studies from the inner tropical belt and the outer tropical belt. A detailed list is given in Table 4.1.

Study	Location	Area size	Soils	Main vegetation	Annual rainfall (mm)	Dry season	Wet season	Dominant runoff processes/major runoff contributors
Dykes & Thornes (2000)	Northwest Borneo, Brunei,	Kuala Belalong Field Studies Centre, hillslope study	(orthis) Acrisols	mixed dipterocarp rainforest	4000-5000	All year rainfall, with highest rainfall from May to November		Subsurface stormflow/ return flow
Elsenbeer & Lack (1996)	Western Amazonia	La Cuenca, 0.75 ha	Ultisols, Inceptisols	rainforest	3300	All year rainfall, with totals below 100 mm month^{-1} from June to September and totals around 900 mm month^{-1} from December to March		Fast flowpaths: Overland flow, return flow
Elsenbeer & Vertessy (2000)	Western Amazonia	La Cuenca, 0.75 ha	Ultisols, Inceptisols	rainforest				Overland flow, near surface flow
Chaves et al. (2008)	Southwest Amazon Basin, Brazil	2 study sites at Rancho Grande 1.37/0.73 ha	Ultisols, Ocisols, Inceptisosl, Entisols	forest, pasture	2330	All year rainfall, with totals below 100 mm month^{-1} from June to August and higher values from September to May		Forest: througfall, pasture: overland flow
Negishi et al. (2007)	Malaysia	Bukit Tarek Experimental Catchment, 0.328 km^2	not specified	Rain forest	2800	all year rainfall , with peaks in May and November		Shallow groundwater and subsurface flow paths
Godsey et al. (2004)	Central Panama	Lutz creek, 9.37 ha; Conrad Trail Stream, 40.2 ha	Acrisol, Oxisols	Rain forest	2600	January to May	June – December	Strong overland flow influence for Lutz Creek, lower influence in Conrad Trail Stream
Wickel et al. (2008)	Eastern Amazonia, Brazil	2 subcatchments of Cumaro catchment 0.1 – 0.34 km^2	Ultisols	Mix of agriculture and secondary forest	2500	Dry spell from October to December, rainfall ≤ 50 mm day $^{-1}$)	Frequent rainfall between January and September	direct runoff from saturated source areas
Goller et al. (2005)	Ecuador	3 micro catchments 0.08-0.13 km^2	Dystrudepts, Eutrudepts	Tropical rainforest	2182	All year rainfall, wettest month June (281 mm), driest month November ~80 mm)		Vertical& lateral pathways, event water dominated stormflow

Table 4.1: Comparison of studies on runoff generation carried out in inner and outer tropical regions (information is given as available from specific literature).

In contrast to the dominance of baseflow during stormflow generation in most temperate regions, Elsenbeer and Lack (1996) confirmed the importance of overland flow during stormflow generation in a small Amazonian watershed. Their study site receives 3300 mm mean annual precipitation and has a period with lower precipitation rates between June and September. They found that overland flow was generated over the whole year, independent from the season, and that overland flow often occurred as return flow (from soil pipes). Subsequent investigations in the same region indicated that near-surface flow paths are important contributors to runoff generation, but are difficult to separate into overland flow and pipeflow because they are coupled and overlap in response time (Elsenbeer and Vertessy, 2000). A review of Elsenbeer (2001) also emphasized the importance of near-surface and overland flow paths in Acrisol landscapes in tropical rainforests for runoff generation. Chaves et al. (2008) identified that groundwater and shallow soil components only delivered 43% of the annual discharge in the south-western Brazilian Amazon basin, which is congruent with the suggestions of Elsenbeer (2001). Mean annual rainfall within their study site is 2330 mm, with a period of lower rainfall from June to August. Wickel et al. (2008) also conducted a study on runoff generation in Brazil (2500 mm annual precipitation, dry season from October to December) and revealed direct runoff from saturated source areas in the catchment as a main driver for runoff generation during stormflow. A further hint on the importance of event water is given by Goller et al. (2005). They found that two of three storm events in a tropical mountainous rain forest in Ecuador were mainly driven by event water. The Ecuadorian catchment receives an annual mean of 2182 mm rainfall, where November is the driest month (~80 mm). Godsey et al. (2004) investigated runoff processes of a small, forested area in central Pánama (Lutz Creek). There, mean annual rainfall amounts to 2600 mm and is characterized by a dry season typically lasting from January to May. They also outlined a strong overland flow signal in their stream flow but assigned certain variation in intensity between two study areas. Nevertheless, those results correspond with suggestions from Elsenbeer and Lack (1996). Although a forested study area in Borneo, Southeast Asia, presented by Dykes and Thornes (2000) gains considerably higher amounts of rainfall (4000-5000 mm per year), they identified overland flow as rare and its occurrence likewise as return flow. Further hints on the importance of shallow groundwater and subsurface flow paths, such as preferential flow, can be found in the publication by Negishi et al. (2007). Within their Malaysian study site, rainfall reaches an annual mean input of 2800 mm with peaks in May and November.

Albeit most of the studies agree with the importance of overland flow or shallow subsurface flow on runoff generation within tropical areas (Table 4.1), the on-going dominant processes are still among the most difficult and least understood (Montanari et al., 2008). However, only very few studies investigate hydrological processes in regions, which are characterized by bimodal rainfall distribution, a distinct dry season (rainfall ≤ 20 mm month^{-1}) and less than 2000 mm mean annual rainfall (Table 4.1). None of the studies listed above, was carried out in regions where rainfall is completely absent or close to zero over several months. A West African based study presented by Giertz and Diekkrüger (2003) may close this gap. They investigated runoff generation in a catchment in Benin where mean annual rainfall reaches 1100 mm and occurs within a unimodal rainy season from May to October. Interflow was identified as the dominant runoff generating process along the hillslope. Later, Giertz et al. (2006) stated that shallow subsurface flow and interflow were identified in most studies as predominant runoff processes under tropical forests. This is underlined by studies listed in Table 4.1.

The Phang Khum Experimental Watershed in Northern Thailand was subject to studies on overland flow enhancement with regard to soil erosion, conducted by Ziegler et al. (2000). The catchment underlies a bimodal rainfall regime with annual totals between 1200 and 1300 mm. They found that overland flow occurred very fast under disturbed soil conditions (i.e. soil compaction along unpaved roads or foot paths and agricultural areas). Horton overland flow was monitored on initially dry soils immediately after the onset of artificial rainfall, whereas less compacted agricultural areas required a higher amount of rainfall to produce overland flow. Kahl et al. (2007) suggested the importance of interflow with regard to transport of solutes in the Mae Sa Noi subcatchment, which is close to the study area of Ziegler et al. (2000).

The preceding studies of Kahl et al. (2007, 2008, 2010) motivated the current investigation. The importance of interflow was suggested, due to concentration peaks of monitored pesticides along the recession limb of the hydrograph. This pattern was seen as transport of these compounds by a delayed flow component, i.e. interflow or lateral preferential flow. To elaborate the suggestions, the presented study aims to identify and quantify the dynamics of runoff generation in a narrow and steep V-shaped tropical catchment, characterized by a bimodal rainfall distribution with distinct wet and dry season. The suitability of several tracers for hydrograph separation in such tropical environments needs to be tested and hydrograph separation should be applied to quantify and trace the dynamics of runoff components.

Despite the rainfall variability between inner and outer tropics, no clear difference of runoff generation processes can be withdrawn from available literature, so far. Additional absence of research on runoff generation in steep, tropical catchment areas (Dykes and Thornes, 2000; Chapell, 2010), highlights the importance of this paper to improve the knowledge on hydrological processes in such areas.

4.2 Materials and methods

4.2.1 Study area

The study area is a part of the Mae Sa watershed (77 km²), which is located 35 km northwest of Chiang Mai in northern Thailand.

Measurements were conducted in the Mae Sa Noi subcatchment (7 km²) (Figure 4.1), which is a very narrow and steep V-shaped (Figure 4.1b) valley with an elevation ranging from 850 to 1560 m.a.s.l.

The creek shows mountainous characteristics with a rocky streambed and an average bed slope of 11% over a length of 2.6 km. Soils are mainly Acrisols and Cambisols (Figure4.1b) on paragneiss and granite. Both soil types show a sharp decrease of hydraulic conductivity with increasing depth (Schuler, 2008). Spohrer et al. (2005) classified a soil profile in the sub-catchment as an umbric Acrisol: bulk density (1.1-1.3 g cm^{-3}) and clay content (41 -51%), which increased within the first 100 cm. While the soil porosity showed a constant decrease (58 – 52%) over depth, hydraulic conductivity varied little. Within the first 20 cm, hydraulic conductivity dropped from 1.04 cm d^{-1} to 0.54 cm d^{-1}. A slight increase to 0.7 cm d^{-1} at 40 cm was observed, followed by a reduction to 0.2 cm d^{-1} in the layer below (Spohrer et al., 2005). However, an increase of water content between 45 and 70 cm depth was reported by Kahl (2003) in the frame of a plot scale experiment. During some early irrigation experiments in the litchi orchard, soil moisture was monitored not only within the experiment, but also for control fields, which remained undisturbed during the experiments. Soil moisture contents ranging from 16 to 30% were registered at depths of 50 cm during that time (Jantschke, 2002).

Kahl et al. (2007) observed macropores with diameters between 1-10 cm mainly at depths of 60-90 cm at the same hillslope and observed a decrease in the areal density of macropores dependent on depth.

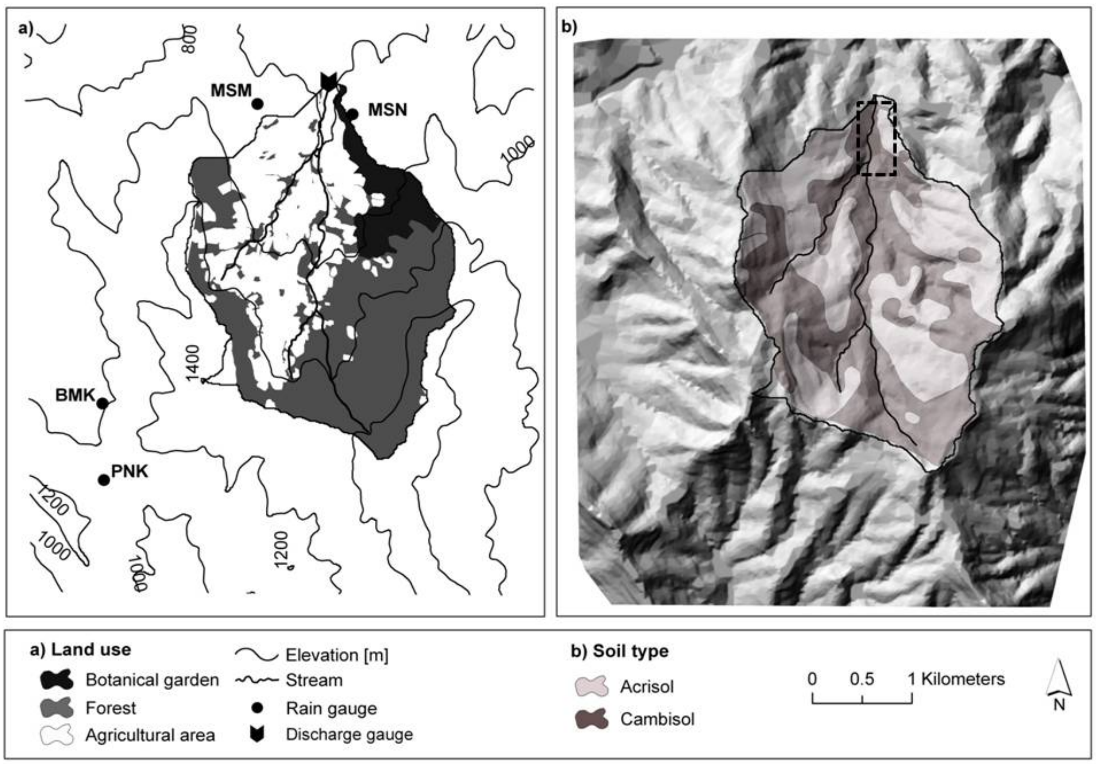

Figure 4.1: Mae Sa Noi subcatchment with (a) measurement devices (MSM, MSN, BMK and PNK), land use in 2008 (modified after M. Lippe, SFB 564, Subproject C4.1) and (b) soil types (modified after Schuler et al., 2008), topography and sampling area (black square).

The main vegetation types in Mae Sa Noi are secondary forest and agricultural crops (Figure 4.1a). The dry dipterocarp forest consists of a variety of evergreen and deciduous tree species. It also hosts scattered tree plantations with *Tectona grandis*, *Litchi chinensis* and *Mangifera indica*, for example. Around 30% of the Mae Sa Noi area is covered by agricultural land, which can mainly be split into field crops (30%) and litchi (50%) (Schreinemachers and Sirijinda, 2008). Major field crops are cabbage and bell pepper, which are cultivated all year round and are irrigated if needed.

The sampling site itself was located along a hill slope in the lower catchment area (Figure 4.1b), which is covered by an abandoned litchi orchard. This orchard was abandoned in 2006 and was not agriculturally used anymore since that time. This implies that no fertilizers had been applied several months before and during the sampling period. The climate in the area is controlled by the monsoon with distinct wet (May to October) and dry (November to April) seasons and a mean annual rainfall of 1200 mm. Based on mean annual discharge of 623 mm a^{-1} (long term runoff coefficient 0.52) evapotranspiration results in 577 mm a^{-1}. The average annual air temperature is 21°C and relative humidity ranges between 40% and 100%.

4.2.2 Measurements

Within the Mae Sa Noi subcatchment a weather station (MSN), a rain gauge (MSM) and a discharge gauge were operated. Two additional rain gauges (BMK and PNK) were close-by and covered the spatial variability of the rainfall (Figure 4.1a). During events, the rainfall data were extracted from stations closest to the discharge flume, MSN and MSM (Figure 4.1a). To ensure the data quality, or to fill gaps in case of e.g. a device failure, rainfall records were compared with the closest stations, BMK and PNK (Figure 4.1a).The variability among the stations was evaluated in terms of representativeness for each rainfall event during the field experiments by cross-correlation coefficients (CCR). CCR was computed among the rain gauges and between each rain gauge and discharge measurement. The analysis was based on monthly data series with a resolution of 10 minutes resulting in CCR per month and station. If more details on CCR between stations were needed, a higher temporal resolution was applied, i.e. days or single events. The mean annual rainfall input for the Mae Sa Noi subcatchment was based on records of the stations MSN and MSM.

Water level was measured at a fixed, rectangular cross section (Figure 4.1a) using an ISCO ultrasonic sensor at the discharge gauge. A stage-discharge rating curve was established by salt dilution measurements for different water levels in order to convert water level into discharge.

During September 2007 (E1), October 2007 (E2) and October 2008 (E3) three event-based field measuring campaigns were carried out to investigate runoff generation in the Mae Sa Noi subcatchment. In the frame of another sampling campaign in August 2009 (E4) and September 2009 (E5) two additional events were sampled (Duffner, 2010).

4.2.3 Sampling of the components

During the measuring campaigns, the followings components were sampled: rainfall, surface runoff, shallow subsurface flow, groundwater and stormflow. The terms component and end-member may be used interchangeable in the following text. Surface runoff (SUR) is defined as the component which flows above soil surface during and/or shortly after events. Shallow subsurface flow (SUB) is defined as water that seeps from the soil at the hill slope foot along the riverbed (Figure 4.2). Shallow subsurface flow is assumed to laterally flow along the hill slope between the bedrock and the soil cover, being forced to ex-filtrate at the end of the slope (Figure 4.2).

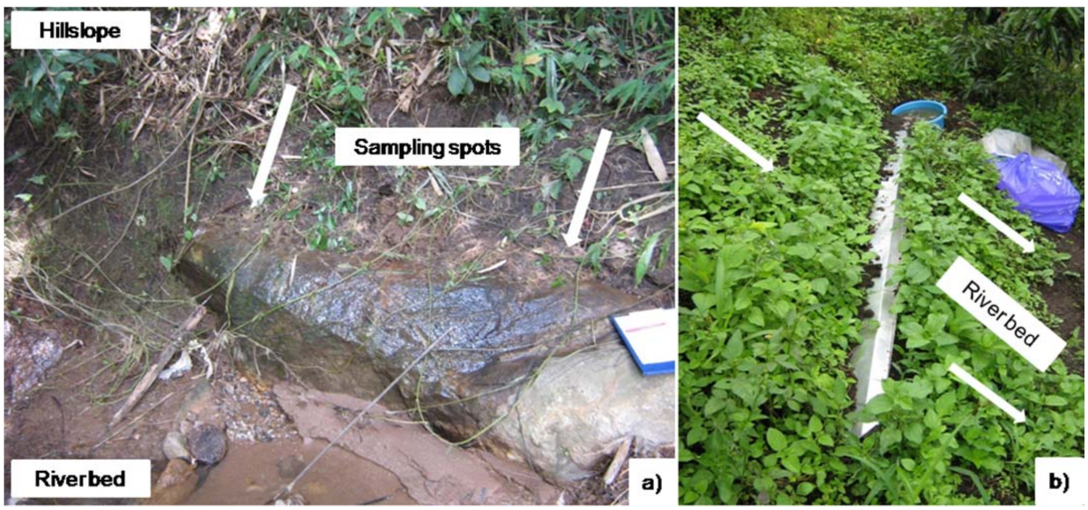

Figure 4.2. Sampling of surface runoff (SUR) and (shallow) subsurface flow (SUB) at the study site (black square, Figure 4.1b). Left picture (4.2a) shows the seep, which is defined as subsurface flow, right picture (4.2b) shows one of the steel gutters, which were used to measure surface runoff along the hillslope.

Because of wet and dry seasons, the subsurface flow is temporal (episodic) and not active throughout the whole year. Once established, it appears until rainfall events are intermittent and it is assumed to be mainly fed by macropore flow in the unsaturated zone along the hill slope. Discharge during the rainy season is assumed to be sustained by a mixture of groundwater and contributions from saturated zones. This mixture is named groundwater (GW) component within this study and is represented by the average concentration measured in between events. It must be stated that a splitting of both contributors is not possible and that the contributed proportions may vary in an unknown amount. Since the subcatchment is very steep and valley bottoms or riparian zones are rare, groundwater must originate from deeper soil layers and/or fissured and fractured rocks. The saturated zones may be distributed across the subcatchment and are most likely highly dynamic. All named components are assumed to generate stormflow (SF) in varying magnitudes.

Rainfall samples were collected in a bulk collector and extracted immediately after or during a rainfall event. Surface runoff was collected along the hill slope close to the discharge gauge (Figure 4.1a) by stainless steel gutters. These metal gutters were installed slope-parallel with a gentle inclination to route the water towards a bulk collector at the end of each gutter (Figure 4.2b). The samples were extracted during or immediately after rainfall events. In 2009, two additional gutters at different positions extended the installation across the hill slope to cover the spatial variability of surface runoff. The distance between those gutters ranged between 50 and 100 m, covering a stretch of roughly 300 m along the slope (Figure 4.1b). A mixture of surface runoff with return flow along the hill slope could not be excluded, although the samples were extracted directly during or after rainfall events.

Shallow subsurface flow was sampled at three spots close to the discharge gauge (Figure 4.1b) along the river banks (Figure 4.2a). The soil cover above the bedrock at the sampling points was around 50 cm. Samples were collected with a resolution of 15-20 minutes during events. Additional samples were taken before, after and randomly in between events.

The hydrochemical signature of the groundwater end-member was obtained from samples collected during rainless periods and directly prior stormflow events from the stream. In order to apply representative end-member signature, the average concentration of all samples related to an event was defined as groundwater component. During the rainy season, sporadic groundwater samples were collected along the main reach.

Stormflow samples were obtained every 5-10 minutes and are considered as a mixture of all components mentioned above.

Electrical conductivity (EC) of each sample was measured in-situ using a conductivity meter (WinLab Data Line, Windhaus Labortechnik, Germany). The analysis of major ions (Cl^-, NO_3^-, SO_4^{2-}, NH_4^+, Na^+, K^+, Ca^{2+}, and Mg^{2+}) was carried out in the laboratory at the Department of Chemistry, Chiang Mai University in Thailand using ion chromatography (Ion chromatograph, Metrohm). Silica samples were analyzed by ICP-OES (Inductively Coupled Plasma - Optical Emission Spectrometry, Perkin Elmer). Detection limits for each ion and for silica are listed in Table 4.3. Analytical errors of silica concentration were specified as ±10%, those of the major ions as ±7% (personal communication, Department of Chemistry, Chiang Mai University).

4.2.4 Hydrograph separation

To divide the hydrograph into its flow components, a three-component hydrograph separation was performed. The chemically-based hydrograph separation relies on the principle of mixing, where equations of continuity and mass balance govern the quantity of tracer flow. The following equations define a three-component separation (Ogunkoya and Jenkins 1993)

$$\begin{aligned} Q_T &= Q_{GW} + Q_{SUB} + Q_{SUR} \\ Q_T C_T &= Q_{GW} C_{GW} + Q_{SUB} C_{SUB} + Q_{SUR} C_{SUR} \end{aligned} \qquad \textit{(Eq. 4.1)}$$

where Q_T, Q_{GW} and Q_{SUB} and Q_{SUR} (Q in $m^3\ s^{-1}$) represent volumes of the measured discharge (Q_T), groundwater (*GW*), subsurface flow (*SUB*) and surface runoff (*SUR*) (see definition in Chapter 4.2.3), while C_T, C_{GW}, C_{SUB}, C_{SUR}, are the equivalent solute concentrations ($mg\ L^{-1}$) or electrical conductivities ($\mu S\ cm^{-1}$). The method is based on several assumptions, which are described in the literature (e.g. Sklash and Farvolden, 1979). Note, however, that the method is only applicable if the components are chemically distinguishable and if tracers are conservative or their fluctuations measurable.

Genereux (1998) showed a detailed example of the propagation of uncertainty for a two-component hydrograph separation including uncertainties of laboratory analysis. The propagation of uncertainty for a three-component hydrograph separation was derived from the demonstrated equations according to Genereux (1998) and uncertainties of the end-members and laboratory analysis were included.

4.2.5 Mixing plots

Mixing plots, as shown in Christophersen et al. (1990), were used to explore the physico-chemical extends of stormflow during an event. The basic assumption of such mixing plots or mixing triangles is that discharge during events is generated by different runoff components. Each of those runoff components must be chemically distinguishable from the others and must be involved in runoff generation. Those components provide a range of concentration of hydrochemical compounds in the shape of a triangle. Since the stormflow was assumed to be a mixture of the chosen components, the hydrochemical concentrations measured during stormflow were expected to be within the boundary of this triangle. If this is true for the monitored data, the chosen components are presumably representative, as they cover the hydro-chemical pattern of the stormflow. If the stormflow concentration is not framed by the concentration of the components, the selected components are either non-conservative, non-distinguishable or non-representative.

4.3 Results

4.3.1 Rainfall records

Annual rainfall and the amount of rainy days at the stations MSM, MSN, BMK and PNK are given in Table 4.2. Rainfall differed much in its temporal and spatial distribution: among all three observed years, 2008 had the highest spatio-temporal variability. Due to the distinct spatial variability of rainfall, some discharge peaks at the flume were observed while no rainfall was measured at the close-by rain gauges (MSN and MSM). During E1, there was only very little rainfall recorded at the lower stations (MSN and MSM, 0.7 mm).

Table 4.2: Annual rainfall and the number of rainy days recorded at four weather stations (For the location of the stations see Figure 4.1).

Station	2007		2008		2009	
	[mm]	[days]	[mm]	[days]	[mm]	[days]
PNK	1222	122	1311	139	1123	105
BMK	1400	121	1426	143	847	70
MSM	1228	118	1137	131	785	98
MSN	1309	132	761	78	719	91
Average	1289	115	1159	123	869	91
Standard deviation	83	6	290	30	178	15

To identify whether the data transfer between the stations is reasonable, the temporal resolution of the CCR was decreased. Single rainfall events between all four stations recorded two days prior and after E1 were used as input data for the CCR. For the single events within these 4 days, CCR ranged between 0.6 and 0.8. Hence, the transferability of rainfall data between the upper (BMK and PNK) and lower (MSM and MSN, Figure 4.1) rain gauges was considered as representative and was applied for the evaluation of E1. Ultimately, the cross-correlation between the two lower rain gauges (MSM and MSN) and measured discharge resulted in CCR = 0.6 with a lag time of 60 minutes between onset of rainfall and discharge peak for September and CCR = 0.7 for October. Discharge and rainfall from the upper two gauges (BMK and PNK) correlated well after a lag time of 80 minutes (CCR = 0.6).

4.3.2 Event-based measurements

Rainfall during E1 had a low intensity with a total amount of 6.9 mm in 50 minutes and was recorded only at the stations PNK and BMK (Figure 4.3a). Discharge peaked to 0.42 $m^3\ s^{-1}$ ($60\ L\ s^{-1}\ km^{-2}$) within 20 minutes and caused a decline in EC by 36 $\mu S\ cm^{-1}$ within the same period (Figure 4.3c). Major anions showed similar dynamics. The drop of silica and the rise of Cl^- prior the event were probably induced by an earlier event. A clear decrease in the concentration of Cl^- and silica coincided with the rise of the hydrograph (Figure 4.3b). The concentration of Ca^{2+} (Figure 4.3c) was reduced by 10 $mg\ L^{-1}$along the recession limb. Na^+, Mg^{2+} and K^+ behaved similar during the event (Figure 4.3c).

Event E2 was monitored a few days later, on October 9, 2007. Total rainfall yielded 17.2 mm in 40 minutes and was recorded at all four stations. The discharge of E2 rose to 0.46 $m^3\ s^{-1}$ ($65.7\ L\ s^{-1}\ km^{-2}$) (Figure 4.4a) after 60 minutes of rainfall. EC (Figure 4.4c) rapidly sank by 53 $\mu S\ cm^{-1}$. Silica concentrations were lowered by 4 $mg\ L^{-1}$ (Figure 4.4b). The dynamics of the major cations are given in Figure 4.4c. A decrease in concentration with the beginning of the peak flow was observed for all measured ions. The sharpest drop was monitored for Ca^{2+}, (15 $mg\ L^{-1}$), the lowest for Na^+. The most significant increase was observed for K^+ (10 $mg\ L^{-1}$). Initial concentrations were reached by all major cations and Cl^-, but not by silica.

Compared to surface runoff, major ion concentrations and EC values of shallow subsurface flow were stable during E1 and E2 (Table 4.3). Only silica concentrations varied remarkably.

In fact, silica concentration of shallow subsurface flow showed high fluctuations between samples from rainy days (7.5 ± 1.1 $mg\ L^{-1}$) and dry days (19.4 ± 0.9 $mg\ L^{-1}$).

During the field campaign in 2008 (E3), only surface runoff and groundwater could be sampled. Shallow subsurface flow was not activated at the time of sampling because of late onset of the rainy season. EC values dropped by 40 µS cm^{-1} with rising discharge.

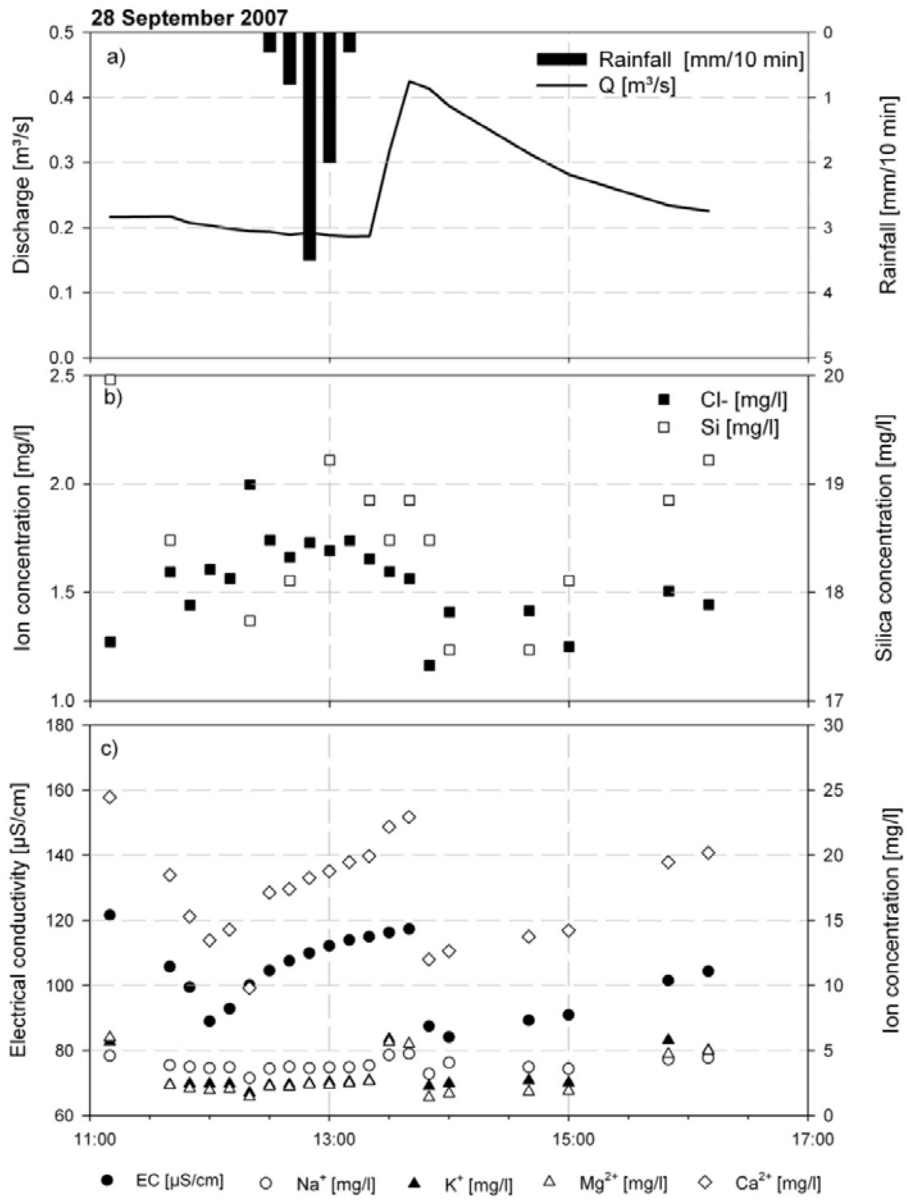

Figure 4.3: Event E1 on September 28, 2007: a) discharge and rainfall, b) silica and Cl^- concentrations, and c) concentrations of Na^+, Mg^{2+}, K^+ and Ca^{2+} and EC values.

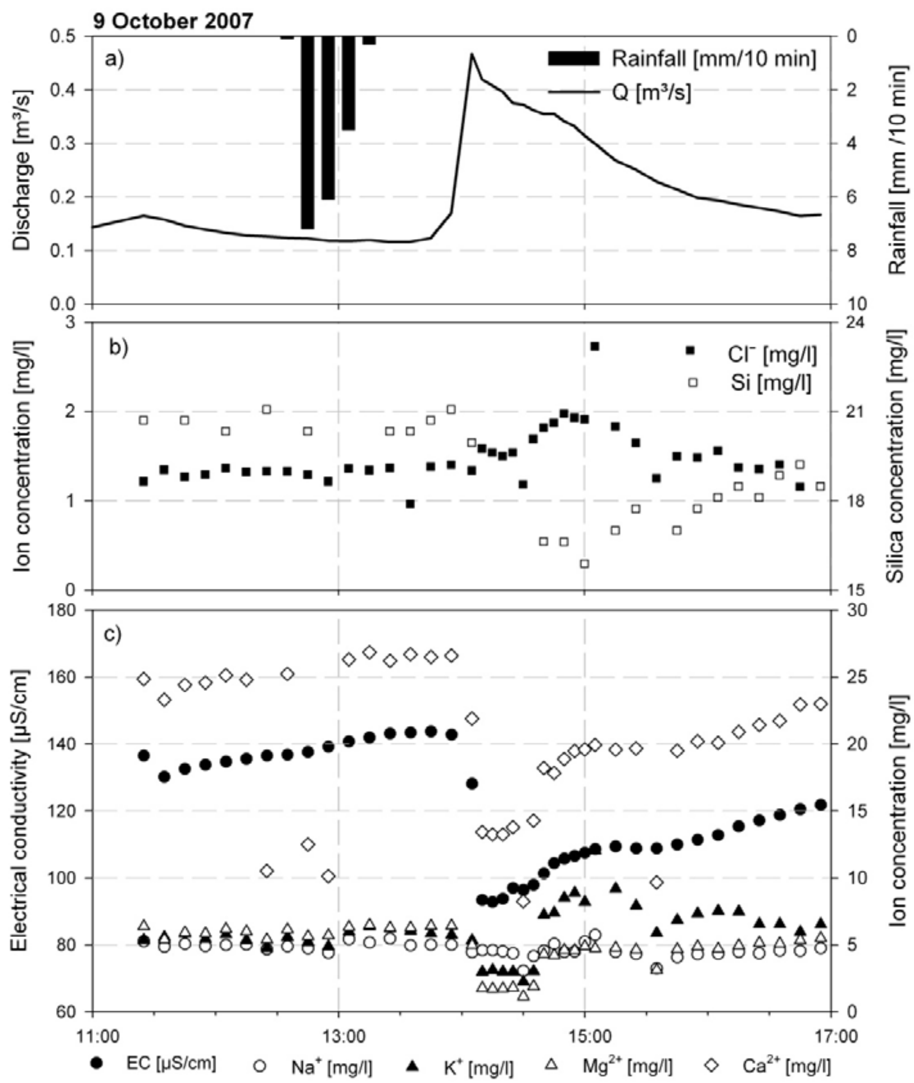

Figure 4.4: Event E2 on October 9, 2007: a) discharge and rainfall, b) silica and Cl^- concentration, and c) concentrations of Na^+, Mg^{2+}, K^+, Ca^{2+} and discharge.

During the two events in 2009 (E4 and E5), only EC and silica concentration were measured. For both events, rainfall data from the closest stations (MSN and MSM) were available. E4 was initiated by 10.6 mm rainfall. Discharge slowly increased from 0.1 m^3 s^{-1} to 0.28 m^3 s^{-1} (40.0 L s^{-1} km^{-2}) (Figure 4.5a). Silica concentration declined by 2.5 mg L^{-1} (Figure 4.5b). The reduction of EC values occurred gradually (Figure 4.5b) and reached 139 µS cm^{-1} after 50 minutes.

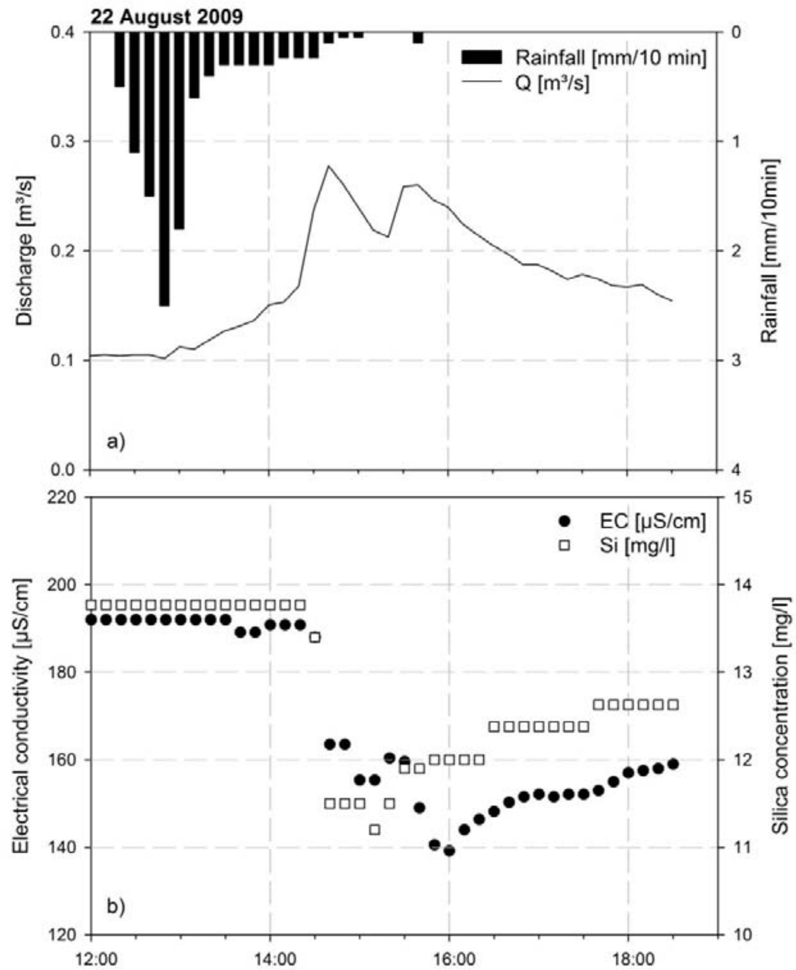

Figure 4.5: Event on August 22, 2009 (E4) showing a) rainfall and discharge and b) EC values and silica.

On September 15, 2009, E5 received 17.6 mm rainfall within 70 minutes. Discharge peaked with 0.6 m³ s^{-1} (85.7 L $s^{-1}km^{2-1}$) within 60 minutes (Figure 4.6a). During the rise of the hydrograph, EC and the silica concentration fell by 35 µS cm^{-1} 3 mg L^{-1}, respectively (Figure 4.6b).

The ionic balance of applied samples was checked according to Appelo and Postma (2005). The results showed gaps of up to -30%, which are explained by missing HCO_3^- analysis.

For each component, mean and standard deviation of concentrations are listed in Table 4.3. EC values of stream flow were generally higher in 2009 and silica had lower concentrations in 2009.

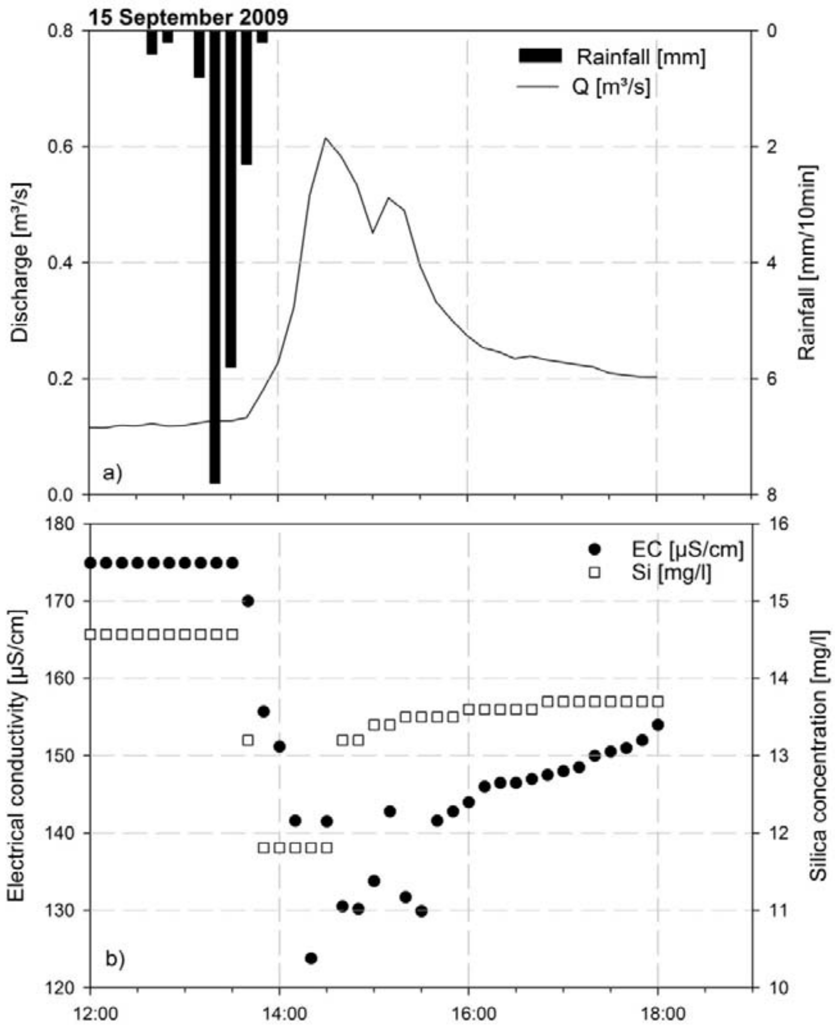

Figure 4.6: Event on September 15, 2009 (E5) showing a) rainfall and discharge and b) EC values and silica.

Table 4.3 reveals that EC values of shallow subsurface flow were lower than the ones of surface runoff, which was also the case for most major ions and silica. Most major ions, which are commonly used for hydrograph separation (i.e. Cl^-) were hardly distinguishable between the components. Considerable differences were identified for K^+ and Ca^{2+}. The Ca^{2+} concentration in groundwater for E1 and E2 showed good correlations with EC ($0.8 \leq CCR \geq 0.86$) and silica ($0.8 \leq CCR \geq 0.82$).

Table 4.3: Electrical conductivity and ion concentrations in water samples of baseflow, interflow, surface runoff and rainfall taken during September - October 2007 and August - September 2009.

		Groundwater (n=20/15)*	Shallow subsurface flow (n=20/10)*	Surface runoff (n=7/7)*	Rainfall (n=4/0)*
		Mean ± standard deviation			
	*DL***	*2007*			
EC [µS/cm]	-	135.86 ± 9.22	29.35 ± 1.04	37.95 ± 23.21	9.48 ± 5.88
Silica [mg/l]	0.012	19.89 ± 1.10	14.64± 6.18	11.84 ± 0.88	n.a.
Cl^- [mg/l]	0.011	1.31 ± 0.12	0.07 ± 0.03	0.97 ±0.78	0.42 ± 0.47
NO_3^- [mg/l]	0.009	2.45 ± 0.46	3.39 ± 0.94	5.29 ± 3.29	0.69 ± 0.37
SO_4^{2-} [mg/l]	0.007	1.41 ± 0.18	0.13 ± 0.02	2.29 ± 1.54	0.83 ± 0.72
Na^+ [mg/l]	0.008	4.90 ± 0.36	4.62 ± 0.79	0.27 ± 0.19	0.29 ± 0.34
NH_4^+ [mg/l]	0.014	n.d.	n.d.	5.52 ± 3.17	0.72 ± 0.23
K^+ [mg/l]	0.040	5.46 ± 0.85	1.72 ± 0.27	7.62 ± 3.47	0.39 ± 0.24
Ca^{2+} [mg/l]	0.030	22.90 ± 5.63	1.20 ± 0.31	1.55 ± 0.8	0.52 ± 0.28
Mg^{2+} [mg/l]	0.031	5.89 ± 0.95	0.16 ± 0.02	0.63 ± 0.37	0.12 ± 0.04
		2009			
		(n= 24/24)*	**(n=12/7)***	**(n=6/6)***	**(n=3/3)***
EC [µS/cm]	-	184.78± 14.09	35.17±5.60	58.43±12.41	5.35±2.51
Silica [mg/l]	0.012	14.7± 0.60	9.06±1.71	1.32±0.15	0.09±0.01

(n.a.: not available; n.d.: not detected; *numbers of silica samples vary and are given on the second position. ** DL: Detection limit.)

4.3.3 Mixing plots

Mixing diagrams were plotted for E1, E2, E4 and E5 based on EC and silica concentrations (Figure 4.7). Event E1 (Figure 4.7) was framed by SUR, SUB and GW, although some samples were above the GW end-member concentration

For the remaining events, E2 (Figure 4.7b), E4 (Figure 4.7c) and E5 (Figure 4.7d), all concentrations were satisfactory enclosed by the end-members. Some stormflow samples of E2 were very close to groundwater concentration. E4 and E5 came up with some outliers.

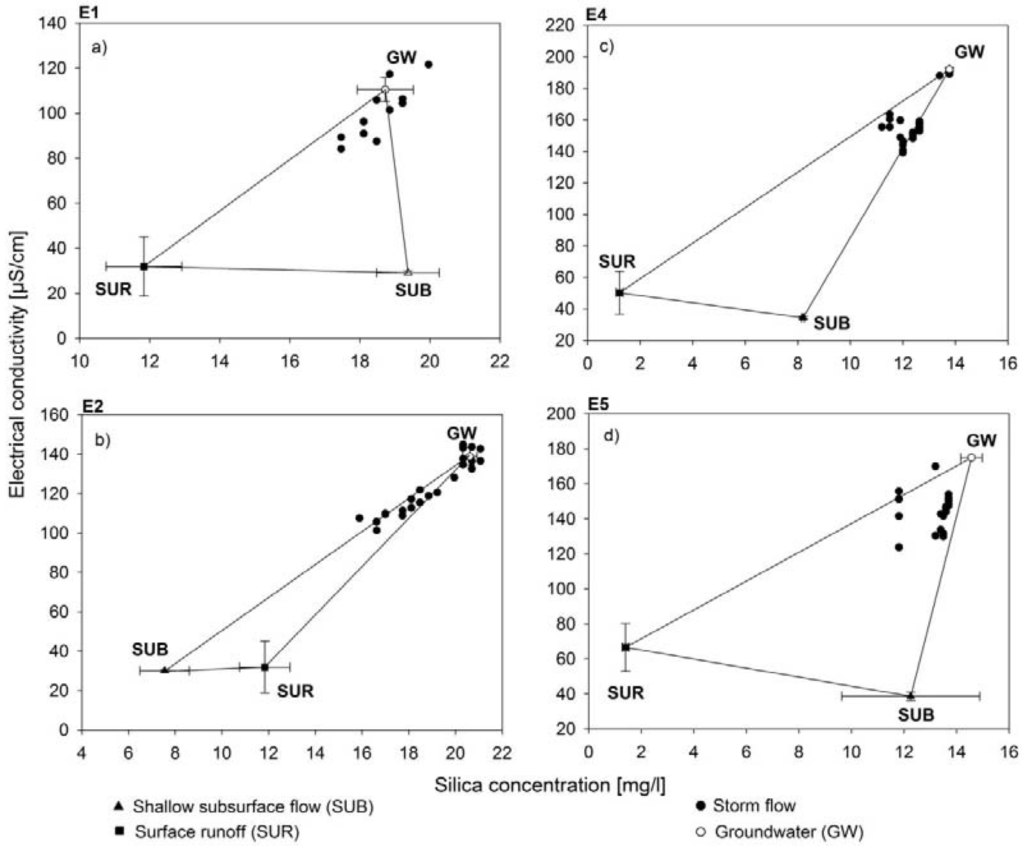

Figure 4.7: Hydrochemical mixing diagrams for a) September 28, 2007 (E1), b) October 9, 2007 (E2), c) August 22, 2009 (E4) and d) September 15, 2009 (E5) based on end-members of shallow subsurface flow (SUB), surface runoff (SUR) and groundwater (GW). Bars indicate standard deviations

4.3.4 Hydrograph separation

A three-component hydrograph separation based on silica concentrations and EC values was performed for E1, E2, E4 and E5 (Figure 4.8). Due to absence of the shallow subsurface flow component, E3 was separated into two components, resulting in a dominance of groundwater, which will not be further assessed in this study.

Major ions were not applied for the three-component separation as the concentrations and/or the differences between the components were too low. Nevertheless, the results will be used for a qualitative assessment in the discussion later on.

During event E1 (Figure 4.8a), the discharge was mainly composed of groundwater (62%) and shallow subsurface flow (36%), while the fraction of surface runoff was very small (2%). Groundwater was the first component which rose, followed by shallow subsurface flow. A first peak of surface runoff coincides with the one of groundwater. E2 received 67% of groundwater (Figure 4.8b). The pronounced shoulder of the recession limb was mainly constituted by groundwater and to a smaller extent by shallow subsurface flow and surface runoff. Compared to the groundwater peak, shallow subsurface flow (20%) was slightly delayed. Surface runoff (13%) showed a peak during a gentle shoulder along the hydrograph.

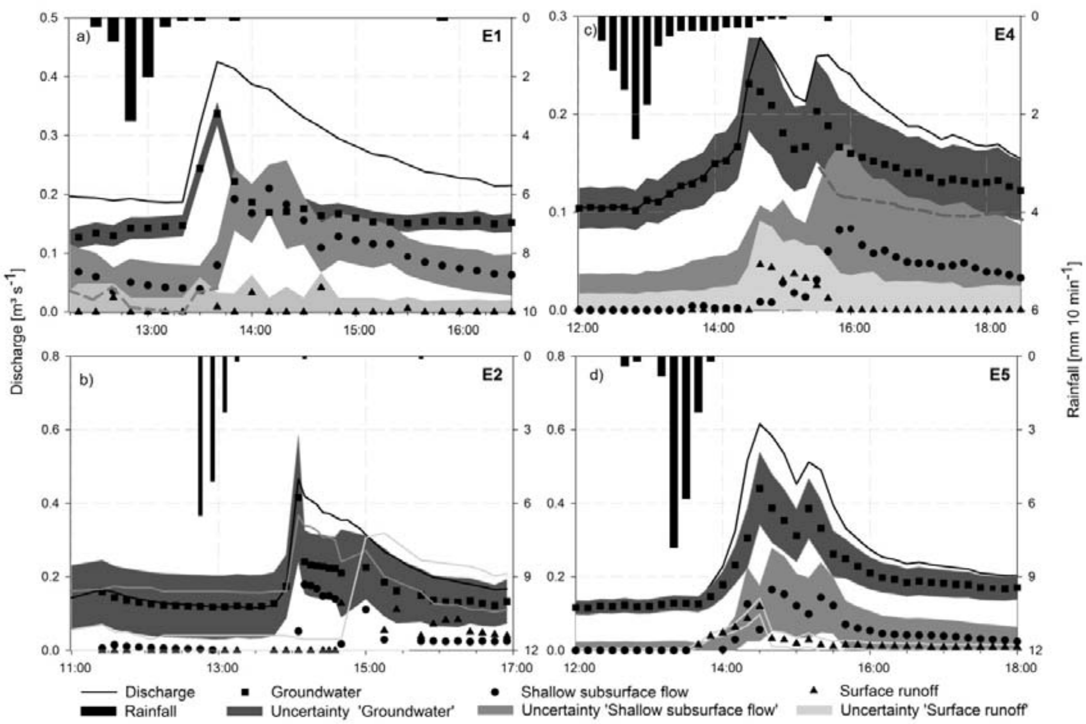

Figure 4.8: Results of the three-component hydrograph separation and uncertainty bands for the monitored events: a) E1 (September 28, 2007), b) E2 (October 9, 2007), c) E4 (August 22, 2009) and d) E4 (September 15, 2009). Uncertainty is depicted with lines or areas, depending on overlay and intersections.

To test the reliability of the separated groundwater fractions for E1 and E2, a two-component hydrograph separation based on Ca^{2+}, EC and silica was conducted. Besides groundwater as an end-member, shallow subsurface flow was chosen as an additional component. All approaches (Ca^{2+}, EC and silica) delivered similar fractions for the groundwater component, ranging between 82% (silica), 84% (EC) and 87% (Ca^{2+}) for E2.

The fluctuations among the results were also small for the separation of E2, for which 68% (silica), 74% (EC) and 76% (Ca^{2+}) were computed as groundwater contribution.
For the event in October 2008 (E3), no three-component hydrograph separation was carried out, because shallow subsurface flow was not active at that time.
In 2009, both runoff events were dominated by groundwater (E4: 80%; E5: 76%). While the role of surface runoff (2%) was marginal (Figure 4.8c), shallow subsurface flow contributed some 18 % to stormflow. Next to the groundwater component, shallow subsurface flow contribution was identified with 17% and surface runoff with 7% (Figure 4.8d).
The derived uncertainties for each fraction are depicted in Figure 4.8. Overall uncertainties are satisfying and do not weaken the order of contribution of the flow components. The errors of surface runoff are particularly high towards the end of E2. These errors and the uncertainties of shallow subsurface flow within E4 were the largest one within the analysis.

4.4 Discussion

Geochemical tracers are common tools for chemically based hydrograph separations and are applied in different regions of the world. Nevertheless, application of certain geochemical tracers in specific regions may be limited by environmental characteristics such as geology, climate, soil or land use.

4.4.1 Hydrochemical analysis and hydrograph separation

Silica and EC are commonly used tracers, and their suitability has been proven for tropical regions (Elsenbeer et al., 1994, Mul et al., 2008) and for study sites in the temperate climate zone (i.e. Hoeg et al., 2000). These studies reported a drop in EC values and silica concentration with the onset of the stormflow, which is consistent with the presented data. The decline can be explained by a mixture of groundwater with surface runoff and shallow subsurface flow, of which both show lower EC values and silica concentrations than groundwater. Whereas EC is a variable which is correlated with the ion concentration of solutes, silica originates mainly from weathering processes. Therefore, water from deeper sources is considered to have higher silica concentration (e.g. Scanlon et al., 2001), because of longer residence and contact time. This is well represented in the data as silica concentrations in groundwater were the highest among the components. It supports the assumption, that groundwater is fed by deeper soil layers, from fissures and fractures in the rock and saprolite zones in the catchment. Both tracers are well distinguishable among the components.

Besides EC and silica, K^+ has been described in literature as suitable tracer for hydrograph separation, particularly to divide overland flow and shallow subsurface flow from groundwater. Sharp rises of K^+ with the onset of fast flow components were reported from tropical (e.g. Elsenbeer et al., 1995, Kinner and Stallard, 2004, Mul et al., 2008) and temperate study sites (Uhlenbrook et al., 2008). Within the present study, a similar pattern was present during E2: K^+ concentration increased shortly after peak flow. Additional indicators that favour K^+ as a suitable tracer for surface runoff are given by the fact that throughout the monitored period, K^+ values in surface runoff were higher than concentrations in shallow subsurface flow. This finding matches well with measured data from Schuler (2008), who identified higher K^+ values in the topsoil (up to 20 cm) with decreasing concentration in the subsoil of a soil profile at the same study site. Since shallow subsurface flow samples were extracted from a soil depth of about 50 cm, the lower concentrations are congruent with Schuler (2008). If monitored in higher spatial and temporal resolution, K^+ can be used as a 'dynamic' tracer for surface runoff in the presented area.

Christophersen et al. (1990) pointed at Ca^{2+} as an indicator for water from deeper soil layers at their temperate study site. Although monitoring a tropical site, high concentration of Ca^{2+} were found in groundwater (Table 4.3), suggesting a different, deeper source for this component than the one for shallow subsurface flow and surface runoff. This pattern is congruent with the veritably mineral depletion (including Ca^{2+}) of the present soils within the first meter of soil cover (Schuler, 2008). Also, the similar behavior of Ca^{2+} and silica may be considered as a hint for a conjoint source. The peak of Cl^- during E2 is rather difficult to explain. Samples of surface runoff and shallow subsurface flow were collected from an abandoned litchi plantation (no agricultural management) and delivered very low concentrations of Cl^-. The observed peak during the runoff event cannot be explained by any of the observed components. Cl^- peaks during stormflow may therefore be caused by agricultural areas upstream, which were not covered by the sampling. The low concentrations of Cl^- in all components (GW, SUB, SUR) and the presence of small agricultural areas within the catchment hamper the suitability of Cl^- as a tracer for this particular study site. However, the low concentrations of Cl^- also point to a minor influence of agricultural management on the water samples within the study area. Monitored concentrations of NO_3^- in the stream were as low as 2.45 mg L^{-1} on average and suggest no influence of agricultural practices on our samples within the catchment during the monitoring period. Low NO_3^- concentrations in surface runoff also consolidate the observation that the sampling site was not under influence of fertilizer during the sampling period.

The observed drop of Na^+ and Mg^{2+} concentration at the beginning of the stormflow was also described by Mul et al. (2008). However, the difference of concentrations among the monitored components was not significant. Thus, both ions were not suitable as geochemical tracers under present conditions. To bypass the limitations of non-distinguishable concentrations among the components, or their non-conservative behavior, the application of isotopes (i.e. ^{18}O, ^{2}H) for hydrograph separation should be considered.

An additional hint for runoff generation can be seen in the ion concentrations and EC values of surface runoff and shallow subsurface flow. Most of the measured ion concentrations and EC values of surface runoff water were larger than those of shallow subsurface water. Surface runoff is assumed to flow quickly at the soil surface. Hence, the contact time between water and soil is limited and ion concentrations and EC values close to concentrations in rainfall would be expected. During the presented events, surface runoff showed an enrichment of ion concentration compared to shallow subsurface flow. Only silica concentration was found to be higher in shallow subsurface flow than in surface runoff. This may be explained by soil chemical investigations by Schuler (2008). Schuler reported maximum ion concentrations in the soil within the first 10 cm and a clear decrease below 20 cm. The hydrochemical composition of surface runoff indicates an infiltration of the water into the topsoil at an uphill position. While laterally flowing downhill in the topsoil, the water may have been forced by bedrock or topography to ex-filtrate along the hill slope. The observed surface runoff during the events may therefore be return flow, instead. The difficulty of a separation of both flow components in a tropical environment has already been stated by Elsenbeer et al. (1994) and can be consolidated for the presented study site.

The enriched silica concentration of shallow subsurface flow and the low ion concentration observations by Schuler (2008) can also deliver explanations. Here, the highest clay contents in the soil were found between 40 and 70 cm. In contrast, the measured ion concentrations within this 40 to 70 cm depth were lower than the ones in the first 20 cm. Similar characteristics of silica concentration and EC values were reported by Negishi et al. (2007) from a Malaysian study site. They sampled bedrock seep and pipe flow for which silica concentrations of bedrock seep were highest and EC values were the lowest among the observed components.

Combining the soil chemistry with our analysis results, a possible pathway for silica-rich and low-ion concentrated water is a rapid bypass of the upper soil layer. This is enabled by vertical macropores (McDonnell, 1990). Kienzler and Naef (2008) also stated that vertical macropores and lateral preferential flow paths are able to transfer water quickly and directly into streams. For the present study site, Kahl et al. (2007) identified preferential interflow at depths of 60-90 cm at the same study site in a preceding plot experiment. However, such flow paths were not backed up by additional hydrometric monitoring.

Hydrograph separation based on silica and EC revealed that all stormflow events were dominated by groundwater. Although EC is considered as a non-conservative tracer, the high temporal resolution of the monitoring allows the application within a hydrograph separation. Nevertheless, a comparative two-component hydrograph separation based on EC, silica and Ca^{2+} was computed and backed up the suitability of EC. All approaches delivered similar results, which strengthens the results of the three-component hydrograph separation, where EC was included as tracer. Shallow subsurface flow contributed the second largest fraction, followed by surface runoff. The order of the components, GW > SUB > SUR is congruent with most studies from temperate regions (Peters and Ratcliffe, 1998; Uhlenbrook and Hoeg, 2003), but deviates from finding in tropical areas (Table 4.1). For instance, Goller et al. (2005) monitored event water fractions of up to 80% from a study site in Ecuador, which received much more rainfall than the present study site and has no distinct dry season. Schellekens et al. (2004) also reported a dominance of fast flow components from their catchment south of Puerto Rico during stormflow. The fast flow components (SUB and SUR) within the presented study did not deliver such large fractions to stormflow. This is certainly due to lower amounts of rainfall received by our study site, compared to the mentioned studies (Table 4.1). Investigations, which particularly suggest an important contribution of overland flow to stormflow generation, were carried out in regions with considerably higher amounts of rainfall throughout the year (e.g. Elsenbeer and Lack, 1996; Godsey et al., 2004; Chaves et al., 2008) (Table 4.1). Due to different rainfall patterns, a comparison between those studies and the presented one is difficult. The lower fractions of surface runoff identified in the presented separation approach can be explained by the amount of rainfall and is also congruent with reported results from Ziegler et al. (2000). They stated that overland flow enhancement on undisturbed soils needs high amounts of rainfall. If forests dominate study catchments, overland flow is rare, and subsurface flow component are more important (e.g. Wickel et al., 2008; Chaves et al., 2008; Negishi et al., 2007; Table 4.1). Studies that are equivalent to the environmental conditions of the presented one are given by Negishi et al. (2007) and Giertz et al. (2006). Negishi et al. (2007) identified shallow groundwater as the main contributor to stormflow at a Malaysian study site with a bimodal rainfall distribution equal to the one of the presented study area. Nevertheless, the amount of rainfall within the Malaysian study site was higher than the one in Mae Sa Noi. Although shallow groundwater was not included as a specific component for monitoring in the presented study, groundwater clearly dominated stormflow generation of the observed events. This may be explained by the understanding of this component within this study as a mixture of groundwater and contributions from saturated zones in the catchment. Also, the groundwater component was sampled in the stream and because of shallow soils and steep hillslopes shallow groundwater may contribute to that component, too. During rainfall events, the saturated zone contributions may deliver higher fractions. However, this could not be backed up by samples.

Giertz et al. (2006) emphasized the importance of shallow subsurface flow (i.e. interflow) in a study site in Benin that received same amount of annual rainfall as the Mae Sa Noi catchment. Shallow subsurface flow also contributed considerable amounts to stormflow generation in the Mae Sa Noi catchment. Despite the different soil types in the Beninese catchment, the results from the presented study can be arranged with the reports from Giertz and Diekkrüger (2003) and Giertz et al. (2006).

4.4.2 Stormflow dynamics

The dynamics of the separated fractions also reveal some insight on stormflow generation. The increase of the groundwater component with the onset of the hydrograph during each event may be driven by water from the upper part of the catchment. Williams et al. (2002) found that the speed of kinematic response within a catchment was greater than pore water velocity. Such kinematic response could cause a rapid rise of the groundwater component in the beginning of the hydrograph. The authors also stated that this process depends on slope and soil moisture. Since the catchment is particularly steep and the rainy season was already progressed during the time of monitoring, this process may be further favored. Although hydrometric information on soil moisture was not available, the characteristic of soil properties may support this postulation. While Acrisols appear with a weak microstructure, the macrostructures are massive and the fast downward movement can only be supported by macropores. Schuler (2008) and Kahl et al. (2007) identified large vertical macropores in the soil layer, allowing a quick downward transfer of water. This may cause a quick dis- and recharge of water in the fissures, fractures and saprolite zone and hence, a rapid rice of groundwater in the stream during stormflow events. The 'fill and spill' hypothesis by Tromp-van Meerveld and McDonnell (2006) could also be an explanation for the rapid rise of the groundwater component during stormflow. Tromp-van Meerveld and McDonnell (2006) argue that bedrock micro-topography along hillslopes influence the contribution of subsurface saturated areas to stormflow. Bedrock depressions are filled, and as soon the water level in the depressions rises high enough, water in such saturated zones spills over the depression and contributes to stream flow. Because of steep slopes and shallow soils along the Mae Sa Noi hillslopes, this is a valid theory during the rainy season.

The lag time of surface runoff differed slightly among the events, but for most events, the peak occurred after the groundwater peak. Low intense rainfall events were observed, which explain the moderate fractions of surface runoff (2-20%) and the slow reaction. As stated above, the significant rise of K^+ concentration was identical with the occurrence of surface runoff during E2. Throughout E1, E2 and E5 the fraction of surface runoff appeared later than shallow subsurface flow. This pattern was different for E4, which had the highest rainfall intensity among the observed events and where surface runoff peaks occurred before shallow subsurface flow. E4 also was the earliest monitored event in the course of the monitored period.

The third component, shallow subsurface flow, was observed in 2007 and 2009, but not in 2008. In 2008, total rainfall was more variable than in the other two years (Table 4.2) and the first seasonal maximum occurred later. Also, the number of rainy days per station fluctuated more, resulting in an unequal distribution of rainfall within the catchment during that year. This highlights the importance of temporal and spatial continuity of rainfall input to trigger shallow subsurface flow along the hillslopes. Kahl et al. (2007) already discussed that a threshold value is needed to activate shallow subsurface flow (so-called interflow in their publication) along a hillslope in the study site.

4.4.3 Representativeness of the study site

Although we only monitored four events with low rainfall intensity, runoff patterns of all events were comparable with regard to dynamics, initial volumes and peak flow. Regarding the computed uncertainties, the separated fractions may deviate from the presented amounts, but the order of contributions of the components is maintained. During E2, the fraction of surface runoff seems to be underestimated, which may be caused by the dimension of the rainfall event. Nevertheless, the dominance of groundwater during the event is still valid.

Some of the monitored concentrations and EC values during stormflow were not exactly bound within the chemical triangles. This may reduce the reliability of the statements gained from the evaluated events. However, as the majority of the measured concentrations and values were within the triangles, a reasonable choice of the end-members is defensible.

The spatial representativeness of surface runoff sampling was improved during the 2009 campaign. The extended collection did not reveal significant differences among the samples, but it should be considered to extend the sampling of both, surface runoff and shallow subsurface flow, across the whole catchment in future studies. Also, groundwater levels and soil moisture were not monitored during the study. This hampers the interpretation of the results and subsurface processes remain speculative to a certain degree.

Although the monitored years differed much in the amount and distribution of rainfall, the results are very much alike. An exception is given by the sampling approach in 2008. While shallow subsurface flow was active at the same time in 2007 and 2009, no leakage could be found in 2008. This is caused most likely by a belayed onset of the rainy season and complicates the transferability of the findings to further events in the catchment. Therefore, a combination of runoff generation studies with a high spatio-temporal rainfall monitoring for such highly dynamic catchments is required.

As most of the catchment area is occupied by secondary forests and managed tree plantations, the representativeness of the sampling site located in an abandoned litchi plantation should be balanced. Although an influence of agricultural practices or management on the study site can be excluded, in some parts of the catchment small agricultural fields may affect runoff generation. Still, soil cover (leaves, weed, etc) and soil properties for both habitats are very similar (Schuler, 2008), which suggests the usefulness of the selected site. With regard to an underestimation of surface runoff within this area, it is rather assumed that undisturbed forest would rather lower the contributions (i.e. Dykes and Thornes, 2000).

Despite these limitations and uncertainties, the presented study is beneficial for the progress in understanding runoff generation in this particular tropical, mountainous catchment for which no runoff investigations are available so far. The field observations delivered some insights into the hydrochemical and hydrological dynamics of the study area during single events. Those results certainly serve as a basis for further, more detailed studies and can be used as evaluation of rainfall-runoff models or on solute transports in the catchment.

4.5 Summary and conclusion

The present study was conducted in a remote catchment in the outer tropics. For such catchments, only very few data on runoff generation are available. Suitable tracers were identified for hydrograph separation and data of four monitored stormflow events were analyzed. Silica and EC were found to be useful tracers in the monitored environment. K^+ may be considered as an indicator for surface runoff dynamics and Ca^{2+} may serve as a groundwater marker. For quantitative conclusions both cations must be monitored with a high spatio-temporal distribution. Other major ions were not found to be useful for geochemical separation approaches in the monitored period. Concentrations were either too low or not distinguishable among the components. To bypass this limitation, isotope tracers could be considered as another tool to elucidate runoff generation processes in this catchment. The three-component hydrograph separation revealed groundwater as the major source of stormflow during all monitored events, followed by shallow subsurface flow and surface runoff. However, the hydrochemical data indicate a complex system of flow paths within the study catchment, which would be needed to be investigated with a higher spatial-temporal resolution in future. Especially the relation between rainfall and the occurrence of shallow subsurface flow in the course of the rainy season needs more attention. This flow component might be of particular interest when focusing on losses of agrochemicals to stream waters.

Acknowledgements

We thank Ittipon Sodsaard and Mai Tanarumgruang for their indispensable help during data collection in the field and assistance in the lab. We also would like to acknowledge the contributions of four anonymous reviewers that helped to improve this publication significantly. This research was funded by Deutsche Forschungsgemeinschaft (German Research Foundation) and was a part of the Collaborative Research Programme SFB 564.

5 Publication 3 - Short-term dynamics of pesticide concentrations and loads in a river of an agricultural watershed in the outer tropics

Sangchan, W.[1], Hugenschmidt, C.[2], Ingwersen, J.[1], Schwadorf, K.[3], Thavornyutikarn, P.[4], Pansombat, K.[5], Streck, T.[1]

[1]Institute of Soil Science and Land Evaluation, Biogeophysics, University of Hohenheim, 70593 Stuttgart, Germany. [2]Institute for Natural Resource Conservation, Department of Hydrology and Water Resources Management, Christian-Albrechts-Universität zu Kiel, 24098 Kiel, Germany.
[3]State Institute for Agricultural Chemistry, University of Hohenheim, 70593 Stuttgart, Germany.
[4]Department of Chemistry, Faculty of Science, Chiang Mai University, 50200 Chiang Mai, Thailand. [5]Department of Soil Science and Conservation, Faculty of Agriculture, Chiang Mai University, 50200 Chiang Mai, Thailand.

Agriculture, Ecosystems & Environment
(published)

Abstract

The intensification of agriculture in the mountainous regions of northern Thailand has led to an increased input of agrochemicals, which may be lost to streams and contaminate the surface water of the lowlands. The present study quantifies the dynamics of pesticide loads in a tropical river during three runoff events. To elucidate the processes involved in pesticide transport from agricultural fields to the stream water we used a high temporal resolution of sampling (1 hour) and applied a time series analysis. Water samples were analyzed for seven pesticides (atrazine, chlorothalonil, chlorpyrifos, cypermethrin, dichlorvos, α- and β-endosulfan). Six of the seven pesticides were detected in the river water. Only dichlorvos was below the detection limit in all samples. In particular, pesticides with low K_{oc} value such as atrazine and dimethoate were transported during the runoff peaks. In case of chlorothalonil, chlorpyrifos, α- and β-endosulfan and cypermethrin, short concentration peaks lasting about one hour were detected during the falling limbs of the runoff peaks, indicating that a fast and sporadic sub-surface flow component (e.g. preferential interflow) plays an important role as a transport pathway. Our study demonstrates that in tropical areas sampling schemes with a high temporal resolution are needed to adequately assess the pesticide contamination of rivers. Otherwise, extreme situations may remain unsampled.

5.1 Introduction

The increasing demand for agricultural products and the urbanization in lowland areas has led to the expansion of permanent cultivation to the vulnerable slopes of the mountainous areas in northern Thailand. To protect crops from diseases and to increase crop yields, the application of pesticides has been intensified during the last decades. The intensive and/or careless use of pesticides may contaminate soil and water, causing environmental problems and posing a risk to human health, both in the uplands and lowlands (Stuetz et al., 2001; Kruawal et al., 2005; Panuwet et al., 2008).

The environmental fate of pesticides has been extensively studied in temperate zones (e.g., Kreuger, 1998; Riise et al. 2004; Müller et al., 2006) and mediterranean zones (e.g., Louchart et al., 2004; Oliver et al., 2012). However, little is known about pesticide dynamics in tropical regions (Reichenberger et al., 2002; Castillo et al., 2000; Polidoro et al., 2009). To our knowledge, only few studies have investigated the transport of pesticides in the tropics in real field situations. In northern Thailand, the climate is characterized by the sequence of distinct rainy and dry seasons. Crops are grown and pesticides sprayed in the rainy season with heavy rainfall and runoff. Thus, pesticide contamination in water resources is a relevant environmental issue in this region. Understanding dynamics of pesticides in agricultural watersheds is crucial for working out effective mitigation and management strategies.

Rainfall-induced surface runoff is considered an important transport pathway of pesticide loss from agricultural fields. Ng and Clegg (1997) analyzed the contribution of different flow components to the transport of atrazine in the Nissouri Creek in Canada. The loss with surface runoff was about twice that of interflow and baseflow. Sub-surface transport, however, may also considerably contribute to total loss. Kladivko et al. (1991) and Brown et al. (1995) found that pesticide concentrations increased at the start of discharge events, and that they rapidly decreased with the recession limb of hydrograph. This type of transport is often called "event-driven". It is hypothesized that the early part of an event is dominated by rapid flow processes such as surface runoff and sub-surface transport by preferential water flow. Later, matrix flow becomes more important, so that solutes are retarded in soil, and thus pesticide concentrations in leachate are much lower (Kladivko et al., 1991).

The present study was conducted in the Mae Sa watershed in northern Thailand. In previous studies within the Mae Sa watershed the fate of pesticides after application to a sloped litchi orchard was investigated at the plot and at the hillslope scale. The results show that macropores caused significant preferential transport in vertical (Ciglasch et al., 2005) and lateral direction (Kahl et al., 2008). The extent of preferential flow and transport strongly depended on rainfall and antecedent soil moisture (Kahl et al., 2007and Kahl et al., 2008). Additionally, simulations based on a two-domain reservoir model indicate that under wet soil conditions, "old" water may be pressed into the preferential flow pathways by very small rainfall events, leading to desorption of pesticides from the pore walls. Therefore, preferential interflow must be considered as an important transport process for pesticides in the mountainous areas of northern Thailand (Kahl et al., 2010).

Studies on the plot and field scale under relatively well defined conditions allow to investigate in detail the influence of selected factors such as application time, rainfall intensity or antecedent soil wetness on pesticide loss. These studies, however, can give only a limited picture of the real situation at the catchment scale. At this scale, additional factors control transport and loss of pesticides from the application area to water bodies. Differences in agricultural practices and cropping systems create a large variability of a pesticide application in time and space. Moussa et al. (2003), for example, reported that ditch networks may play an important role for water flow characteristics such as runoff volume, lag time, and form of runoff peak. The spatial distribution of the agriculturally used areas may also influence pesticide losses during flood events (Frey et al., 2009; Wohlfahrt et al., 2010).

The aim of our study was to gain a better understanding of the transport of seven pesticides with widely differing physicochemical properties (log K_{oc} 1.5-4.9) under wet-dry tropical conditions at the catchment scale. The watershed under study can be regarded as representative for agricultural mountainous watersheds in northern Thailand and elsewhere with similar climatic conditions. Based on a high-resolution sampling scheme and a time series analysis, we deduced potential transport pathways from observed pesticide concentration patterns. We investigated three rainfall events: one event at the beginning of the rainy season when soils were dry and two events in the middle and towards the end of the rainy season when soil moisture was high.

5.2 Materials and Methods

5.2.1 Description of the study area

The Mae Sa watershed is located 30 km northwest of Chiang Mai in northern Thailand. The total area of the watershed is 77 km^2 (Figure 5.1). The agricultural land use in the catchment was mapped based on a SPOT 5 image centered at N19°1'4" E98°49'24" taken on 6 November 2006 (Figure 5.2) (GISTDA 2007). About 24% of the watershed is in agricultural use, whereby this land use class covers also a small fraction of settlements. The remaining 76% are covered by deciduous forest, evergreen forest and mixed forests (Figure 5.2). The fraction of agricultural area in the headwater sub-catchment was 28.5%. This area is mainly used for growing vegetables (cabbage, bean, chayote etc.), fruit (litchi) and flower production (gerbera, chrysanthemum, etc.). In the headwater area (28 km^2), the proportion of agricultural area and particularly the number of greenhouses is higher than in the lower parts of the watershed.

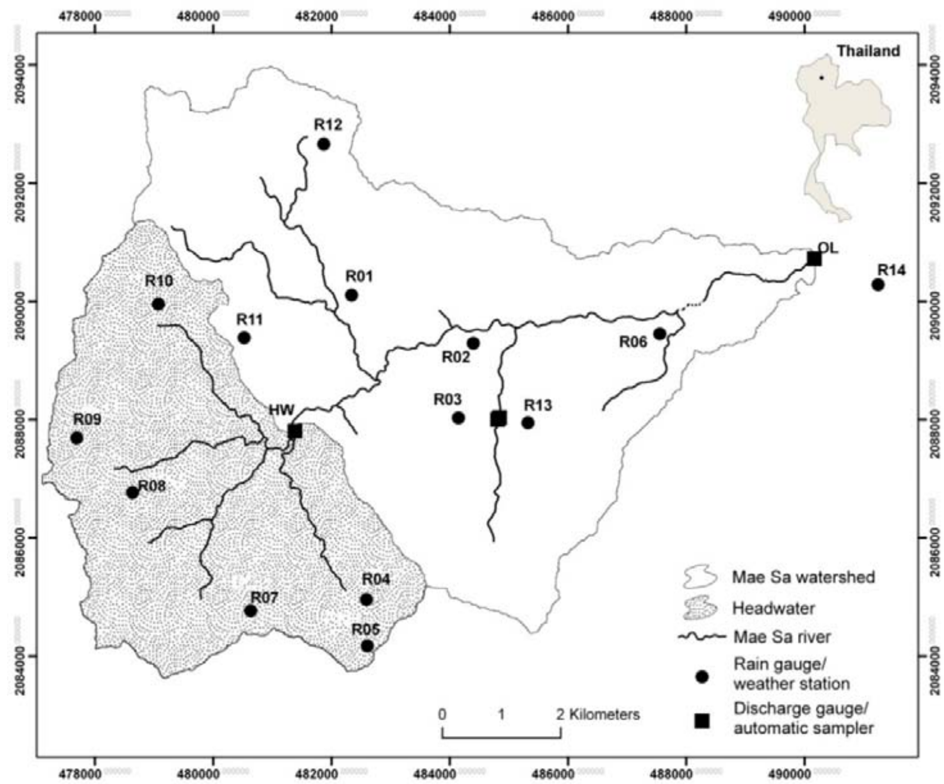

Figure 5.1: Mae Sa watershed (North Thailand) with sampling locations and measurement network.

Dominant soil types in the watershed are Acrisols and Cambisols, with a highly developed macropore network (Schuler, 2008). Top soil texture of the Acrisols (0.0-0.2 m) is clay loam, while that of the Cambisols varies from clay loam to sandy clay loam (Schuler, 2008; Spohrer et al., 2006). The parent material is mainly granite and paragneiss. The catchment is characterized by steep slopes and narrow valleys. The altitude ranges from 350 to 1540 m above sea level (m.a.s.l.). The average slope is 36%, with large differences from the headwater (HW) towards the outlet (OL).

The climate is tropical with distinct rainy (May to October) and dry seasons (November to April). Mean annual air temperature and mean annual rainfall in 2004 - 2010 were 21.0^{o}C and 1250 mm, respectively (Thai Meteorological Department, 2011). The total rainfall in 2008 was 1236 mm, which is close to the average annual rainfall between 2004 and 2010. The typical crops are grown in the rainy season (June to September). Off-season fruits, such as Litchi, and temperate crops, such as carrot, white radish etc., are cultivated in winter (November to February). Most agricultural areas are located in the valleys following the river network (see Figure 5.2).

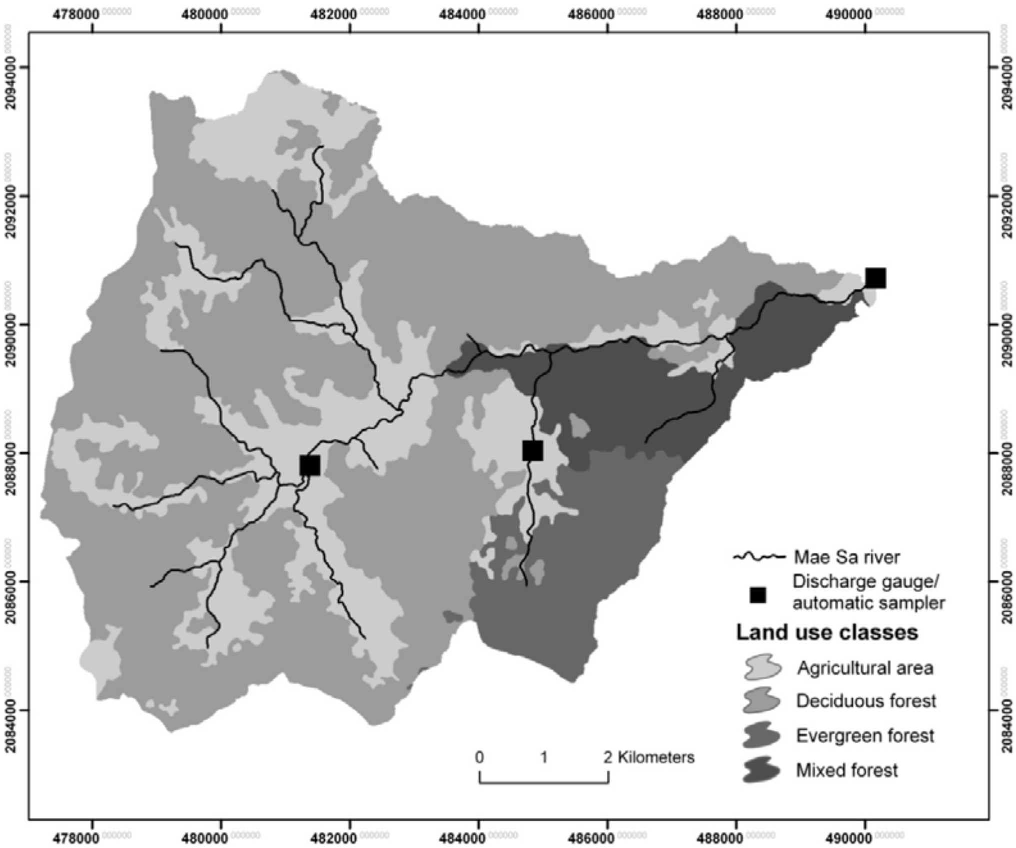

Figure 5.2: Land use in the Mae Sa watershed, 2006.

The occurrence of surface runoff is typical for the rainy season. In 2008, the average discharge of the HW and the entire watershed was 2.34 and 1.36 mm d^{-1}, respectively. The maximum flow rate at the HW station was 14.6 mm d^{-1} (with a peak of 14.0 $m^3 s^{-1}$), which occurred on 21 August 2008. At the OL station, the maximum flow was recorded as 8.5 mm d^{-1} (with a peak of 21.5 $m^3 s^{-1}$) on 6 September 2008.

5.2.2 Pesticide selection

We selected seven pesticides frequently applied by the farmers in the Mae Sa watershed. Their properties are given in Table 5.1.

Table 5.1: Physico-chemical properties of the investigated pesticides.

	Water solubility[a]	Log K_{oc} [b]	Half life in water
Pesticide	**[mg L^{-1}]**	**[L kg^{-1}]**	**[days]**
Dichlorvos	10,000	1.7	7[c]
Atrazine	28	2.0	30[c]
Dimethoate	25,000	1.5	8[d]
Chlorothalonil	0.6	2.9	49[c]
Chlorpyrifos	2	3.9	35-78[d]
Endosulfan	0.32	4.1	28[d]
Cypermethrin	0.01	4.9	> 50[e]

Data from [a]EXTOXNET (1996), [b]Footprint PPDB (2011), [c]PAN database (2008), [d]Howard (1991) and [e]EPA (1989)

According to a survey by Schreinemachers and Sirijinda (2008), dichlorvos, chlorpyrifos, cypermethrin, and chlorothalonil are intensively used in bell pepper, chrysanthemum, and white cabbage production (Table 5.2).

Endosulfan and dimethoate were included because they had been detected in a previous study in the Mae Sa River (Ciglasch et al., 2006). Although not mentioned in Schreinemacher's survey, atrazine was included because we had found significant concentrations in preliminary investigations.

Table 5.2: Major crops and usage of investigated pesticide in the Mae Sa watershed 2007 (Schreinemachers and Sirijinda, 2008).

	Insecticide					Fungicide
Crop	**Dichlorvos**	**Dimethoate**	**Chlorpyrifos**	**Endosulfan**	**Cypermethrin**	**Chlorothalonil**
Bell pepper	x		x		x	x
Chrysan-themum	x		x		x	x
White cabbage	x		x	x	x	
Bush bean	x					x
Chinese cabbage	x		x		x	
Litchi	x		x		x	x
Chayote	x					x
Potato		x				
Paddy rice			x		x	

5.2.3 Field measurements and data analysis

Stream flow and pesticide loads originating from the headwater catchment were measured at the HW gauge (767 m.a.s.l.; 28 km^2), those originating from the entire watershed at the OL gauge (345 m.a.s.l.; 77 km^2). At each station, the water level was continuously recorded using an ultra sonic water level sensor (710 Ultrasonic module, Teledyne ISCO Inc., USA). The conversion into discharge volume was based on calibration data taken by an acoustic flow meter (OTT ADC, Germany). Discharge data were recorded in 10-min intervals.

Each gauging station was equipped with an automatic water sampler (6712 Portable sampler, Teledyne ISCO Inc., USA). The first runoff event was sampled on the beginning of the rainy season from 2 May to 7 May 2008. Two further events were sampled in the middle and close to the end of the rainy season. The second campaign was conducted from 20 to 24 August and the third event was sampled from 13 to 17 September 2008.

During the sampling campaigns (each 3-4 days long), composite samples were taken at hourly resolution. Each composite sample (300 mL) was mixed from six 50 mL samples drawn from the river every 10 minutes. The decision of which samples to use for analysis was made later in the lab, based on measured discharge. To characterize the background concentrations before the discharge peak (16 h in case of the May event, and 8 h in case of the August and September event), samples were selected with a 4-hourly resolution. The beginning of increasing discharge was determined visually. In the automatic sampler and later, sampling bottles were cooled with ice. Within one day, they were transported to the lab. Samples were stored in a refrigerator at 4°C in the lab and processed during the following two to three days.

Rainfall data

To quantify the rainfall within the watershed, a network of twelve automatic rain gauges (Type 441301, 0.2 mm resolution, Fischer GmbH, Germany) was installed (Figure 5.1). The rain gauges were distributed over the whole catchment area and cover the major elevation levels. Additionally, the rainfall data of two neighboring weather stations were included. All stations were operated with 10-min resolution. The average rainfall within the catchment was computed after Shaw (1988):

$$\bar{R} = \frac{1}{A}\sum_{i=1}^{n} R_i A_i \qquad \textit{(Eq. 5.1)}$$

Here, R_i (mm) is the rainfall measured at the i-th rain gauge, the symbol n stands for the number of rain gauges, A (km^2) is the total area of the catchment and A_i (km^2) is the Thiessen polygon area of the i-th gauge. In the case of HW rainfall, only the parts of the Thiessen polygons located in the headwater area were used to calculate the amount of rainfall.

Runoff coefficient

The runoff coefficient (RC) is defined here as the percentage of rainfall that appears as runoff during an event. Rainfall related to a particular flood event was included from the point in time when discharge started to rise until it started to fall again. Runoff volume directly generated by rainfall was determined by using an automated two-component hydrograph separation method separating baseflow and direct flow (Arnold et al., 1995; Arnold and Allen, 1999). This Baseflow Filter Program is also available from http://swatmodel.tamu.edu/software/baseflow-filter-program. The RC was calculated from the quotient between direct flow and rainfall.

Time series analysis

To relate rainfall, discharge and pesticide concentrations in the stream to each other, a time series analysis was conducted. Cross-correlation coefficients (CCC) between variables *x* and *y* were computed as

$$CCC = \frac{\sum_t (x_{t+\tau} - \bar{x})(\bar{y}_t - \bar{y})}{\sqrt{\sum_t (x_{t+\tau} - \bar{x})^2 \sum (y_t - \bar{y})^2}} \qquad \textit{(Eq. 5.2)}$$

where τ is the time lag in hours, and x_t and y_t are the values of the correlation variables at time *t*. The symbols $\bar{x}$ and $\bar{y}$ denote the means of *x* and *y*, respectively. CCCs were calculated for rainfall and stream discharge, rainfall and pesticide concentration in stream water, and stream discharge and pesticide concentration with $0 \leq \tau \leq 300$ min (HW, May: 565 data points; OL, May: 708 data points; HW, August: 346 data points; OL, August: 417 data points). The time series analysis was performed with the statistical software package SPSS (Version 16.0, SPSS Inc., USA) using 95% confidence intervals.

Pesticide extraction and analysis

Pesticides were concentrated from water samples by solid phase extraction (SPE) (Supelclean™ Envi-Carb, *Graphitized Non-Porous Caron,* surface area 100 m^2 g^{-1}, particle size 120/400 mesh, 0.5 g, 6 mL; Supelco, USA). Prior to extraction, all samples were filtered through a glass fiber filter (GF/F, 0.4 µm; Whatman Inc., USA) to remove suspended particle material. To condition and deactivate the sorbent, the cartridges were rinsed with 8 mL of a dichloromethane: methanol mixture (9:1, v v^{-1}), 3 mL methanol, and 25 mL of ascorbic acid (γ = 10 g L^{-1}; this solution was brought to pH 2 using hydrochloric acid). After this conditioning step, 400 mL of the filtered water samples were sucked through a SPE cartridge at a flow-rate of about 5 mL min^{-1} using a vacuum pump. After the sample load, air was sucked through the cartridges for approximately 5 min. At the end, the cartridges were packed in bags, sealed, and stored in the freezer (-18 °C). As shown by Anyusheva et al. (2012), samples processed in this way can be stored without significant pesticide loss for up to nine months. After having been prepared as described above, the samples were shipped to Germany within approximately 24 h using solid carbon dioxide as cooling agent. They were stored at -20°C until extraction and analysis.

To remove possible water from the sample, air was again sucked through the sorbent for 5 min followed by rinsing with 1.5 mL of methanol. Subsequently, the SPE cartridges were eluted with 10 mL of acetone, 15 mL of a dichloromethane: methanol mixture (9:1, v v^{-1}), and 30 mL of tert-butyl methyl ether (TBME). The flow-rate of all solvents was restricted to less than 2 mL min^{-1}. The eluted solutions were collected in conical flasks, and two drops of toluene were added as a keeper before evaporating to almost dryness. The residues were re-dissolved in 1 mL of a mixture of cyclohexane and toluene (9:1, v v^{-1}). These solutions were used for analysis.

Analytical procedure

The elutes were analyzed by capillary-GC and partly by GC-MS. For capillary-GC analysis, two differently equipped GCs were operated: Firstly, a Hewlett Packard HP 6890 gas chromatograph equipped with an organophosphate pesticide capillary column, Rtx®-OPPesticides (length 30 m, I.D. 0.25 mm, film thickness 0.25 µm; Restek, USA), and a nitrogen-phosphorus detector (NPD, with Blos-bead; Agilent Technologies, USA), and secondly, an Agilent Technologies 7890 GC equipped with an HP-5 capillary column (length 30 m, I.D. 0.32 mm, film thickness 0.25 µm) and a micro-electron capture detector (µ-ECD). Dichlorvos, dimethoate, and atrazine were analyzed by GC-NPD. Chlorothalonil, chlorpyrifos, (α,β)endosulfan, and cypermethrin were analyzed by GC-µ-ECD.

The inlets of both GCs were programmable temperature vaporization (PTV) injectors (Model UNIS; Joint Analytical Systems GmbH, Germany), which were operated in the pulsed splitless mode. The advantage of this pulsed splitless mode is better resolution and response (e.g., Godula et al., 1999). The starting temperature in PTV was 125°C. The temperature was held constant for 0.2 min and then raised to 300°C at a rate of 250°C min^{-1} with GG-NPD or 750°C min^{-1} with GC-µECD. Here, temperature was held constant for 25 min. The PTV inlet pressure in the beginning was set to 159 kPa and pressure was increased during the pulsed splitless mode for 1.5 min to 207 kPa. The injection volume was 1 µL. The temperature of the GC oven was initially set to 90°C, held constant for 2 min, ramped to 300°C at 15°C min^{-1} and then held constant for 10 min. High purity grade helium was used as carrier gas in constant flow mode (2 mL min^{-1}). The NPD temperature was set to 310°C and operated at the following gas flows. H_2-flow: 3 mL min^{-1}, air-flow: 60 mL min^{-1}, constant make-up (N_2) + carrier gas flow:

20 mL min^{-1}. The bead-voltage ranged from 0.8 to 0.96 V within 4 months, which caused an offset current of approximately 10 pA. The µ-ECD temperature was also set to 300°C.

Capillary-GC results of selected samples, i.e. samples with outstanding high peak concentrations, were confirmed by GC-MS (GCQ; Finnigan MAT, USA). The MS was equipped with capillary column FactorFour VF-5MS (length 30 m, I.D. 0.25 mm, film thickness 0.25 µm; Varian, USA). The injector of the GC-MS system was operated in the splitless mode (-0.2 to 1.5 min) at constant inlet temperature of 230°C. As carrier gas, helium was used in constant flow mode at 40 cm s^{-1}. At the beginning the GC oven temperature was set to 90°C, held for 2 min and raised to 290°C at a rate of 15°C min^{-1}. Then, temperature was held constant for 10 min. The temperature of the transfer line between the GC and ion trap detector was set to 300°C. Electron impact ionization (EI) was performed at 70 eV. Fragments within the m/z (mass-to-charge ratio) range from 75 to 430 atomic mass units (amu) were collected and analyzed. Mass spectra from the sample chromatograms were compared to mass spectra of the pure substances measured with the same instrument and under the same operating conditions and to mass spectra published in literature, e.g. from the NIST Chemistry WebBook. Limits of detection (LOD), recoveries, and relative standard deviations (RSD) of the pesticide analysis are given in Table 5.3.

Table 5.3: Limit of detection (LOD) and recoveries of pesticides in water and sediment samples.

		% Recovery (RSD)	
Pesticide	**LOD [ng L^{-1}]**	**In water (n=3)**	**In sediment (n=9)**
Dichlorvos[a]	0.1	60 (8)	41 (16)
Dimethoate[a]	0.5	117 (16)	175 (7)
Atrazine[a]	2	113 (7)	103 (5)
Chlorothalonil[b]	1	58 (27)	79 (5)
Chlorpyrifos[b]	0.3	106 (5)	112 (1)
α-endosulfan[b]	0.1	91 (9)	90 (1)
β-endosulfan[b]	0.1	101 (7)	96 (2)
Cypermethrin[b]	2	69 (4)	104 (3)

[§]RSD = relative standard deviation, [a] Analyzed by GC-NPD, [b] Analyzed by GC-µECD.

Pesticide load calculation

Pesticide loads were calculated by multiplying the hourly stream flow volume with the average pesticide concentration of stream water of that period. Concentrations below the detection limit were set to zero. At both gauging stations, the average areal pesticide loads (g km^{-2}) were computed to compare the pesticide losses between the two catchments. For that, the cumulative pesticide loads were divided by the catchment area of arable land (km^2) assigned to each gauging station.

5.3 Results

5.3.1 Hydrological event characterization

The response of runoff to rainfall varied remarkably between the sampling events (Figure 5.3). The first event, a minor discharge peak, was sampled at the beginning of the rainy season in May.

The HW sub-catchment received 56 mm rainfall during 44 h, which led to two runoff peaks, one after about 1 h with a maximum flow of 2.5 $m^3 s^{-1}$ and a smaller one with a maximum flow of 1.9 $m^3 s^{-1}$ which followed 7 h later. The RC of the event was 0.8% (Table 5.4). On average, the rainfall in the whole catchment was 45 during a period of 48 h. The peak flow at the OL station occurred about 4 h later with a smaller peak flow of 2.8 $m^3 s^{-1}$. A larger peak, with a flow rate of 3.8 $m^3 s^{-1}$, appeared about 14 h later. The RC was also 0.8% (Table 5.4). The in-stream travel time between the main runoff peaks between HW and OL station was about 4 h.

The second and the third events were sampled in the middle and towards the end of the rainy season in August and September. Other than with the first event, sharp discharge peaks were observed at both stations. At HW, the event sampled in August was the highest runoff event in 2008 (Figure 5.3). A total rainfall of 9.9 mm over a period of 7 h initiated runoff within 1 h. Peak flow was 14 $m^3 s^{-1}$. With 13.1%, the RC was considerably higher than that of the first event (Table 5.4).

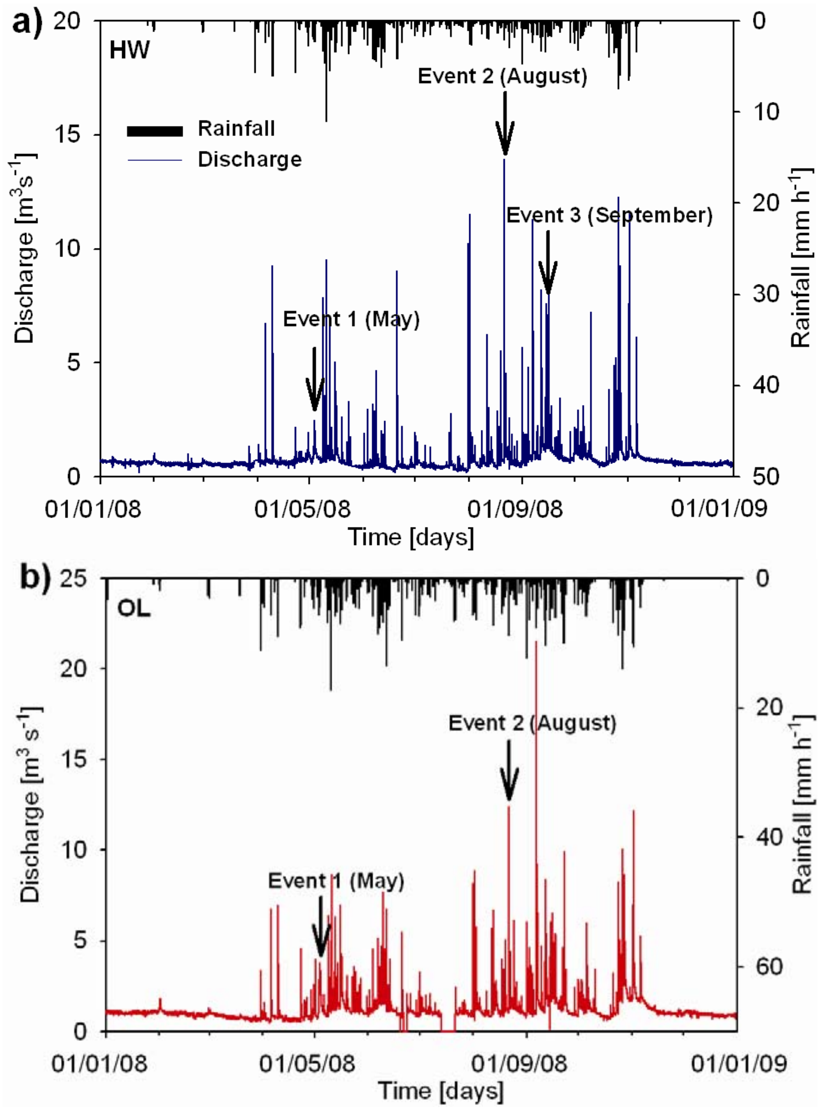

Figure 5.3: Time-series of rainfall and discharge in 2008 and three sampling events at the two stations: (a) the HW, and (b) the OL.

Table 5.4: Hydrological characteristics of the runoff events monitored at the headwater (HW) and the outlet (OL) station.

Hydrological characteristics	**Event 1 2.-7.05.08**		**Event 2 (20.-24.08.08)**		**Event 3 (13.-17.09.08)**		
	HW1	**OL1**	**HW2**	**OL2**	**HW3[a]**	**HW3[b]**	**HW3[c]**
Rainfall (mm)	56	45	9.9	10.9	13.7	11.7	5.2
Mean rainfall intensity (mm h^{-1})	1.3	0.89	1.4	1.1	1.9	1.5	0.52
Maximum rainfall intensity (mm h^{-1})	6.5	5.7	5.6	7.1	8.4	3.2	4.6
Total runoff (mm)	6.6	6.7	4.7	2.2	5.7	9.2	1.7
Direct flow (mm)	0.44	0.36	1.3	0.52	1.0	1.2	0.66
Runoff coefficient (%)	0.8	0.8	13.1	4.8	7.3	10.2	12.7
Peak discharge (m^3 s^{-1})	2.5	3.8	14.0	12.4	7.6	7.1	7.9

§ The three main runoff peaks during the HW3 event: [a] 14 September 2008, [b] 15 September 2008 and [c] 16 September 2008.

In the whole catchment, total rainfall was slightly higher (10.9 mm). Peak flow amounted to 12.4 $m^3 s^{-1}$, 3 h after the start of rainfall. RC was 4.8%. The in-stream travel time between both stations was 3 h (see below) and hence shorter than in May. Because of a technical failure at the OL station, in September the pesticide data are only available at the HW station. Five runoff peaks were observed during the sampling campaign. In this study, we will only consider the hydrological characteristics of the three main events. On the first main event, the total rainfall amounted to 13.7 mm. It resulted in a discharge peak of 7.6 $m^3 s^{-1}$ within 50 min (Figure 5.6). A slightly lower discharge peak (7.1 $m^3 s^{-1}$) was observed on 15 September triggered by a total rainfall of 11.7 mm. The highest discharge peak (7.9 $m^3 s^{-1}$) was measured on 16 September. It was initiated by a relatively lower rainfall amount (5.2 mm). The RCs of the three September events was 7.3, 10.2 and 12.7%.

5.3.2 Pesticide concentrations in the stream

Table 5.5 summarises the range of pesticide concentrations and their frequency of detection (measured concentration > LOD) in stream samples taken at the HW and OL stations. The number of detected pesticides was highest during the May event. Six out of seven pesticides analyzed were detected in the Mae Sa River (exception: dichlorvos).

The dynamics of rainfall, stream discharge, and pesticide concentrations for the three events are shown on chemographs in Figure 5.4 to Figure 5.6. At the HW station, the concentration of atrazine increased with increasing discharge and peaked to 0.12 µg L^{-1} between the two runoff peaks (Figure 5.4a). After rainfall had ended, several smaller atrazine peaks were observed on the falling limb of the recession curve. At the OL station, with the beginning of the rain event, atrazine concentrations in stream water closely followed the runoff curve with a delay of about 3 h to reach a maximum of 0.4 µg L^{-1} (Figure 5.4b). After the first runoff peak, atrazine concentrations declined gradually to a low level, but concentrations remained higher than before the event. In the course of the second runoff peak and the following recession phase, no significant additional concentration peaks were observed.

Dimethoate peaked within the same time frame as atrazine, with a maximum concentration of 0.6 µg L^{-1} at the HW station (Figure 5.4c). Several post-event concentration peaks were detected during the following recession phase. At the OL station, dimethoate concentration also increased after the first runoff peak but not as pronounced as atrazine. Similar to HW, smaller post-event peaks (<0.2 µg L^{-1}) were also observed at the OL station.

Table 5.5: Ranges and mean of pesticide concentrations, and frequency of detection (concentration > LOD) measured at headwater (HW) and outlet (OL) stations during three rain events.

	Headwater station (HW)									Outlet station (OL)					
	May event			August event			September event			May event			August event		
	Range	Mean	Samples >LOD	Range	Mean	Samples >LOD	Range	Mean	Samples >LOD	Range	Mean	Samples >LOD	Range	Mean	Samples >LOD
Pesticide	[µg kg^{-1}]	[µg kg^{-1}]	[%]	[µg kg^{-1}]	[µg kg^{-1}]	[%]	[µg kg^{-1}]	[µg kg^{-1}]	[%]	[µg kg^{-1}]	[µg kg^{-1}]	[%]	[µg kg^{-1}]	[µg kg^{-1}]	[%]
Atrazine	0.01 - 0.1	0.03	42	n.d.	n.d.	n.d.	n.d.	n.d.	n.d.	0.004-0.4	0.07	96	n.d.	n.d.	n.d.
Dimethoate	0.003 - 0.6	0.10	93	0.07-0.3	0.07	67	n.d.	n.d.	n.d.	0.005-0.2	0.06	89	0.06-0.4	0.07	69
Chlorothalonil	0.01 - 0.6	0.04	98	n.d.	n.d.	n.d.	0.01-0.07	0.01	38	0.003-0.07	0.02	87	n.d.	n.d.	n.d.
Chlorpyrifos	0.008 - 0.5	0.08	98	0.04-9.7	0.65	95	0.01-0.04	0.01	38	0.002-0.1	0.04	90	0.04-0.9	0.2	94
Endosulfan	0.002 - 0.09	0.02	95	n.d.	n.d.	n.d.	n.d.	n.d.	n.d.	0.006-0.05	0.01	91	n.d.	n.d.	n.d.
Cypermethrin	0.008 - 0.2	0.06	82	0.002-0.05	0.01	44	n.d.	n.d.	n.d.	0.01-0.2	0.02	39	0.003-0.008	0.004	79

§ n.d. = not detected; LOD: limit of detection

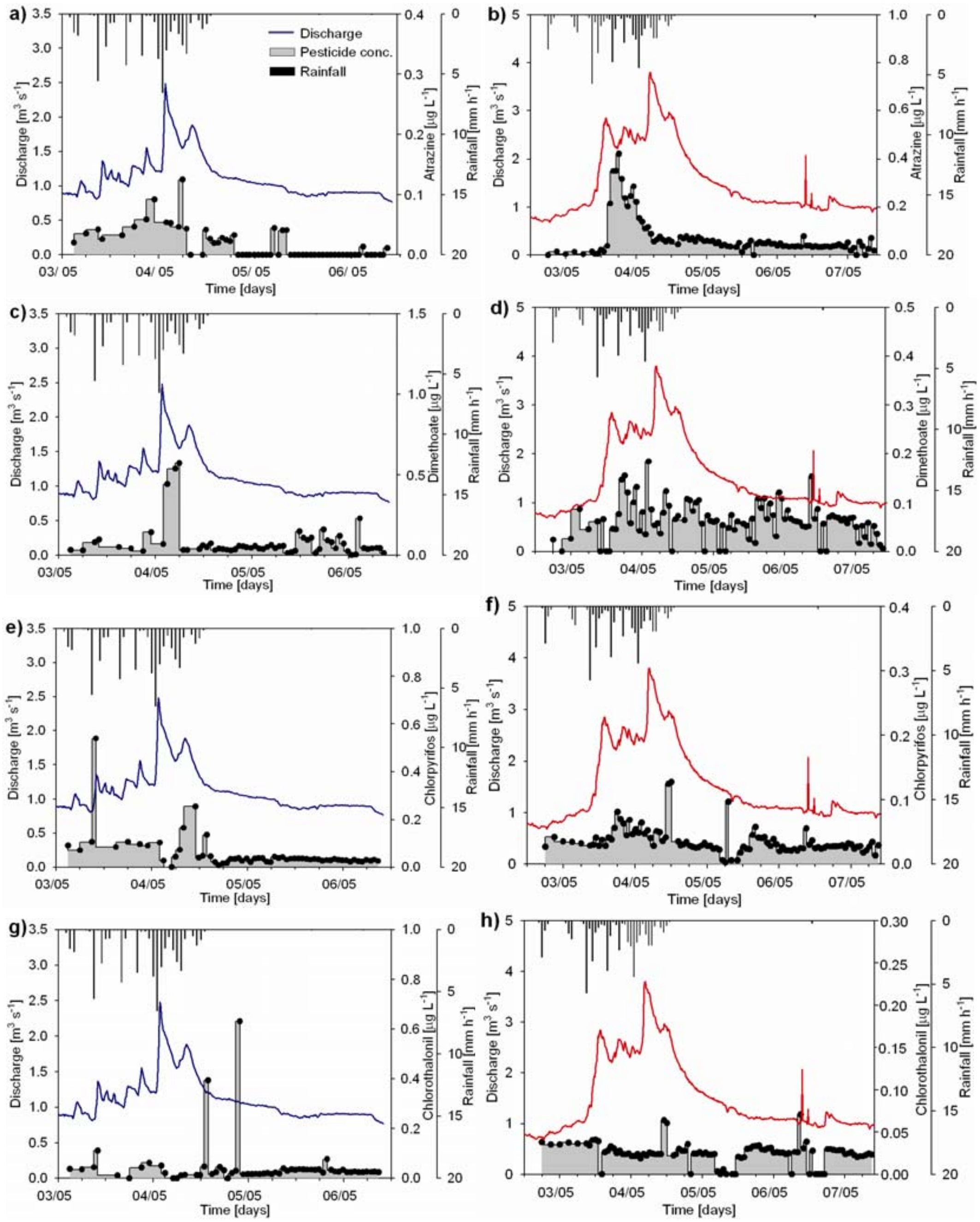

Figure 5.4: Concentrations of six pesticides, discharge, and rainfall data during the May event. Left column: headwater (HW) station. Right column: outlet (OL) station. Pesticides: (a,b) atrazine, (c,d) dimethoate, (e,f) chlorpyrifos, (g,h) chlorothalonil, (i,j) endosulfan, (k,l) cypermethrin.

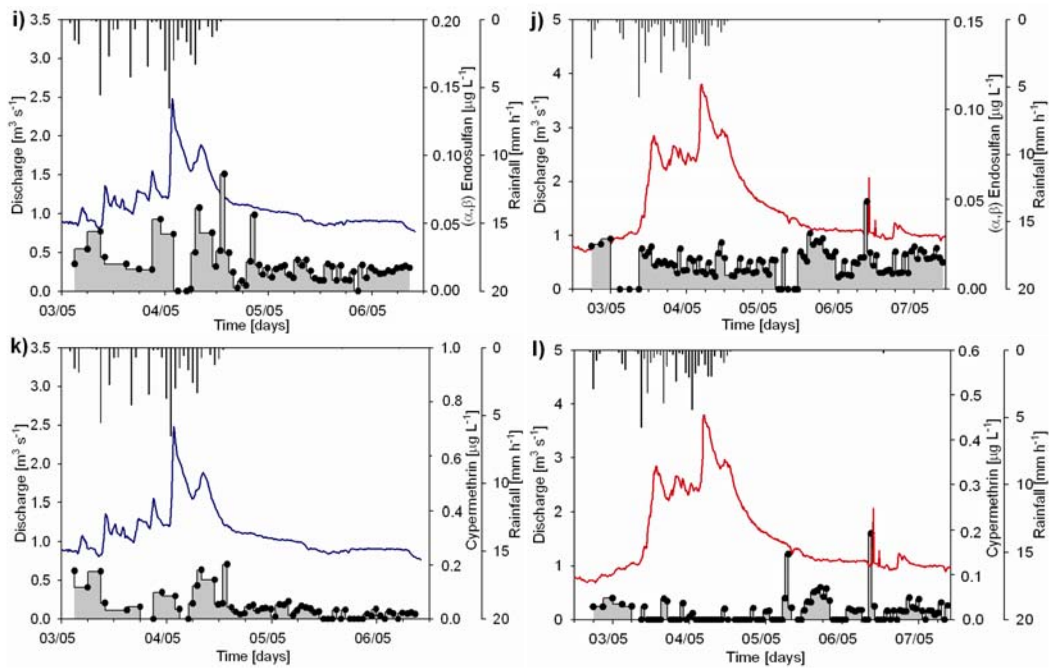

Figure 5.4 (continued): Concentrations of six pesticides, discharge, and rainfall data during the May event. Left column: headwater (HW) station. Right column: outlet (OL) station. Pesticides: (a,b) atrazine, (c,d) dimethoate, (e,f) chlorpyrifos, (g,h) chlorothalonil, (i,j) endosulfan, (k,l) cypermethrin.

With chlorpyrifos, a single peak (0.6 µg L^{-1}) was detected before the runoff peak at the HW station. Additional chlorpyrifos peaks occurred after the runoff peak during the following phase of increasing discharge. No clear post-event concentration peaks were observed at that station (Figure 5.4e). At the OL station, chlorpyrifos increased only slightly with the onset of increasing discharge. Three concentration peaks in the range of 0.1 µg L^{-1} were sporadically observed along the recession limb of the runoff curve (Figure 5.4f).

Concentrations of chlorothalonil remained at a low level before and during the increase of discharge, but two remarkable concentrations peaks were detected along the recession limb, with a maximum concentration of 0.6 µg L^{-1} at the HW station (Figure 5.4g). Also at the OL station the concentrations of chlorothalonil were quite constant during the entire event. Only three samples showed concentrations above 0.05 µg L^{-1} during the phase of decreasing discharge (Figure 5.4h). The endosulfan concentrations reported in Figure 5.4 are the sum of the isomers α-and β-endosulfan. Concentrations peaked at the initial phase of the event. The highest concentration was found later during the falling limb of the runoff curve (Figure 5.4i). At the OL station, most concentrations of endosulfan were below 0.03 µg L^{-1}. They were approximately constant during the event. Only one concentration peak of 0.05 µg L^{-1} was observed on the falling limb of the hydrograph. Cypermethrin concentrations at the HW station were already as high as 0.2 µg L^{-1} before the discharge distinctly increased. Slightly lower concentrations were measured during the increase of the runoff peak. Close to the end of the main decrease, cypermethrin peaked again at 0.2 µg L^{-1} (Figure 5.4k). At the OL station, the concentration pattern was similar to that at the HW station. Only some small peaks of cypermethrin were detected during the discharge increase, whereas the main peaks appeared sporadically during the recession phase of the runoff, with a maximum concentration of 0.2 µg L^{-1} (Figure 5.4l). Note that the concentrations of all pesticides increased remarkably with the steep, but small runoff peak on 6 May.

Pesticide dynamics during the mid-rainy season event in August are shown in Figure 5.5. Only three of the seven pesticides investigated, namely dimethoate, chlorpyrifos and cypermethrin, were detected in the water samples.

At the HW station, dimethoate concentrations increased as discharge increased peaked at 0.3 µg L^{-1} shortly after the runoff peak, and gradually declined during recession (Figure 5.5a). At the OL station, only dimethoate showed this pattern (Figure 5.5b). Extremely high concentrations of chlorpyrifos (up to 9.7 µg L^{-1}) were detected at the HW station during the recession. The concentration peak showed up later in stream water than in the case of dimethoate (Figure 5.5c). During the runoff peak, only very low concentrations of chlorpyrifos were found. The concentration pattern at the OL station was very similar to that of the HW station, but the concentration peak was broader and the maximum concentration (0.9 µg L^{-1}) was much lower than at the HW station (Figure 5.5d).

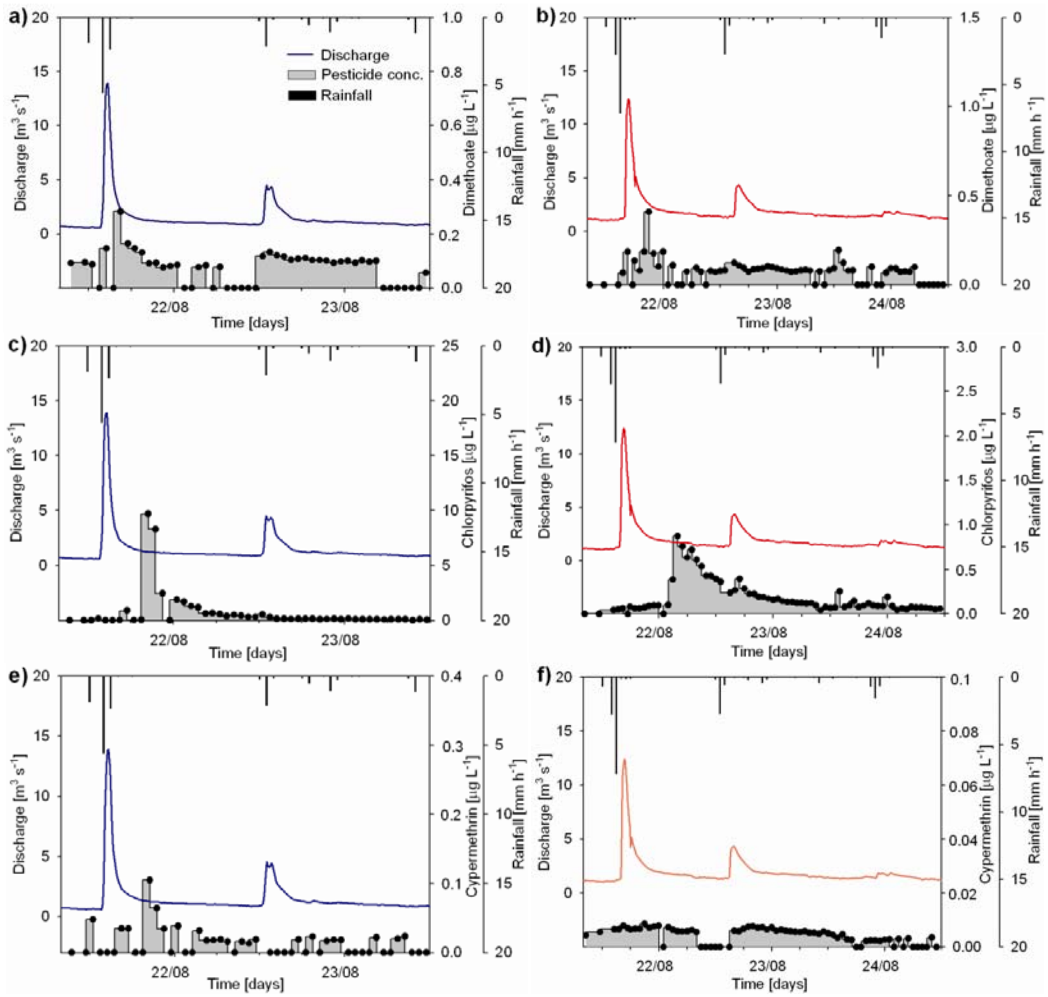

Figure 5.5: Concentrations of three pesticides, discharge, and rainfall data during the August event. Left column: headwater (HW) station. Right column: outlet (OL) station. Pesticides: (a,b) dimethoate, (c,d) chlorpyrifos, and (e,f) cypermethrin. The other pesticides were not detected.

Cypermethrin values reached 0.05 µg L^{-1} prior the runoff event at the HW station. The pesticide concentration decreased during the runoff peak and increased again to a maximum of 0.1 µg L^{-1} at the end of recession limb (Figure 5.5e). No clear post-event peak of cypermethrin was detected. The cypermethrin concentration at the OL station showed no significant peaks. During the entire event, the concentrations of this pesticide were low (0.003-0.008 µg L^{-1}) (Figure 5.5f).

In September, only chlorothalonil and chlopyrifos were detected at the HW station during the sampled runoff events (Figure 5.6).

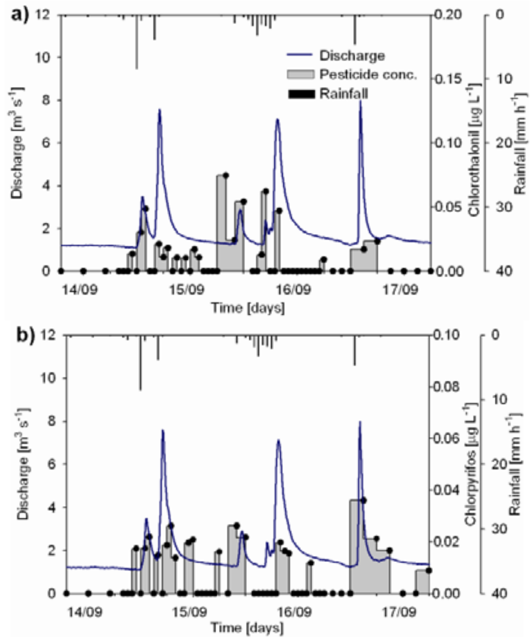

Figure 5.6: Concentrations of two pesticides, discharge, and rainfall data during the September event at headwater (HW) station. Pesticides: (a) chlorothalonil (b) chlorpyrifos. The other pesticides were not detected.

Similarly to the previous event, we found a delay between peak concentration and peak flow. Chlorothalonil peaked with 0.05 µg L^{-1} the first time during the small runoff peak that preceded the main runoff event on 14 September (Figure 5.6a). It peaked the second time with 0.07 µg L^{-1}, 14 h after the discharge peak of the runoff event (on 14 September). Similar to chlorothalonil, several concentration peaks of chlorpyrifos were detected sporadically between the peak flows of 14 and 15 September. The highest concentrations of this insecticide (0.04 µg L^{-1}) were measured during the discharge peak of 16 September (Figure 5.6b).

5.3.3 Pesticide loads

Table 5.6 gives total (mass) and average areal (mass per unit area) loads of dissolved pesticides at both gauge stations. During the May event at the OL station, the total load of most pesticides was higher than at the HW station, in case of atrazine by a factor of ten. Only in case of cypermethrin, the total load at OL was lower than at HW. At OL, the highest average areal loads were those of atrazine and dimethoate. At HW, the loads of dimethoate and chlopyrifos were the highest. In August, a very high load of chlorpyrifos

(20.1 g km^{-2}) was observed at the HW station. The average areal loads of all investigated pesticides were higher than at OL. In September, when pesticide loads were determined only at HW, the loads were generally lower (Table 5.6).

5.3.4 Time series analysis

To better understand the observed pesticide concentration patterns, we performed a time series analysis with atrazine and cypermethrin, atrazine being a weakly-sorbing, cypermethrin being strongly sorbing pesticide. The analysis was carried out for the May event.

At HW, the highest CCC between rainfall and discharge occurs at about one hour (Figure 5.7a, c). At OL, the time lag is 4 h (Figure 5.7b, d). At HW, the CCC between discharge and atrazine concentration is highest at zero time lag, implying quick transport of atrazine. At OL, the highest cross-correlation between discharge and atrazine concentration occurs at a time lag of 3 h. In May, no significant correlation between atrazine and discharge was found at time lags > 14 h.

Table 5.6: Pesticide load at headwater (HW) and outlet (OL) stations during three runoff events.

	Headwater station						Outlet station			
	May event		August event		September event		May event		August event	
Pesticide	Total load [g]	Areal load [g km^{-2}]	Total load [g]	Areal load [g km^{-2}]	Total load [g]	Areal load [g km^{-2}]	Total load [g]	Areal load [g km^{-2}]	Total load [g]	Areal load [g km^{-2}]
Atrazine	4.9	0.62	n.d.	n.d.	n.d.	n.d.	50.5	2.7	n.d.	n.d.
Dimethoate	21.4	2.7	24.6	3.1	n.d.	n.d.	37.9	2.0	43.9	2.4
Chlorothalonil	10.2	1.3	n.d.	n.d.	4.4	0.55	14.8	0.80	n.d.	n.d.
Chlorpyrifos	14.5	1.8	159.3	20.1	3.2	0.41	23.0	1.2	84.7	4.5
Endosulfan	5.0	0.63	n.d.	n.d.	n.d.	n.d.	8.0	0.43	n.d.	n.d.
Cypermethrin	11.4	1.4	3.1	0.39	n.d.	n.d.	7.9	0.43	2.5	0.1

[§] Agricultural land use in 2006: headwater catchment 7.9 km^2, entire catchment 18.5 km^2 (GISTDA, 2007)

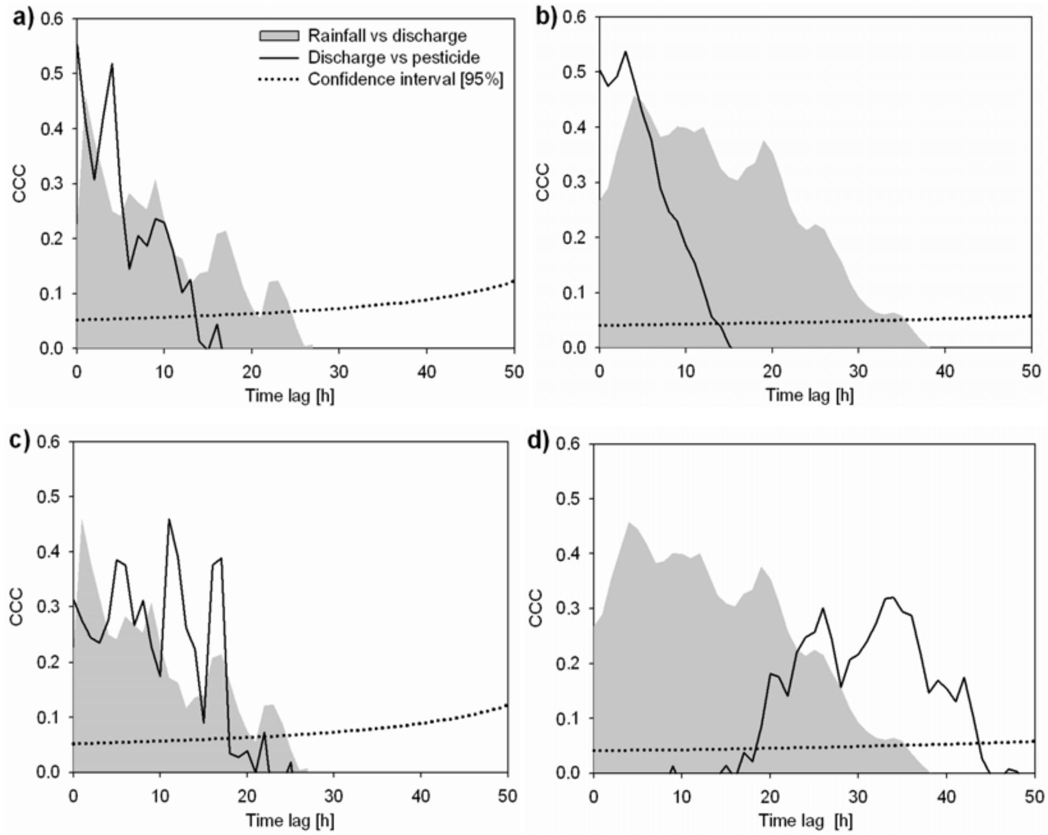

Figure 5.7: Cross-correlograms of rainfall, discharge and pesticide concentration at the HW (left panel) and OL (right panel) stations in May: (a,b) atrazine, and (c,d) cypermethrin.

Cypermethrin shows a different pattern. At HW, the maximum CCC between discharge and cypermethrin concentration was found at a time lag of 11 h (Figure 5.7c). At OL, the cross-correlation between discharge and concentration was even zero at time lags of up to 18 h (Figure 5.7d). Here, highest CCCs between discharge and cypermethrin concentration were found at time lags of 26 and 33 h.

Figure 5.8 compares cross-correlations involving chlorpyrifos during the three events. During the May event, at HW several peaks of CCCs between discharge and chlorpyrifos concentration appeared at the early part of the event (Figure 5.8a). At OL, chlorpyrifos showed a continuous response to discharge, with largest CCC between time lags 0 and 6 h (Figure 5.8b).

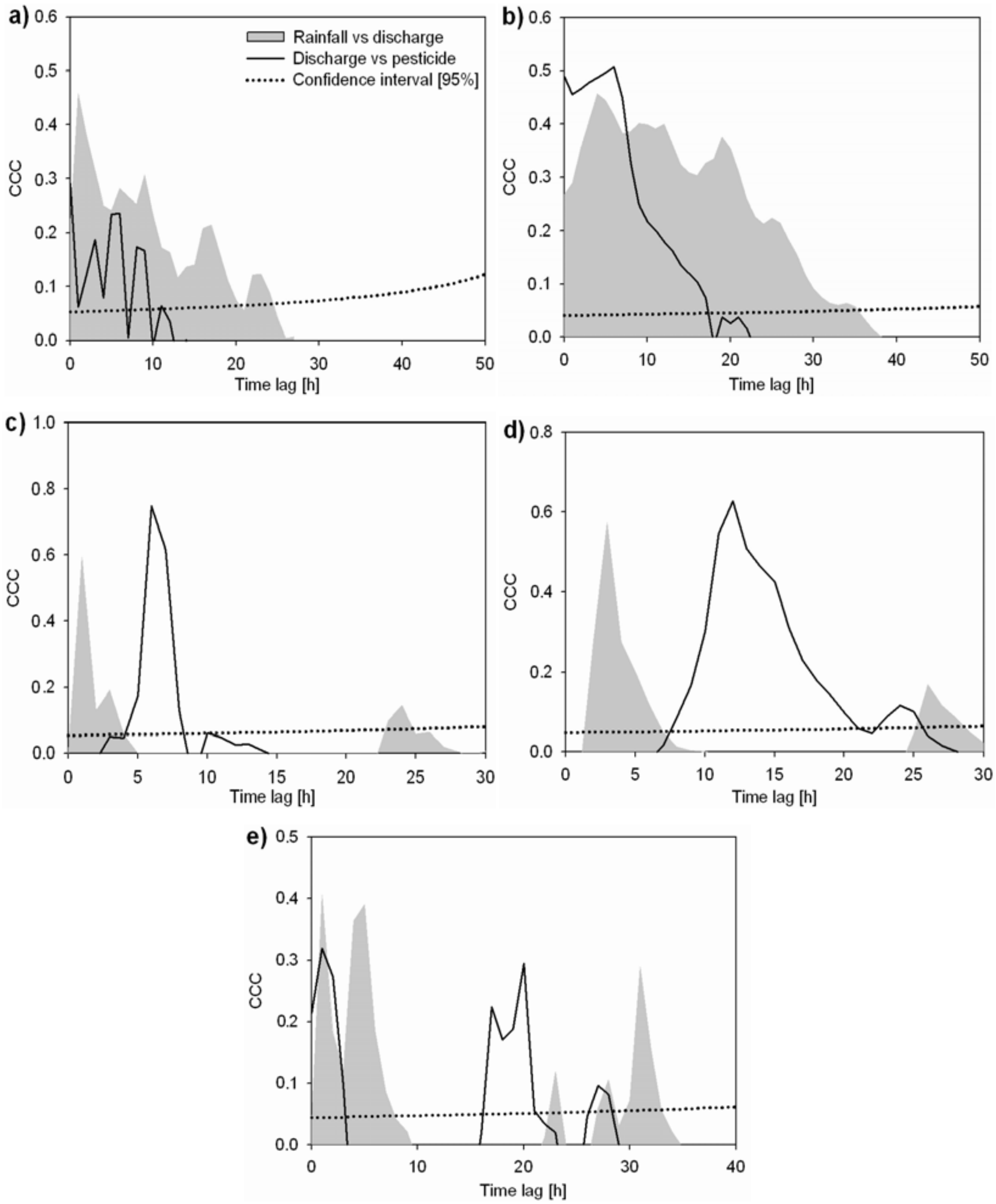

Figure 5.8: Cross-correlograms of rainfall, discharge and pesticide concentration: for HW (left panel) and OL (right panel): (a,b) chlorpyrifos in May, (c,d) chlorpyrifos in August, (e) chlorpyrifos in September.

During the August event, the rainfall-runoff response at HW occurred within one hour. Chlorpyrifos was not observed during the recession limb. The CCC of chlorpyrifos was highest at a 6 h lag time (Figure 5.8c). At OL, the in-stream pattern of chlorpyrifos during discharge was similar as that observed at HW with the peak of chlorpyrifos at a lag time of 12 h after the discharge peak (Figure 5.8d).

During the September event, at HW the two rainfall-runoff responses peaked at time lag 1 and 5 h (Figure 5.8e). An additional pronounced CCC between rainfall and runoff was found at a time lag of 23 and 31 h. Discharge and chlorpyrifos are correlated at very small time-lags and at time lags of 17, 20 and 27 h. The latter CCC peaks do not coincide with highest rainfall-runoff cross-correlations (Figure 5.8e).

5.4 Discussion

5.4.1 Pesticide concentration patterns

Transport mechanisms and pathways of pesticides form a central link between agro-ecosystems and their surrounding environmental compartments. We observed three different concentration patterns of pesticides: (a) increase during the rainfall events as discharge increases, (b) sporadic high values during the falling limb of the runoff peak, and (c) low but more or less continuous values on a baseline level.

On the May event, the first pattern cannot be clearly attributed to a specific transport pathway because the processes contributing to discharge are too complex: several rain events caused overlapping hydrographs. Our time series analysis suggests that a fast flow component, such as surface runoff, which, in some areas, may contribute up to 75% of the total pesticide load (Ng and Clegg, 1997), significantly contributed to the total pesticide load. The highest cross-correlations between discharge and pesticide concentration were observed at short time lags. For example, the highest cross-correlation between atrazine concentration and discharge occurred at time lags between 0 and 3 h at OL; at larger time lags (> 14 h) it vanished (Figure 5.7b). In addition, however, the concentration peaks of more strongly sorbing pesticides such as chlorpyrifos were somewhat delayed to those of less strongly sorbing pesticides such as dimethoate (see Figure 5.4c and 5.4e on 4 May). This chromatographic behaviour points to an interaction with a matrix, probably during transport along a sub-surface pathway (Kahl et al., 2010). Hence, during the May event the pesticide transport was probably controlled by both surface runoff and sub-surface flow.

Our findings agree well with the results of previous studies. Leu et al. (2005) and Duffner (2010) reported that in agricultural catchments atrazine losses were event-driven with concentrations increasing almost simultaneously with increasing discharge and peaking with peak flow. Oliver et al. (2012) also found a strong relationship between peak concentrations of pesticides and peak flow during runoff events, particularly when log K_{oc} < 3. In case of chlorpyrifos (log K_{oc} 3.9), however, they found that the concentration in stream water increased as the hydrograph increased, but it did not decrease as the hydrograph decreased.

The second concentration pattern, the appearance of sporadic post-event pesticide peaks on the falling limb of the runoff curve, was most clearly observed with the more strongly sorbing pesticides such as chlorpyrifos (Figure 5.4e, f), chlorothalonil (Figure 5.4g, h), endosulfan (Figure 5.4i, j), and cypermethrin (Figure 5.4k, l). This incidence is even clearer in the August event, where the hydrograph consisted of two clearly separated runoff peaks, simplifying interpretation. Chlorpyrifos did not peak with the runoff peak but appeared in the river water about 6 h later at the HW station and 12 h later at the OL station (Figure 5.5c, d). Moreover, in the third event in September, the sporadic appearance of chlorothalonil and chlorpyrifos after the peak flows confirmed this type of input pattern (Figure 5.6a, b). In a study of pesticide transport at the hillslope scale in the Mae Sa watershed Kahl et al. (2008) found a similar concentration pattern. Supported by a modelling study, they attributed the appearance of the pesticide peaks at the falling limbs of the runoff curve to preferential subsurface flow (Kahl et al., 2010). Because in the present study the pesticides were not applied under controlled conditions, we can not fully exclude that the observed sporadic pesticide peaks are the result of point sources or local spills. However, we are convinced that the low concentrations in between the sporadic peaks are not an artefact due to sampling, sample preparation or analysis errors. The sampling volume was always determined with a graduated cylinder. A failure of the sampling unit would have been detected immediately. All water samples were prepared and analyzed under exact the same standard conditions. For six of the seven pesticides the analytical method had a high reproducibility (RSD < 20%). Only in case of chlorothalonil, the variability of the method was somewhat higher (RSD = 27%).

The third concentration pattern, steady, but low pesticide concentrations, cannot be explained by the fast transport mechanisms mentioned above. Instead, it points to a continuous leaching of pesticides with the base flow, especially during periods after rainfall. The atrazine concentrations during the recession phase in May at the OL station (Figure 5.4b) are a good example for this pattern.

Our observations agree well with the results of Leu et al. (2004). These authors also observed sustained elevated atrazine concentrations during the long-lasting tailing of discharge after a heavy rainfall. They assigned this finding to a pesticide pool in the saturated zone, which was filled up by vertical fast components during the rain event and subsequently leached to the river over a longer period.

5.4.2 Hydrological implications

Provided that transport is chromatographical, strongly sorbing pesticides should have longer travel times and appear at lower concentrations compared to weakly sorbing pesticides. This holds true when there is sufficient time for interaction between pesticides and soil. In case of a preferential transport, however, the time available for sorption and degradation is drastically reduced, which may lead to an almost direct transfer of pesticides to surface waters (Müller et al., 2003).

At the beginning of the rainy season in May, soils were still rather dry. At low water content, the preferential flow paths are not well connected and the potential of pesticide leaching is low. The detection of high K_{oc} substances, i.e. chlorpyrifos (Figure 5.4e), endosulfan (Figure 5.4i) and cypermethrin (Figure 5.4g) at the HW station shows that retardation did not have a major impact on the loss rates of the pesticides and their temporal dynamics.

As indicated by the higher RCs in August and September the soils in the catchment were wetter as a consequence of the cumulated high rainfalls in the previous months. Antecedent rainfall has an important role in that it increases soil water content which may trigger preferential flow (Kahl et al., 2007) and the leaching of pesticides (Flury, 1996; Lewan et al., 2009). Pesticides may be dissolved in pre-event water and sorb to walls of macropores. Later during a rainfall event, water may travel within macropores through the soil and leach previously sorbed pesticides to the river. Pesticide peaks will be caused by the drainage of a mixture of old and new water. This process is significantly delayed in comparison to surface runoff because the travel distance in the pores is larger and the travel velocity lower (Duffner, 2010; Kahl et al., 2010).

5.4.3 Comparison of pesticide loads between HW and OL gauge

The pesticide concentration patterns as well as the set of detected pesticides were similar at both stations. The fast increase of discharge during rainfall and the appearance of pesticide peaks shortly thereafter (see e.g., atrazine (Figure 5.4a, b), dimethoate (Figure 5.4c, d) and chlorpyrifos (Figure 5.4c, d)) at the HW station, however, indicate a quicker and more sensitive hydrological response at HW than at OL. The steep slopes of the headwater area foster the rapid transfer of water to the stream network. The longer delay between rainfall, discharge and pesticide peaks at the OL station reflects the travel distance from precipitation and application area.

Other than at the HW station, at the OL station two smooth pesticide curves were obtained for atrazine in May and chlorpyrifos in August. A possible explanation is that pesticide losses at the outlet of the catchment are an integral from spatially distributed pesticide sources over the fields located upstream. The larger the upstream area, the more fields contribute to the pesticide load and the smoother is the integrated concentration curve. Obviously, the smoothness of the signal will also depend on the uniformity of application time and rates.

The average areal pesticides loads can tentatively be used to trace back pesticide use in the watershed. Average areal loads of atrazine and dimethoate were highest at the OL gauge. While at HW dimethoate was also lost at high quantities, the average areal load of atrazine was much lower, suggesting that the major atrazine sources were located downstream of the HW gauge. The average areal losses of chlorpyrifos, dimethoate and cypermethrin in the headwater area were higher than those in the whole watershed. This finding suggests that the three pesticides were mainly applied within the HW area, where around 471 greenhouses were in operation (Schreinemachers et. al., 2009). The cultivation per cropping cycle of bell pepper and chrysanthemum under greenhouses requires intensive use of pesticides. The environmental impacts of pesticide used with these two crops are relatively high compared to the other field crops (Schreinemachers et al., 2009).

5.4.4 Implications for the design of appropriate sampling schemes

During rainfall and several hours after rainfall, maximum concentrations of many pesticides such as chlorpyrifos (9.7 µg L^{-1}), chlorothalonil (0.6 µg L^{-1}), and endosulfan (0.09 µg L^{-1}) exceeded the European limits for pesticides in surface water (chlorpyrifos: 0.03 µg L^{-1}; endosulfan: 0.005 µg L^{-1}) and/or the Canadian water quality guidelines for protection of aquatic life (chlorothalonil: 0.18 µg L^{-1}; chlorpyrifos: 0.0035 µg L^{-1}; endosulfan 0.02 µg L^{-1}). However, they do not exceed the limit of the Thai quality standard of surface water issued by the National Environmental Board (1994) of 50 µg L^{-1} for total organochlorines.

Most of the pesticides showed highly dynamic concentration patterns. Highest concentrations were detected both during initiation of runoff and during the longer recession phase. These extreme events were shortly pulsed and lasted less than one hour. This highly dynamic nature of pesticide input to surface waters should have consequences for monitoring schemes and ecotoxicological tests. In our study we took samples every 10 minutes and mixed six samples to one composite sample, ending up with an hourly resolution. Using a monitoring strategy with a lower temporal resolution would lead to an erroneous assessment of the water quality status. This point was stressed by Holvoet et al. (2007). They stated that the current ecotoxicological testing and risk assessment approaches need to be tuned to the specific dynamics of pesticides in surface waters. While conventional ecotoxicological tests assume a constant dose of a contaminant to an organism, the stress of the aquatic ecosystem induced by pesticides is characterized by short and multiple-pulsed extreme events.

Pesticide monitoring can be used to strengthen confidence in environmental and ecological exposure estimates. Understanding the fate of pesticides in aquatic environments and assessing their potential effects on non-target organisms are important for protecting environmental and human health. During single rainfall events, the transport pattern of pesticides is highly complex. This must be considered in the design of sampling schemes for pesticide monitoring and ecological risk assessment. To ensure accurate monitoring, high-resolution sampling schemes are needed. Using a too low temporal resolution would result in a biased assessment of the water quality status (see also Holvoet et al., 2007). Also Reinert et al. (2002) pointed to the importance of pulsed concentrations of pesticides and time varying exposure for ecotoxicological testing and risk assessment approaches. Moreover, the average exposure may not lead to an adequate estimate of toxic effects. Pesticide properties and input patterns must be taken into account for choosing an adequate sampling period. We observed a high pesticide exposure during the initiation of rainfall and runoff peak but also during the later recession phase.

5.5 Summary and conclusions

Six out of seven pesticides applied by local farmers were detected in the Mae Sa River. Measured concentrations exceeded European Union and Canadian limits for pesticides in surface water but were far below the Thai limits. Pesticide loss was related to sorption strength, but other factors interfered. We identified three different pesticide input patterns. The first pattern – increasing concentrations during the rainfall events as discharge increases – suggests transport with surface runoff. The second pattern – sporadic high concentrations during the falling limb of the runoff peaks –was mostly observed with pesticides of medium to high K_{oc} ($2.5 < \log K_{oc} < 5$) such as chlorpyrifos, chlorothalonil, endosulfan, and cypermetrin. It points to a sporadic sub-surface flow component (e.g., preferential interflow). The third pattern – low but more or less continuous concentrations on a baseline level – is probably related to some long-term storage in the underground.

The highly dynamic nature of pesticide input into surface water has important implications for the design of representative monitoring schemes and ecotoxicological risk assessment. The sampling scheme must be set up in a way to capture the peaks during the rain events and peak runoffs, but also the short and pulsed peaks during the following recession phases. Sampling schemes with a high temporal resolution are therefore advisable.

Acknowledgements

We thank Juthasiri Rohitrattana for her support in collecting pesticide samples and performing the pesticide analyses in the frame of her master thesis in May 2008. We thank Dr. Alan Ziegler for his support in comparing discharge data in the Mae Sa watershed. Many thanks go to Matthias Bannwarth for his land use mapping and to Ittipon Sodsaard, Mai Tanamrungruang, and Christian Halle for their technical assistance. We also thank Dr. Rudolf Frank of Landesanstalt für Landwirtschaftliche Chemie for his vital support in pesticide analysis. We gratefully acknowledge the financial support by Deutsche Forschungsgemeinschaft (DFG) in the frame of SFB 564 (The Uplands Program).

6 Publication 4 - Simulation of streamflow components in a mountainous catchment in northern Thailand with SWAT, using the ANSELM calibration approach

M. A. Bannwarth[1,], C. Hugenschmidt[1], W. Sangchan[1], M. Lamers[1], J. Ingwersen[1], A. D. Ziegler[2], T. Streck[1]

[1]Institute of Soil Science and Land Evaluation, Biogeophysics Section, University of Hohenheim, Germany.[2]Department of Geography, National University of Singapore, Singapore.

Hydrological Processes
(submitted)

Abstract

Highland agriculture is intensifying rapidly in Southeast-Asia leading to alarming high applications of agrochemicals. Understanding the fate of these contaminants requires carefully planned monitoring programs, and in most cases, accurate simulation of hydrological pathways into and through water bodies. We simulate runoff in a steep mountainous catchment in tropical SE Asia. To overcome calibration difficulties related to the mountainous topography, we introduce a new calibration method, named ANSELM (A Nash-Sutcliffe Efficiency Likelihood Match), which allows the assignment of optimal parameters to different hydrological response units in simulations of stream discharge with the SWAT (Soil and Water Assessment Tool) hydrological model. ANSELM performed better than the Parasol calibration tool built into SWAT in terms of model efficiency and computation time. The most sensitive model parameters were those related to baseflow generation, surface runoff generation, flow routing, and soil moisture change. The coupling of SWAT with ANSELM yielded reasonable simulations of both wet- and dry-season storm hydrographs. Nash-Sutcliffe model efficiencies for daily stream flow during two validation years were 0.77 and 0.87. These values are in the upper range or even higher than those reported for other SWAT model applications in temperate or tropical regions. The different flow components were realistically simulated by SWAT, and showed a similar behavior in all the study years, despite inter-annual climatic differences. The realistic partitioning of total streamflow into its contributing components will be an important factor for using this hydrological model to simulate solute transport in the future.

6.1 Introduction

Sustainable use of natural resources is of increasing importance in mountainous regions of Southeast Asia where highland agriculture is intensifying rapidly (Schreinemachers and Sirijinda, 2008). Over the last few decades, cropping periods have expanded; and increasing fertilizer and pesticide inputs are required to sustain crop yields and overcome diminishing soil fertility (Bruun et al., 2009). Agrochemical contaminants are of great environmental concern because of the potential to leach into aquatic systems where they may threaten aquatic life and human health (Sangchan et al., 2013; Ziegler et al., 2009). Understanding the threat of these contaminants not only requires carefully planned monitoring programs, but in some cases, accurate simulation of contaminant transport into and through stream systems.

Reliable simulations are only possible if the hydrological model is soundly calibrated and tested. Both procedures strongly depend on data availability and quality. Previous investigations within our study area in northern Thailand revealed that contaminants such as pesticides tend to be transported to stream water by lateral subsurface flow (Sangchan et al., 2012; Duffner et al., 2012; Kahl et al., 2007; Kahl et al., 2008). Duffner et al. (2012) and Hugenschmidt et al. (2010) pointed to a considerable fraction of shallow subsurface flow (i.e. lateral flow) on total flow during single events in a small subcatchment at the site. This finding implies that a model, which is intended to be used to simulate the transport of contaminants, must not only be calibrated with regard to a precise reproduction of the water balance and discharge dynamics, but also with a reasonable partitioning of runoff generating flow components.

Of the vast number of hydrological models available, only a few are capable of simulating complex land management operations and pesticide transport at catchment scale. One of these models is the Soil and Water Assessment Tool (SWAT; Arnold et al., 1998), which has been applied frequently to watersheds worldwide (see Gassman et al., 2007). Most SWAT applications have been carried out in temperate regions (i.e. Neitsch et al., 2011; Larose et al., 2007; Green and van Griensven, 2008; Ullrich and Volk, 2009). The number of SWAT model studies carried out in tropical or subtropical regions, however, is increasing (Schuol et al., 2008; Tripathi et al., 2003; Ndomba et al., 2008; Setegn et al., 2010; Strauch et al., 2012). Nevertheless, most applications focus only on water balance (Table 6.1). This is particularly true for studies conducted in Thailand. Kuntiyawichai et al. (2011), for example, performed SWAT simulations to evaluate flood management options in the 4145 km² large Yang River basin in northeast Thailand. Another SWAT application was carried out by Reungsang et al. (2010) in a subbasin of the 7000km² Chi River. SWAT reproduced the monitored runoff well, but the R^2 never exceeded 0.72. Phomcha et al. (2011) simulated discharge in the Lam Shonti watershed (357 km²) in central Thailand, where the elevation ranges between 100 and 700 m above sea level and land use was dominated by forest and agriculture. The SWAT model performed well but the study demonstrated some shortcomings in predicting stream during the dry season. Collectively, none of the SWAT model applications in Thailand have been carried out in catchments with less than 100 km² (Table 6.1). Also, catchments with steep orography have not been simulated. Furthermore, none of the studies focused on simulating solute runoff or transport partitioning.

Manual calibration of model parameters is a time and labor intensive task that does not necessarily yield the best parameter set. Hence, automatic calibration techniques are widely applied nowadays. Examples for frequently used automatic calibration techniques are: (a) Markov-Chain Monte-Carlo (MC^2) methods, which derive optimal parameters from a large number of runs with different parameter sets (Metropolis et al., 1953); (b) Shuffled Complex Evolution (SCE), which uses an intelligent search algorithm to find the best parameter distribution (Duan et al., 1988); and (c) Sequential Uncertainty Fitting (SUFI-2), which uses the uncertainty bands of MC^2 runs for optimization (Abbaspour et al., 2004).

Calibration of complex models is hampered by uncertainties in input data as well as by limitations of model structure and parameterization. One complicating issue is often the lack of model flexibility to accurately represent catchment heterogeneity and scale processes. Several techniques have been developed to assess model uncertainties including Bayesian approaches (e.g. Kuczera and Parent, 1998; Ajami et al., 2007), autoregressive error models (e.g. Bates and Campbell, 2001; Duan et al., 1993) and "fuzzy" approaches that do not have strict statistical assumptions (e.g., the Generalized Likelihood Uncertainty Estimation (GLUE; Beven and Binley, 1992)).

The built-in automatic calibration functionality in SWAT is performed with Parasol, a method based on Shuffled Complex Evolution (SCE) algorithm (van Griensven et al., 2006). The major drawback of Parasol relates to the electability of model parameters. To save computer time, Parasol reduces the number of parameters by calibrating all parameters of one modeled category together. This lumped approach limits the possibility to parameterize spatially variable processes in a heterogeneous catchment. To overcome this issue, Lin and Radcliffe (2006) first calibrated a set of lumped parameters across a catchment, then coupled SWAT with the PEST parameter estimation software (Doherty and Johnston, 2003), a code for inverse parameter optimization based on the Gauss-Marquardt-Levenberg algorithm, to account for the spatial variability of some elected parameters. Another tool that is used more frequently is SWAT-CUP (Abbaspour et al., 2004; http://www.eawag.ch/forschung/siam/software/swat/index), which used the SUFI-2 method to support SWAT calibrations. In the latest version, however, SWAT-CUP has evolved into a calibration "swiss-knife", featuring various calibration methods. SWAT users can now select between the standard Parasol method, SUFI-2, and various MC-based methods.

In this work we investigate the applicability of the SWAT model in simulating the discharge dynamics and hydrograph partitioning in a tropical, mountainous headwater catchment. The SWAT model was calibrated and tested on a three-year dataset. For calibration, we developed a new tool: ANSELM (A Nash-Sutcliffe Efficiency Likelihood Match). This calibration tool allows assigning unique parameters to specific soil and land-cover units. The results were compared with the outcome of a Parasol calibration. The performance of the calibrated model is assessed with different efficiency criteria and with the help of an uncertainty analysis. Finally, the composition of the simulated streamflow is evaluated in detail.

Table 6.1: Overview of current studies on streamflow calibration with SWAT in Thailand and climatically comparable regions in Southeast-Asia.

Study	Calibration goal	Study site	Elevation (m above sea level)	Precipitation (mm)	Land use (%)	Number of gauging stations	Simulation period (years)	Model efficiency (streamflow calibration)
Khoi and Suetsugi, 2012	streamflow, sediment	Be River catchment, 7500 km², Central Vietnam	100 – 1000	2400 mm (May – Oct)	51% agriculture, 43% forest, 6% urban and others	1	10 yrs calibration	R^2 = n.a. NSE = 0.8
Reungsang et al., 2012	streamflow	Chi River, Subbasin II, 7000 km², Northeast Thailand	148 – 250	1193 mm (May - Oct)	56% rice, 15% field crops, 10% forest, 6% pasture,13% urban	4	1yr calibration 3 yrs validation	R^2 = 0.77 – 0.88 NSE = 0.55 – 0.79
Kuntiyawichai et al., 2011	streamflow	Yang River, 4145 km², subbasin of Chi River, Northeast Thailand	600 m on average	1390 mm (May – Oct)	4% urban, 60% agriculture, 33% forest, 3% water bodies	1	1yr calibration	R^2 & NSE > 0.85
Phomcha et al., 2011	streamflow	Lam Shonti catchment, 357 km², Central Thailand	100-700	1134 mm (May - Oct)	59% forest, 38% agriculture, 3% others	1	2yrs calibration 2yrs validation	R^2 = 0.895 NSE = 0.848
Graiprab et al., 2010	streamflow, climate projections	2 sub-regions of At Samat subbasin, Chi River, 205 and 438 km², Northeast Thailand	115 – 150	1507 mm (May – Oct)	80% agriculture, 7% forest, 4% urban, 9% water & others	2	8 yrs calibration[a]	R^2 = n.a. NSE = 0.7 - 0.89
Alansi et al., 2009	streamflow forecasting	Upper Bernam River, 1097 km², Malaysia	up to 1830	1800 mm – 3500 mm (May – Oct)	3% urban[b], 11% oil palm[b], 23% rubber[b], 54% forest[b], 2% orchards[b]	1	24 yrs calibration 3 yrs validation	R^2 = 0.65 – 0.82, NSE = 0.62 – 0.81
Alibuyog et al., 2009	streamflow sediment	Kiluya and Kalaignon, subbasins of Manupali catchment, 2 km², Philippines	900 – 2000	2347 mm (Jun – Oct)	17% forest, 29% agriculture, 53% grassland, 1% footpaths	4	1 yr calibration	R^2 = 0.87 – 0.99 NSE = 0.77 – 0.83

[a] Calibration was adopted from model application by Rossi et al., 2009; [b] Land use is given in averages because it changed within the calibration period.

6.2 Material and Methods

6.2.1 Study site

The Mae Sa catchment (18° 54′ N, 98° 54′ E) is located 35 km north-west of Chiang Mai in northern Thailand (Figure 6.1). The catchment has a total area of 77 km² spread over elevations ranging from 325 to 1540 m a.s.l. Sharp relief and narrow valleys dominate the catchment. The mean slope is 36%, but slopes steeper than 100% are abundant.

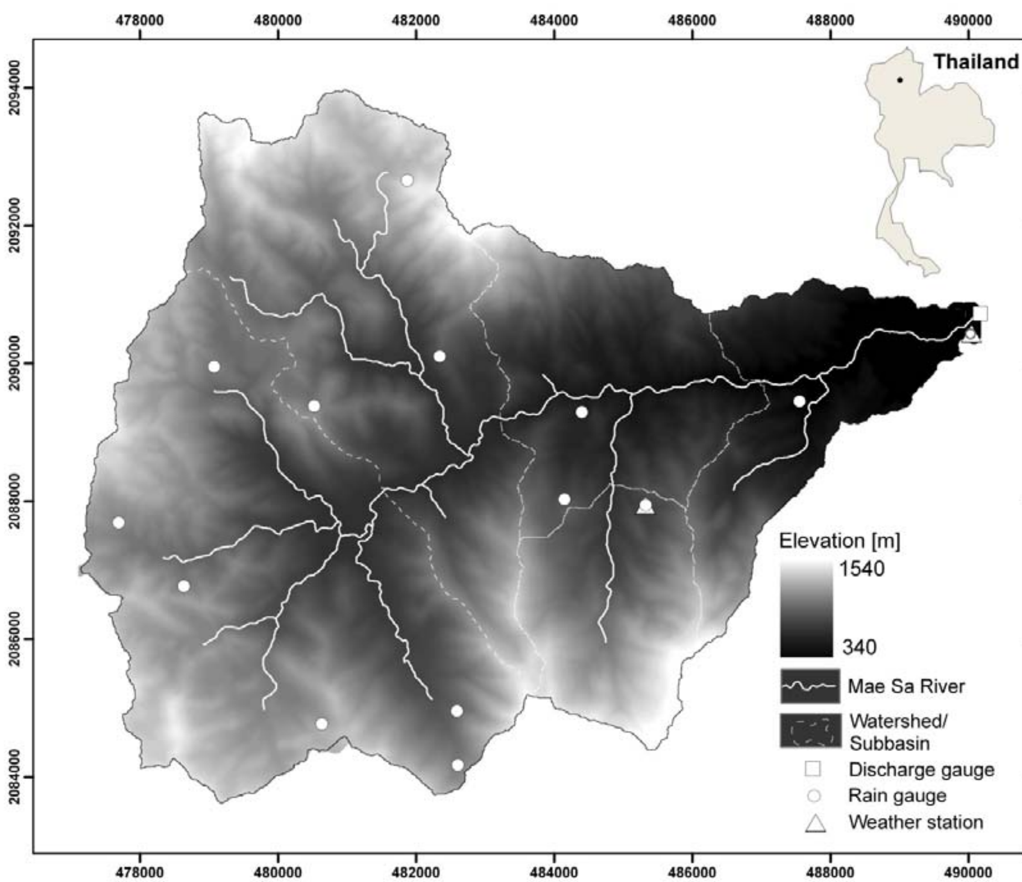

Figure 6.1: Topographic map of the Mae Sa watershed, position of monitoring stations, and the five subbasins used in the SWAT model.

The Mae Sa River is a tributary of the Ping River, one of the major rivers in northern Thailand draining to the Chao Phraya. The river has a length of 12 km; and bed slope ranges between 1 and 20 % (mean = 5%). About 24% of the catchment area is devoted to agriculture. The remaining area is mostly covered by deciduous and evergreen forests of varying degrees of disturbance. Acrisols and Cambisols are the main soil types within the catchment (Schuler, 2008). Mean air temperature is 21°C and annual rainfall is 1250 mm on average (2004 - 2010). The tropical climate in the area is dominated by a rainy season stretching from May to late October, followed by a lengthy dry season (November to April).

6.2.2 Monitoring program and data analysis

Discharge, rainfall and general meteorological variables were monitored in the Mae Sa catchment from July 2007 to December 2010. Solar radiation, rain, air temperature, relative humidity, and wind speed (Thies, Germany; UIT, Germany) were measured at two automated climate stations. Additionally, rainfall was recorded by 12 automatic tipping bucket gauges (Fischer GmbH, Germany) (Figure 6.1). Discharge of the Mae Sa River was monitored at the main catchment outlet at 10-min intervals by an ultrasonic water level sensor (710 Ultrasonic module, Teledyne ISCO Inc., USA). Hand measurements of discharge for establishing the stage-discharge calibration curve were conducted with an acoustic digital current meter (Model ADC, OTT ADC GmbH, Germany) at a broad range of flows. Discharge measurements at the outlet were evaluated against data from another gauging station located 3 km upstream (Ziegler et al., 2013).

6.2.3 The SWAT model

SWAT divides a catchment into subbasins that are each subject to different micro-climatic forcing. Each subbasin is further partitioned into a number of Hydrological Response Units (HRUs) that represent various combinations of land use, soil type and relief. A water budget is computed for each HRU on the basis of evapotranspiration, precipitation, runoff, percolation, and return flow from groundwater and subsurface flow (Neitsch et al., 2011):

$$SW_t = SW_0 + \sum_{i=1}^{t} (R_i - Q_{surf,i} - E_{a,i} - w_{seep,i} - Q_{gw,i}) \qquad (Eq.\ 6.1)$$

where SW_t (mm) is the soil water content at day *t*; SW_0 (mm) stands for initial soil water content; R_i (mm) denotes rainfall depth; $Q_{surf,i}$ (mm) is surface runoff; $E_{a,i}$ (mm) is evapotranspiration; $w_{seep,i}$ (mm) is the water entering the vadose zone from the soil profile; and $Q_{gw,i}$ (mm) is the amount of base flow. In all cases, the subscript i denotes the i-th preceding day.

6.2.4 Setup of the SWAT model and sensitivity analysis

The Mae Sa catchment was divided into five subbasins for simulating discharge generation at a daily time step (Figure 6.1). Preliminary testing suggested that finer subbasin division did not significantly improve simulation results but greatly increased computing time. One rain gauge was selected to represent each subbasin (Figure 6.1). Data from the remaining 9 rain gauges within the Mae Sa catchment were used to fill gaps caused by technical failures. Soil input data were based on prior field work (Schuler, 2008). Elevation and land use were derived from a SPOT 5 image (November 2006; scene center = N19°1'4" E98°49'24"), provided by the Geo-Information and Space Technology Agency (GISTDA, 2007). Parameters for forest vegetation were manually altered from model default values (SWAT2009.mdb; Ver. 2009/Rev481) to align with those of tropical vegetation in the catchment (e.g. increasing maximum of total biomass, LAI and heat units to maturity). Input on management operations were based on interviews with local farmers (Schreinemachers et al., 2011). Following an initial parameterization, a sensitivity analysis was performed with a Latin-hypercube (LH) approach (van Griensven and Meixner, 2007; van Griensven et al., 2006) to identify the ten most sensitive parameters to be used in the subsequent calibration.

6.2.5 Model Calibration

Parasol with SCE searches a global optimum in the parameter space based on the sum of squared residuals (SSQ) or a ranked version of SSQ. Parameters can be updated during the calibration only by assigning new values or adjusting via scalar addition or multiplication (Figure 6.2), either for the whole catchment or for a predefined selection of HRUs. It is not possible to calibrate parameters for specific soil, slope or land-cover units simultaneously. Furthermore, not all parameters can be calibrated.

ANSELM, which is written in Matlab (Version 7.10.0, http://www.mathworks.de), uses the NSE objective function during calibration. It can simultaneously modify values of all parameters separately for different HRU classes. Any SWAT input parameter can be calibrated. ANSELM uses a MC²-calibration approach. It applies a triangular probability density function (pdf) within pre-defined ranges. Range and peak value of the pdf is derived by expert guesses or measurements, the pdf decreases from the peak value linearly to zero at the upper and lower border of the range.

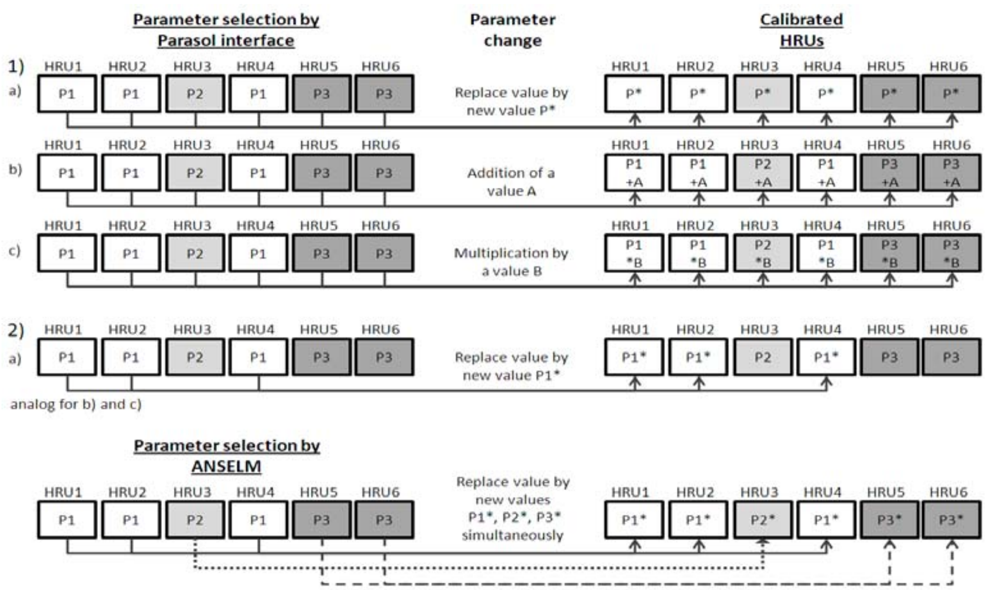

Figure 6.2: Schematic overview of the two calibration tools over six HRUs. PX is related to calibration class X, X=1,…,6 (e.g. the average slope value 1 to the slope class 1).

Model calibration was performed with the 2008 Mae Sa daily time series data. In the first calibration approach using Parasol, the ten most sensitive parameters derived from the sensitivity analysis were selected. As initial values, we used the values of the SWAT model setup. Where applicable, the ranges were set according to the ArcSWAT interface with physically meaningful values (Table 6.2). The maximum number of optimization simulations was limited to 70,000. Other than Parasol, ANSELM allows calibrating a parameter separately for different HRU classes (Figure 6.2). For example, two saturated hydraulic conductivities were calibrated: one for the HRU class Acrisol and one for the HRU class Cambisol. This procedure was applied analogously to the top-ten high-leverage parameters. In total, 42 parameters were calibrated (see Table 6.2).

Table 6.2: Ranking, calibration range and initial values of the ten most sensitive parameters used in calibration of the SWAT model.

Parameter	Rank	Description	Unit	N_HRU[a]	Calibration range[b]	Initial value
Rchrg_Dp	1	Deep aquifer percolation fraction	-	5	0-1	0.05
Gwqmn	2	Threshold depth of water in the shallow aquifer required for return flow to occur	mm	5	0-1000	100
GW_Delay	3	Groundwater delay	days	5	0-200	31
Sol_K	4	Saturated hydraulic conductivity (K_s)	mm/h	2	0-100	10-23
CN2	5	Runoff curve number	-	4	30-95	55-77
Slope	6	Average slope steepness	m/m	5	0-0.99	0.02-0.6
Sol_Awc	7	Available soil water capacity	1	2	0.01-0.5	0.13-0.18
Esco	8	Soil evaporation compensation factor	-	4	0-1	0.9
Alpha_Bf	9	Base flow alpha factor, or recession constant	-	5	0-1	0.048
Slsubbsn	10	Average slope length	m	5	0-200	10-120

[a]Number of different HRU classes. A parameter was simultaneously calibrated for 5 slope classes, 2 soil classes or 4 land use classes, [b] The range depicts parameter values for different HRU classes

Besides the objective functions used during calibration - i.e., the Nash-Sutcliffe efficiency (NSE; Nash and Sutcliffe. 1970) and the sum of squared residuals (SSQ) - we further applied the Kling-Gupta efficiency (KGE; Gupta et al., 2009) for model evaluation. The equations are

$$NSE = \frac{\sum_{t=1}^{n}(q_o^t - q_s^t)^2}{\sum_{t=1}^{n}(q_o^t - \overline{q}_o)^2} \qquad (Eq.\ 6.2)$$

$$SSQ = \sum_{t=1}^{n}(q_o^t - q_s^t)^2 \qquad (Eq.\ 6.3)$$

$$KGE = 1 - \sqrt{(r-1)^2 + (\alpha-1)^2 + (\beta-1)^2} \text{ with } \alpha = \sigma_s / \sigma_o \text{ and } \beta = \overline{q}_s / \overline{q}_o \qquad (Eq.\ 6.4)$$

where q_o^t and q_s^t (m³ s^{-1}) are observed and simulated discharge at time t, respectively. The symbols $\overline{q}_o$ and $\overline{q}_s$ (m³ s^{-1}) stand for mean observed and simulated discharge, respectively. The symbols σ_s and σ_o are the standard deviations of the simulated and observed discharge; and ***r*** denotes the linear correlation coefficient between the simulated and the observed values. The index ***n*** is the number of time steps. The NSE and KGE indices range from -∞ to 1, where 1 denotes the best model efficiency. The SSQ ranges from 0 to ∞, where 0 denotes the best efficiency.

6.2.6 Uncertainty analysis

ANSELM employs a GLUE uncertainty analysis approach (Beven and Binley, 1992) based on the following weighted likelihood equation:

$$w_i = \frac{NSE(i)}{\sum_{j=1}^{N} NSE(j)}, \qquad (Eq.\ 6.5)$$

where w_i is the weight of the i-th behavioral run. A run is set as “behavioral”, when its respective likelihood function (in this case the NSE) is above a certain threshold predefined by the user. The symbols $NSE(i)$ and $NSE(j)$ denote the NSE of the i-th and j-th behavioral run, respectively; and N is the number of behavioral runs. The 95% prediction uncertainty (PU) bands for daily discharge are derived from the cumulative density function of all weighted behavioral runs. The NSE was taken as the likelihood function; and the threshold for non-behavioral runs was set to zero. The zero value was chosen to get broad uncertainty bands that should cover all of our observations. This choice is in line with other GLUE applications using SWAT (Yang et al., 2008; Shen et al., 2012).

The uncertainty analysis in the Parasol calibration follows the approach of van Griensven and Meixner (2007). The method, based on χ^2 statistics (Bard, 1974), divides the sample population in simulations with “good” and “bad” parameter sets. The SCE finds a parameter set consisting of *p* free parameters with lowest SSQ. The threshold of a "good" set is defined by the equation:

$$c = SSQ(\theta^*) \cdot \left(1 + \frac{\chi^2_{P,0.95}}{N-P}\right) \qquad (Eq.\ 6.6)$$

where *N* stands for the number of observations, θ^* denotes the vector with the best parameter values, and $\chi^2_{P,0.95}$ is χ^2 for *P* parameters at a 95% confidence level. The 95% PU bands of daily discharge are derived from the highest and the lowest daily values of all "good" simulations.

6.3 Results

6.3.1 Model calibration and validation

Of the 27 parameters selected by the LH sensitivity tool for discharge optimization, the three most sensitive were those associated with simulating base flow: Rchrg_Dp, Gwqmn, Gw_Delay (Table 6.2). The next most sensitive parameters were the soil parameter Sol_K, which controls water flux in soil and curve number (CN_2), which governs infiltration and thereby surface runoff generation. Our finding that the mean slope parameter of every HRU is the sixth most sensitive parameter demonstrates the importance of topography in SWAT. The only sensitive parameter related to evaporation was Esco, which controls the loss of water by evapotranspiration from deep soil layers. The final calibrated parameter values using Parasol (Parasol-SWAT) and ANSELM (ANSELM-SWAT) are shown in Table 6.3.

The model efficiencies of the simulations of the calibration year (2008) and the validation years (2009 and 2010) are shown in Table 6.4. The simulations were performed with the parameters derived from the final run of both calibration methods respectively. ANSELM-SWAT yielded the best simulation result for the 2008 calibration period: NSE, SSQ and KGE values were 0.83, 27.33, and 0.91, respectively. In the first test period (2009), modeling efficiencies only slightly dropped (NSE = 0.77).

Table 6.3: Calibrated parameter values of the two calibration approaches.

Parameter [a]	Unit	Parasol	ANSELM [b]
Rchrg_Dp	-	0.22	0.11 - 0.253
Gwqmn	mm	335.99	98.12 - 350.67
GW_Delay	days	186.16	24.56 -74.35
Sol_K	mm/h	43.18	9.56 - 27.45
Cn2	-	53.98	36.59 - 66.52
Slope	m/m	0.26	0.047 - 0.658
Sol_Awc	mm/mm	0.5	0.12 - 0.2
Esco	-	0.28	0.26 - 0.43
Alpha_Bf	-	0.149	0.009 - 0.11
Slsubbsn	m	105.25	12.00 - 112.11

[a] Parameter descriptions are listed in Table 6.2

[b] The range depicts parameter values of different HRU classes

Table 6.4: Efficiency indices of the two approaches for the periods of calibration and validation.

	Parasol			ANSELM		
Year	NSE	SSQ	KGE	NSE	SSQ	KGE
2008[a]	0.617	61.63	0.822	0.831	27.33	0.907
2009[b]	0.227	91.80	0.643	0.770	27.80	0.882
2010[b]	0.664	192.9	0.828	0.874	70.89	0.834

[a]Calibration year, [b] Test year, NSE: Nash-Sutcliff efficiency, SSQ: Sum of squared residuals, KGE: Kling-Gupta efficiency. Values are for the best runs of the three calibration approaches.

In contrast, the NSE of Parasol-SWAT significantly decreased from 0.62 in the 2008 calibration simulation to 0.23 during the 2009 test simulation. In the second validation period (2010), the NSE values of both methods were higher than in the calibration year (0.66 and 0.87 for Parasol and ANSLEM, respectively). The better performance in 2010 is related to the fact that the NSE objective function weights being proportional to peak magnitudes. High peaks at the end of 2010 inflated the NSE of both calibration approaches (Figure 6.3). In comparison, the sum of squared residuals (Eq. 6.3) is lowest in 2008 and highest in 2010: e.g., with Parasol-SWAT it increases from 6 to 192, while with ANSELM-SWAT it increases from 27 to 70.

6.3.2 Discharge dynamics

The discharge in the dry periods before and after the rainy season is well captured by ANSELM-SWAT in all three years (Figure 6.3). Year 2009 is an exception: ANSELM-SWAT simulates small discharge peaks in February and March that were not observed at the gauging station. The recession behavior of the hydrograph is well described by ANSELM-SWAT. In comparison, Parasol-SWAT shows severe deficiencies in predicting the recession limbs at the end of the rainy season. Flashy discharge during the rainy season is generally well reproduced by ANSELM-SWAT (Figure 6.3). While the timing of storm peaks is generally modeled adequately, the magnitudes are not, particularly in 2009. Parasol-SWAT simulations match the observations at the end of the dry season (January to April), but they do not perform well at the onset of the rainy season (May to July). The magnitude and recession of discharge

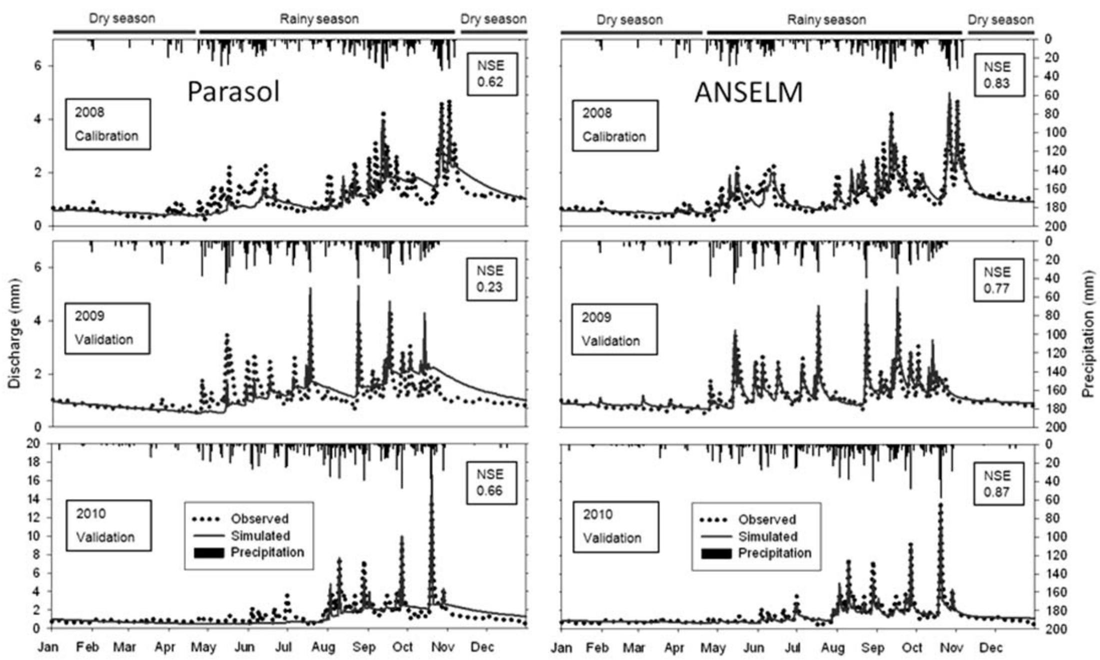

Figure 6.3: Observed and simulated discharge at the outlet of the Mae Sa watershed together with the corresponding precipitation. Left: Final calibration using the Parasol method. Right: Final calibration using the ANSELM method. Note the different scale of the discharge axis in 2010.

The magnitude and recession of discharge peaks markedly deviate from the measured discharge time series. In general, discharge peaks are underestimated; and recession occur too fast in both the calibration and validation periods. At best, Parasol-SWAT only captures the "average" trend of observed discharge in the raining season.

Annual rainfall did not vary greatly for the three years considered (1281 – 1352 mm; Table 6.5). However, annual discharge was greatly different in 2008 and 2009 compared with 2010 (378 - 423 versus 517 mm; Table 6.5). The 2010 rainy season commenced almost four weeks later than in the two previous years, but received the same total amount of rainfall. Several large storms produced larger discharge peaks in 2010 compared to the previous years. Both calibration approaches closely matched the observed 2008 annual discharge (378 mm). For 2009, ANSELM-SWAT and Parasol-SWAT slightly overestimated the annual discharge (423 mm) by 2% and 8% respectively. In 2010, both methods underestimated the annual discharge (517 mm) by 5% (Parasol-SWAT) and 4% (ANSELM-SWAT). The predicted runoff coefficients (ROCs) based on the ANSELM-SWAT simulations were very similar to the observed ROCs (Table 6.5).

Table 6.5: Observed and predicted total annual discharge of the two calibration approaches.

Year	Annual discharge (mm)			Annual runoff coefficient	Annual runoff coefficient	Observed annual precipitation (mm)
	Parasol	ANSELM	Observed	ANSELM	Observed	
2008	371	382	378	0.28	0.28	1352
2009	456	432	423	0.34	0.33	1281
2010	492	496	517	0.37	0.39	1316

6.3.3 Time series uncertainty analysis

The 95% PU bands of the Parasol calibration were generally narrower than those derived by the GLUE analysis with ANSELM (Figure 6.4). Consequently, observed discharge values frequently fell outside the confidence bands of Parasol. Only seven out of 70000 Parasol model runs were identified as "good", based on the threshold Parasol used. The ANSELM approach produced nearly 45,000 runs that were behavioral. The observed time series falls completely within the PU band from the ANSELM simulations. Nevertheless, ANSELM-SWAT does tend to underestimate the baseflow in some sections of the hydrograph. Uncertainty in predicting rainfall event peaks increases proportionally with the peak magnitude - this is true for uncertainty evaluation techniques considered herein.

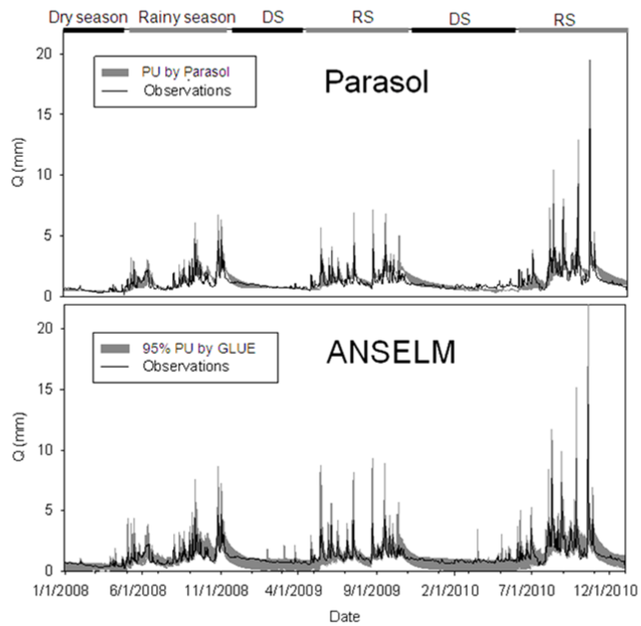

Figure 6.4: Predicted uncertainty bands of the daily discharge for the years 2008 to 2010 for both calibration approaches based on the calibration period 2008.

6.3.4 Simulating flow components

Although observed hydrological conditions were highly variable in time, the dynamics of the discharge was reproduced well during all periods by ANSELM-SWAT (Figure 6.4). Parasol-SWAT, however, was not suited for simulating all flow components. For example, the poorly reproduced recession limbs indicated that lateral flow was not simulated accurately. Because the ANSELM approach yielded the highest values of all objective functions (Table 6.4), its final parameter set was chosen to evaluate the different flow components contributing to the total discharge (Figure 6.5 and 6.6). Despite the given temporal differences between the study years (Figure 6.5), some general flow component trends were observed in all years. Baseflow contributed almost 100% to the streamflow in the very dry period between December and March. The baseflow fraction increased throughout the rainy season with a high near the end of the year. Throughout this behavior, the total contribution by baseflow also increased both in observed and simulated baseflow (Figure 6.5 and 6.5; 2008: From 0.6 to 0.85 mm/day; 2009: From 0.85 to 0.93 mm/day and 2010: 0.93 to 1.0 mm/day).

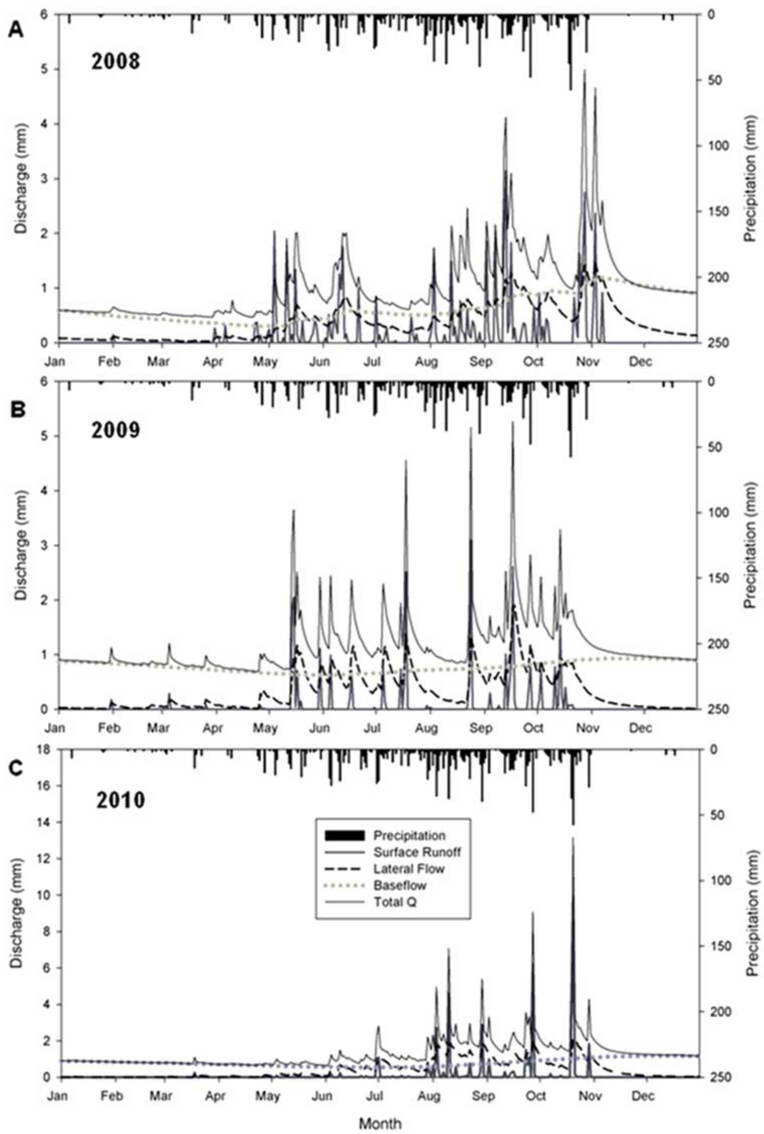

Figure 6.5: Simulation of the flow components by SWAT. The simulation is based on the final ANSELM calibration.

Only substantial basin-wide rainfall contributions would trigger small peaks of surface runoff and lateral flow (Figure 6.5, 6.6A). At the beginning of the wet season as rainfall occurred more frequently, the total streamflow was influenced by both baseflow and lateral flow (as indicated by the near parallel component hydrographs in Figures 6.5, 6.6B). The volume of lateral flow produced during storms increased after the onset of the rainy season (Figure 6.5). This behavior is interrupted by surface runoff peaks, which evolve almost directly at the time of the respective rain event. The magnitude of the peak was controlled by the depth and temporal distribution of rainfall. In the beginning of the rainy season, rain events produced only small surface runoff peaks. In comparison, events at the end of the rainy season often generated very high peaks (e.g., October 2010; Figure 6.5, 6.6C). These high surface runoff peaks dominated storm discharge response. For example, surface runoff contributed 75% of the largest stream discharge peak in late October 2010. Throughout the year, the shapes of the recession limbs of the lateral flow and total stream flow were similar (Figure 6.5, 6.6 D).

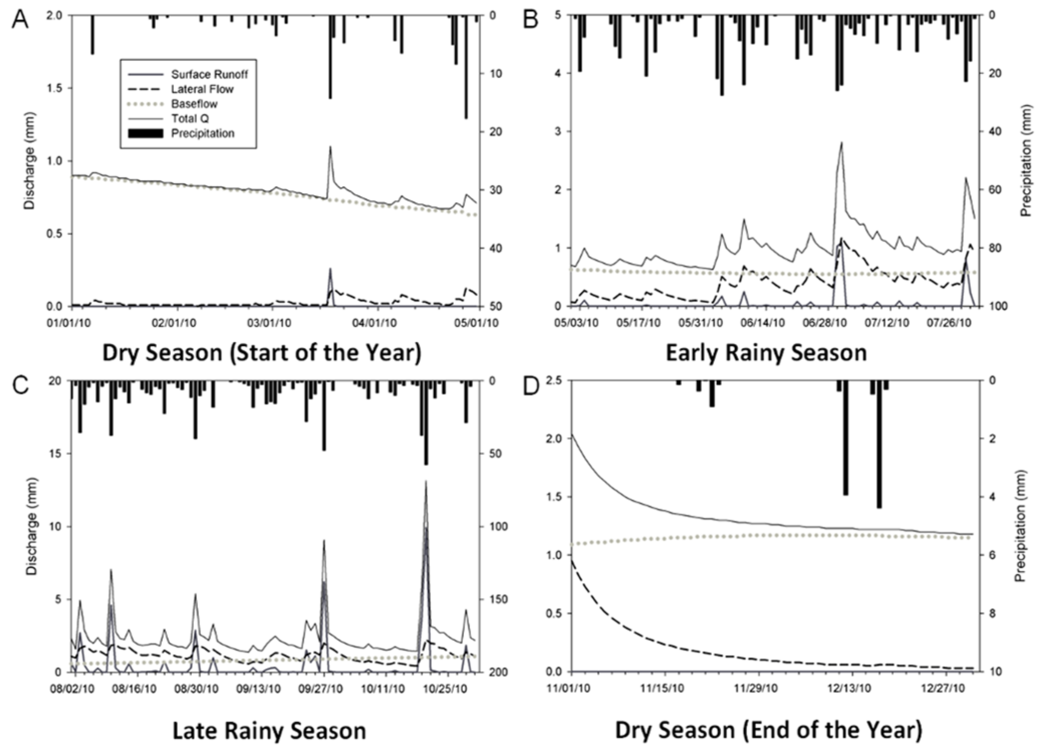

Figure 6.6: Simulation of the flow components by SWAT for four characteristic periods exemplified for the year 2010. The simulations were run with the parameters derived from the final calibration run using ANSELM-SWAT.

6.4 Discussion

6.4.1 Applicability of ANSELM

Both calibration approaches yielded acceptable model efficiencies after 70,000 optimization steps, while Parasol needed approximately 2 hours longer (4% of the total time) for 70.000 steps than ANSELM. However, the ANSELM tool was able to quickly identify acceptable parameter sets (i.e., produce NSE of > 0.5; Moriasi et al., 2007) within less than a 100 optimization steps. In contrast, the Parasol calibration approach required more than 45,000 optimization steps to obtain simulation with a NSE above 0.5. The performance differences could relate to Parasol calibrating 10 parameters and ANSELM 43, with 43 parameters there is a larger degree of freedom to fit the model to the data set. Also the lower final model efficiencies could be attributed to this difference in the parameterization set. Nevertheless, the ANSELM-SWAT coupling proved to be a useful method to calibrate the SWAT model for simulating hydrological response in our tropical catchment.

6.4.2 Discharge Simulations

Discrepancies of measured versus simulated discharge peaks in the 2009 discharge time series could be related to the steep topography and narrow valleys that contribute to the flashy hydrograph behavior in Mae Sa catchment. Limited flood plain areas in the upper portion of the catchment likely result in fast routing of storm flow to the stream system. Also, the geometry and the similar length of the tributaries in the upper part of the catchment support a fast response (Figure 6.1). The relatively equal flow path length from the catchment boundary to each tributary probably causes a sudden response and an overlay of the runoff response at the observation point.

SWAT simulated both the magnitude and timing of peaks in 2008 and 2010 reasonably. The closeness of simulated and observed streamflow in the dry season suggests that the parameters controlling the baseflow conditions, such as Gwqmn, Rchrg_Dp, GW_Delay and Alpha_Bf, are reasonably calibrated. Based on field data from a subcatchment of the Mae Sa watershed by Hugenschmidt et al. (2010) and Duffner et al. (2012), the simulation of the different flow components showed a reasonable partitioning of surface runoff, lateral flow and baseflow. For all events, baseflow (i.e. groundwater) contributed fractions between 62 and 80%. Lateral flow delivered roughly 30%; and surface runoff varied between 2 and 14%, depending on rainfall intensity. The fraction of each flow component varies according to season (Table 6.6). The direct flow components, surface runoff and later flow, are low during the dry season, but increase significantly in the rainy season.

Table 6.6: Mean contribution of the three major flow components to streamflow as simulated using parameter sets identified by Parasol and ANSELM approaches. The values cover the total observation period from 2008 to 2010.

Flow component (%)	Parasol	ANSELM		
	Complete season	Complete season	Rainy season	Dry Season
Surface runoff	6.5	7.3	11.1	0.9
Lateral flow	29.7	28.8	45.2	11.7
Baseflow	63.8	63.9	43.8	87.5

Comparison of our results with others is hampered by the dearth of modeling studies focusing on long-term variation of simulated runoff components in tropical, steep environments. Some experimental studies on various scales and from different tropical environments may lend insight into the reliability of our simulation results. Dykes and Thornes (2000) reported that overland flow rarely occurred during their studies in a steep tropical rainforest catchment in Brunei. The small contribution of annual surface runoff (7%; Table 6.6) computed in the simulations is reasonable because more than 70% of the catchment is covered by forest. They also identified storm flow runoff coefficients of about 0.4. The annual runoff coefficients simulated by ANSELM-SWAT ranges between 0.28 and 0.37 (Table 6.5). Although this seems to be quite low compared with the storm flow runoff coefficients it is still reasonable, as it represents the average of rainy and dry season.

Baseflow dominates the hydrograph during the dry season, but is overwhelmed by lateral flow during rainy season. Lateral flow – in varying nomenclature – is considered to be dominant or at least important in tropical storm flow generation (i.e. Ziegler et al., 2007; Giertz et al., 2006, Wickel et al., 2008). Hence, the simulation of higher fractions of lateral flow during the rainy season is in agreement with evidence from field experiments. Depletion of soil water after the end of the rainy season is adequately represented by the recession of the lateral flow (Figure 6.5, 6.6D). At this time, baseflow is again the dominant streamflow component, sustaining the discharge during the extended period of little rainfall. This stable behavior in hydrological response favors a reasonable fit of the calibration parameters, which allows the use of the model for further specific applications, where a reliable separation of flow components is necessary.

Although rainfall during all years did not differ greatly, runoff was substantially higher toward the end of the 2010 rainy season. This response was probably caused by the belayed onset of the 2010 rainy season, or perhaps by storm differences that caused differences in catchment wetting. The difference in runoff among those years is simulated adequately by SWAT, providing additional evidence for reasonable parameterization of the model. The use of different uncertainty methods by Parasol and ANSELM (χ^2 and GLUE) results in different widths of the confidence bands. Compared with the band generated by the GLUE method, the band generated by χ^2 is so narrow that is does not cover the observations. Furthermore, the χ^2 method covers the parameter uncertainty, while the GLUE method can cover all sources of uncertainty (Beven and Binley, 1992; Beven and Freer, 2001).

6.4.3 Comparison of model performance with other studies

SWAT was not able to simulate the observed hydrograph adequately using default model parameters. Some critical parameters relating to runoff generation (e.g. curve number) and topography were not representative of the tropical, mountainous conditions of the Mae Sa catchment. In addition, baseflow-related parameters were very sensitive in this catchment, where long dry periods cover nearly half of the modeling period. Following an extensive parameter optimization process, the NSEs obtained in this study were reached by SWAT coupled with ANSELM (NSE=0.77-0.87).

Kannan et al. (2007) achieved NSEs of 0.60 simulating discharge within their study site in UK—although they encountered trouble simulating the peaks correctly. Larose et al. (2007) reached NSEs between 0.51-0.66, but had difficulties in reproducing both peak flows and base flows. Tripathi et al. (2003) reported for their monsoon-driven, North Indian catchment that peaks were underestimated in the beginning of the simulations and then over-estimated during latter periods. Phomcha et al. (2011) produced results for their site in central Thailand that were congruent with those reported herein: NSE values > 0.7 were produced during both calibration and testing periods. Elsewhere, Reungsang et al. (2010) achieved R^2 values of ≤ 0.72 for their simulations in a 7000 km² sub-basin of the Chi River in Thailand. And recently, Kuntiyawichai et al. (2011) achieved an NSE as high as 0.85; and they stated that there was also no clear trend in discrepancies between observed and simulated discharge. The studies above and further available SWAT applications for Southeast Asia (Table 6.1) confirm that the model performance obtained within the presented study was in the upper range or even higher than those reported elsewhere, be it in temperate or tropical zones.

6.5 Conclusion and Outlook

The SWAT model was found to be capable of simulating discharge in the 77-km^2 tropical Mae Sa catchment in Thailand at a level of skill equal to or higher than achieved in other catchments worldwide. Part of this success can be attributed to the introduction of the ANSELM tool that allowed assigning unique parameters to specific soil and land-cover units, and thereby leading to a better representation of heterogeneous catchment variables that affect runoff generation. The most sensitive parameters included three related to baseflow generation, as well as others that controlled surface flow generation, runoff routing, and soil moisture dynamics. The calibrated SWAT model produced good simulations of the timing and peaks of rainy season storm events. Simulation of the baseflow in the protracted monsoon dry season was more challenging, yet acceptable. Comparison with results from field experiments in other tropical study sites gives confidence that the separation of the flow components (baseflow, lateral subsurface flow, runoff) all over the seasons is reasonable. Hence, simulations for which the partition of the hydrograph becomes relevant are highly possible. In our case, this initial model evaluation phase provides us with confidence that SWAT, coupled with ANSLEM for calibration, can be applied to intended future simulations of pesticide transport in the catchment.

Acknowledgements

This project was supported by Deutsche Forschungsgemeinschaft (DFG) in the framework of SFB 564 "The Uplands Program" and in part by SARCS grant 95/01/CW-005; APN grants #ARCP2006-06NMY, #ARCP2007-01CMY & #ARCP2007-01CMY; NASA grant NNG04GH59G, and NUS grant R-109-000-092-133. The authors would like to express their gratitude to Dipl.-Math. Anselm Rohland for supporting the development of the ANSELM tool.

7 General discussion

Before hydrology and the transport of agrochemicals within a catchment can properly be simulated by models, investigations on the hydrological characteristic and dynamics of specific solutes need to be performed. As shown in the previous chapters (Chapter 3 - Chapter 6), those issues have been addressed within this thesis and the main research objectives have been answered. In the following, the benefits of these investigations for the different research fields within this thesis will be discussed.

7.1 Rainfall analysis and its importance for hydrological assessment, pesticide transport and modeling

The first part of the presented study focused on the analysis of the spatio-temporal variability of rainfall in the Mae Sa watershed (Chapter 3). The characteristic of rainfall variability in the catchment was identified and the quality of rainfall data that are used in the following model application were checked. Hosting a monitoring density of about 5 km² per rain gauge, this study presents a data set with a high spatial resolution for an environment where monitoring data are extremely rare (Wilk and Andersson, 2000; Dykes, 2000).

Tests with regard to a reduced rain gauge network density revealed that at least nine stations must be operated to remain within the 5% and 10% allowed deviation of the true annual mean. The ANOVA indicated no significant difference between the station means, which was supported by results from the tests, where each station was removed in turn. There, only one station (R02, Figure 3.1) exceeded the 5% and 10% limit in all three years. While the true annual mean is still well reproduced based on nine stations, such reduction may cause imprecise information on spatial and temporal distribution of rainfall. The importance of a dense survey was reflected during the studies on runoff generation, which is described in Chapter 4. Rainfall in the 7 km² Mae Sa Noi subbasin was recorded by four close-by stations (Figure 4.1) and during E1 (Chapter 4) rainfall received by the lower stations (MSN and MSM, Figure 4.1) was non-representative for this particular runoff event. Based on cross correlation analysis of those four stations, a data exchange between the stations was reliable. Hence, the runoff event could be matched to representative rainfall data, which was important for the interpretation of the results. Such findings are in good agreement with a statement by Woods et al. (2000), who stressed that especially in smaller catchments and catchments that respond quickly to rainfall input (i.e. mountainous catchments) a detailed monitoring is necessary. Particularly due to the relevance of spatio-temporal distribution for distinct runoff generation processes (Tetzlaff and Uhlenbrook, 2005), this fact must be considered in studies on solute transport and the application of water quality models. Chaubey et al. (1999) recommend a dense survey of rainfall data as a key input if mass transport is the focus of model applications. Although we only incorporated five of the 14 available rain gauges in the model setup, the leftover stations were used to fill data gaps in the used ones. Due to the choice of stations, we were also able to implement the one with the most complete time series, avoiding gap filling.

As claimed by many authors who performed studies on watersheds within the Southeast Asian region (Walker, 2002; Campling et al., 2001; Noguchi et al., 1996), rainfall in the Mae Sa watershed occurred with a bimodal distribution in all three years. Driven by the monsoon, rainfall starts around April/May and lasts until October, showing two peaks within this period. Wilk and Andersson (2000) report similar pattern for their monsoon-driven study region in India. The data point to a constant temporal pattern of rainfall during the monitored period (Figure 1.5), which may be supportive for the development of a sustainable application technique of agrochemicals in the Mae Sa watershed and/or for the management of water resources. Because pests and diseases pose severe threats to crops during humid periods, the application rate of agrochemicals in the Mae Sa watershed increases (Schreinemachers et al., 2009). In combination with the onset of the rainy season and high rainfall intensities, those agrochemicals easily reach surface waters (Kahl et al., 2008) in high and harmful concentrations (Sangchan et al., 2012, Sangchan et al., 2013). The adjustment of agrochemical application behavior with the onset of the rainy season may help to reduce the leaching rates into stream waters. Additionally, the management of water resources can be planned more suitably, if temporal rainfall characteristics are known.

The monitored hydrographs clearly showed the influence of the monsoon (Figure 1.5) and further temporal patterns. Rainfall from April to December 2077 reached 1299 mm, the years 2008 and 2009 received 1352 mm a^{-1} (January to December) and 1281 mm a^{-1}(January to December), respectively. On first glance, the differences are not distinct, but are revealed by a look at data from the weather station Mae Sa Noi (R13, Figure 3.1, operated since 2003). Here, the difference between 2007 (1540 mm a^{-1}), 2008 (1067 mm a^{-1}) and 2009 (1020 mm a^{-1}) become more obvious. Despite highest rainfall input and highest discharge in 2007 (2007: 531 mm a^{-1}; 2008: 378 mm a^{-1}; 2009: 423 mm a^{-1}) the recession limb in the dry season 2007/2008 dropped faster than in 2008/2009, where discharge was much lower. With regard to stream flow recession and hence water supply during the dry season, it is suggested that seasons with a higher frequency of moderate rainfall events on regular occurrence (Figure 1.5, Figure 1.7) are of greater benefit. Additionally, the leaching of agrochemicals may be hampered by rather less intensive rainy seasons. Pesticide loads in the Mae Sa watershed reported by Sangchan et al. (2013) were notably higher during 2007 than in 2008. The flashy rainfall pattern in 2007 may have supported leaching.

Summarized from many studies, Allamano et al. (2009) state that rainfall amount increases with elevation. Although this relation has been identified for a catchment in Northern Thailand (Kuraji et al., 2001; Dairaku et al., 2004), it is invalid for the Mae Sa watershed. Here, slope was found to have a statistically significant effect on rainfall amount: stations with larger slopes receive higher rainfall totals. Elevation could partially be related with the amount of rainfall, but the results were statistically non-significant. For stations below 1000 m.a.s.l. the coefficient of correlation was only R^2= 0.27. Above the threshold, rainfall decreased with increasing elevation (R^2 = 0.67). In contrast, Marquinez et al. (2003) showed an altitudinal increase of precipitation in a catchment in northern Spain, which was stronger as soon as a threshold of 1000 m.a.s.l. was exceeded. The authors also reported a threshold for slope, which becomes an important covariate at values larger than 12 degrees. It is assumed that both variables, slope and elevation, are interacting.

With regard to losses of agrochemicals, this finding highlights the danger of contamination in the Mae Sa watershed, as postulated by Sangchan et al. (2013). The authors state that the steeper areas (Headwater and Mae Sa Noi, Figure 1.2) show higher losses of agrochemicals and explain it by higher agricultural production intensity and dilution processes towards the downstream area. About 64% of the agricultural land of the Mae Sa watershed on which agrochemicals are heavily applied is located in the steepest parts of the catchment (Schreinemachers and Sirijinda, 2008; Schreinemachers and Sirijinda, 2010). Provided that those regions receive more rainfall due to greater slopes, the high losses of agrochemicals from this area may also be favored by rainfall pattern. Nonetheless, based on hydrological character, pesticide application and topography, the Mae Sa watershed represents a region predestined for environmental contamination.

7.2 Can knowledge of runoff and pesticide dynamics in the Mae Sa watershed be combined?

Within this thesis, runoff generation (Chapter 4) and the dynamics of pesticide during single events (Chapter 5) were investigated. While the pesticide dynamics were surveyed on the catchment scale, runoff generation was explored on the subbasin scale.

Three different patterns of pesticide dynamics were observed during the field analysis. Namely, pesticides that occurred with the rising limb of the hydrograph, pesticides with sporadic concentration peaks along the recession limb and such with low, continuous concentrations. The first two patterns were clearly assigned to fast flow components, such as surface runoff and interflow (Chapter 5). The third one may be transported by baseflow or another indirect flow component. The identified runoff components in Chapter 4, surface runoff, shallow subsurface flow and groundwater, contributed in the same order to total runoff during each monitored event: groundwater > shallow subsurface flow > surface runoff. The monitored events rank above the daily mean discharge (0.05 m^3s^{-1}) but are below the highest daily mean (0.9 m^3s^{-1}). They hence represent some intermediate events in the Mae Sa Noi subbasin.

The questions that rise here are, if the knowledge of runoff generation and pesticide dynamics can be combined and if the information allows a transfer between catchment scales.

Duffner et al. (2012) conducted a follow-up study on hydrograph separation after the application of atrazine and chlorpyrifos in the Mae Sa Noi subbasin. Kahl et al. (2007) already proved that pesticides were transported via interflow or preferential flow along a hillslope in Mae Sa Noi.

Both agrochemicals applied were detected in the stream. Atrazine peaked during the rise of the hydrograph and again along the recession limb and these peaks decreased in the course of the study period. Chlorpyrifos peaked only once after application, which may be explained by volatilization (Ciglasch et al., 2006). The very low concentration over the course of the study period was in agreement with the findings presented in Chapter 5. Because no chlorpyrifos was detected in shallow subsurface flow and groundwater samples, the concentrations must originate from sediment (see Chapter 5). Atrazine was assigned to be transported by surface runoff and shallow subsurface flow (Duffner et al., 2012). Although this study was based on known application rates and application time, the output behavior of both agrochemicals was similar to the one identified in Chapter 5. There, atrazine peaked as well during the rise of the hydrograph and along the recession limb. For both catchment areas, Headwater and Outlet, atrazine is assumed to be lost by fast flow components, favoring a notable contribution of surface runoff and shallow subsurface flow to total runoff. However, the Headwater is more likely comparable to Mae Sa Noi than the Outlet, because of its steepness and land use. In the progress of the rainy season, the differences between the subcatchments become more clearly.

The dynamics of atrazine and other agrochemicals (e.g. dimethoate) occurring along the rising and recession limb speak for an important role of interflow on the catchment scale, but it is, however, apparent from the recession limb that this role becomes less important towards the Outlet. Here, the area is less steep and mostly forested, favoring a higher influence of baseflow and groundwater. Furthermore, runoff from different variable source areas within the whole catchment and interactions in the hyporheic zones are swapped and produce a complex hydrograph. On one side, similar characteristics (soils, geology, rainfall input) of the subbasin may suggest a transfer of identified runoff generation processes to the catchment scale. On the other side, different land use and slightly different topography complicate the transfer. To give a final answer on the transferability and applicability of the results from Chapter 4 to the catchment scale, further investigations are needed. A model application may serve as a helpful tool while testing this theory.

7.3 Hydrological modeling as a tool for testing process assumptions

Hydrological models are used to test theories of runoff generation processes on different scales or even in different catchments (Beven, 2002). Within this study, the SWAT model was tested with regard to its suitability for the Mae Sa watershed (Chapter 6) and its future purpose in pesticide simulations. Data from previous chapters in this thesis were implemented in the model, and, if possible, assumptions and conclusions were tested.

While simulating the water balance of the Mae Sa watershed with the SWAT model, rainfall input was only based on five stations. In disagreement with Sun et al. (2000), who stressed that relatively small differences in rainfall input data might results in comparably large errors in the simulated runoff, the model performed quite well (NSEs: 0.77-0.78, Chapter 6). Furthermore, they emphasize that a higher network density improves the timing of peak flow simulations. Surprisingly, the timing of peak flow within the model application was never of concern, not even during the first, uncalibrated trial runs. Although Chaplot et al. (2005) claims that the simulation output of models strongly depends on the quality of representation of catchment characteristics by spatial input data, it has been reported that the SWAT model is able to perform well with only little spatial information on rainfall. Bieger et al. (2012) performed a SWAT model application in the 3200 km² mountainous Xiangxi catchment, based on only three rain gauges and obtained NSEs values as good as 0.67 and 0.74. With regard to the present study, the amount of rainfall gauges incorporated in the SWAT model may be a problem where the transport of agrochemicals is simulated. This may be due to different relevant runoff components that contribute to mass transport (Chaubey et al.,1999) and due to runoff processes that are depending on spatial rainfall input (Tetzlaff and Uhlenbrook, 2005).

Despite the lower number of rain gauges that was necessary to obtain good NSEs, the application partially agrees with the results from Chapter 3. Some of the runs, in which the stations were randomly excluded while recomputing the annual mean, did not result in a crossing of the confidence interval when 6 or even more stations were excluded. However, the tests were run on the annual mean and the model application was performed on daily rainfall totals, which hampers a direct comparison.

As the SWAT model allows a separation of the total flow into surface runoff, lateral flow and baseflow, we tested if the results of the hydrograph separation from the Mae Sa Noi subbasin (Chapter 4) could be useful for the model application on the catchment scale. Whereas single events were monitored within the study, a baseflow separation was computed for the whole time series. Based on the *Baseflow Filter Programme* (Arnold et al., 1995), the annual contribution of baseflow between 2007 and 2010 for the Mae Sa Noi subbasin ranged between 40% and 51%. The fraction of baseflow during the same period for the Outlet varied between 61% and 76%. This is in good agreement with the results from the simulations, where about 63% of the total flow from 2008 – 2010 were contributed by baseflow (Chapter 6, Table 6.6).

Based on the results from the field investigations described in Chapter 4, the simulation of the different flow components showed a reasonable partitioning of the flow components. Baseflow fractions (i.e. groundwater contributions) ranged between 62%

and 80%. Lateral flow and surface runoff delivered about 30% and up to 14%, respectively. Those results are also congruent with Duffner et al. (2012).
Although the contributions match well on both scales, it must be stated, that the SWAT simulations were long-term, and the field study only focused on single events. Within both field studies (Chapter 4; Duffner et al., 2012), baseflow increased during the course of the hydrograph (Chapter 4, Figure 4.8). During simulations on daily time steps the SWAT model reproduced baseflow as a steady, slightly increasing line (Chapter 6, Figure 6.6). This could be different while simulating runoff on higher temporal resolution. However, with regard to the future purpose of the modeling approach and the knowledge obtained during the short-term pesticide analysis, it is rather important, to reproduce the fast flow components in a precise manner, because they are more likely to affect pesticide transport. In fact, the SWAT model version (SWAT2009.mdb; Ver. 2009/Rev481) we used within this study is not yet able to route pesticides in the baseflow component (Neitsch et al., 2002), which reduced its importance for following pesticide simulations.
In summary, the use of the results from the hydrograph separation in Mae Sa Noi for the runoff simulations of the Mae Sa watershed was possible and processes on the large scale seemed to be similar, based on the model outcome. Still, it must be considered that the SWAT model is a parameter-high model, with many opportunities to adjust the simulated runoff. In Chapter 6, it was demonstrated that different calibration approaches (PARASOL and ANSELM, Table 6.3) delivered similar NSEs, based on different parameter values. Such equifinality issues had been addressed by Beven and Freer (2001), already. Although equifinalty is commonly considered as a problem within model application, because science is supposed to work towards a single correct description of reality (Beven, 2006), it may also represent a chance. As reality is seldom known in detail, this can be seen as a 'positive uncertainty' (Juston et al., 2013). However, to obtain a sound conclusion on the transferability of runoff processes from the subbasin to the catchment scale, further data collection and investigations are needed.

8 Final conclusion

This dissertation intended to build the foundation for simulations of transport of agrochemicals in the Mae Sa watershed by investigating rainfall pattern, hydrological processes, pesticide dynamics and model performance. As a part of the Southeast Asian mountainous region, the Mae Sa watershed represents an area which is currently exposed to more and more pressure due to expansion of settlement and the production of agricultural goods. This fact awards a certain importance to the study, because such catchments are not frequently present in literature.

Annual rainfall in the Mae Sa watershed showed a bimodal distribution, which is in general agreement with other studies from monsoon-driven regions (i. e. Walker, 2002; Negishi et al., 2006). Whereas the timing of peaks (around May and September) was similar within the study period, the magnitude of peaks varied. We tested the differences of stations means (n=14) with an ANOVA and found that, with regard to annual means, the stations did not significantly differ from each other. This was also supported by removal of single stations in turn, before recomputing the total annual mean. Only one station affected the total annual mean in the manner that the 5% and 10% deviation limits of the total annual mean were exceeded. The random exclusion of several stations pointed to the fact that at least 9 stations are necessary to remain within the confidence interval of the annual mean. We analyzed the spatial distribution with GAMMs and revealed that only slope had a significant effect on rainfall amount. This is incoherent with other studies within such type of environment (Dairaku et al., 2004, Kuraji et al., 2009). Elevation was in parts related to rainfall amount by linear regression. Nonetheless, for the whole data set, elevation was statistically not significant. In recap, the study delivers a valuable data set on rainfall distribution for an area that lacks high-resolution rainfall data. We highlighted the notorious variability of rainfall in such regions, as it was stated in earlier studies from different regions within the tropics (Bonell, 1993), and showed the difficulty of detecting that variability. Although slope was statistically significant, additional interactions between variables that have not been monitored within this study, are assumed. For future approaches, it is recommended to combine rainfall data with simulated wind fields, for example, to test if there are additional influences, other than orography.

Based on hydrochemical analysis and electrical conductivity measurements, runoff generation was investigated in the Mae Sa Noi subbasin during four runoff events. Dissolved silica and electrical conductivity were found to be suitable tracers for the Mae Sa Noi subbasin and were used for the three-component hydrograph separation. Most of the other geochemical tracers were not applicable, because either the concentrations were too low, or the components were not distinguishable. Only Potassium was identified as an indicator for surface runoff, which is in agreement with Elsenbeer (2001). To bypass limitations by low concentrations of major ions, environmental isotopes, such as $^{18}O/^{16}O$ or tritium may be applied. The hydrographs of four events were separated into surface runoff, shallow subsurface flow and groundwater. All events were dominated by groundwater, followed by shallow subsurface flow and surface runoff. Giertz and Diekkrüger (2003) and Negishi et al. (2007) pointed at the importance of interflow in their study region, which has similar rainfall input pattern as the Mae Sa watershed. Furthermore, the results of the hydrograph separation strengthened the findings from previous field studies in the subcatchment (Kahl et al., 2007), in which interflow was stated as a key source for pesticide input to stream water. Hence, the results obtained within the field study are assumed to be reasonable.

The short term monitoring of pesticides resulted in three different input patterns, which were similar at both monitoring stations. The first group of pesticides is characterized by a clear concentration rise at the peak of the hydrograph and along the early recession limb. Highly mobile compounds, such as atrazine and dimethoate, are prone to be lost during this phase. Compounds with lower mobility were sporadically detected along the recession limb (i.e. chlorothalonil, chlorpyrifos, etc.). Some of the compounds showed a behavior, similar to a base concentration, which was persistent through the monitoring and rather independent from runoff events (e. g. cypermethrin, endosulfan). Although the results point to notable contributions of fast flow components in the Headwater and Outlet, and pesticide loss pattern of Mae Sa Noi are comparable with the ones on the catchment scale, a transferability of the runoff generation processes between the scales is difficult due to differences in land use and topography. However, to enable the transfer of processes between the catchment and subbasin, more data collection and field analysis are needed.

We successfully calibrated (NSE = 0.77-0.87) the hydrological part of the SWAT model for the Mae Sa watershed and therefore demonstrated its applicability for tropical mountainous areas. Based on the remaining rain gauges (n=9), data gaps in the implemented rain gauges (n=5) were filled in advance and reduced the input uncertainty of rainfall data. Although the discharge peaks were occasionally over- or underestimated, the recession of the hydrograph was generally well reproduced. The performance of the single runoff components during the simulations is of great importance, because the model will be used for pesticide simulations in future. Reproduced fractions were compared with the runoff generation study (Chapter 4) and were found to be in a fairly good agreement.

In conclusion, the investigation on hydrology (Chapter 3 and Chapter 4), pesticide dynamics (Chapter 5) and the calibration of the SWAT model (Chapter 6) provide a solid footing for future studies on long-term scenario-based pesticide simulations. Based on the study results, it will also be possible to analyze the impact of land use changes on water balance and water quality.

9 Summmary

Tropical regions experience dramatic land use changes, which are mainly caused by a rising population, migration and rising food demand. Those regions are very important for global water balance because they receive the highest annual rainfall, and some of the largest rivers of the world are fed by tropical headwaters.

The pollution of water bodies by an increasing application of agrochemicals due to an intensified agricultural land use has recently been recognized as the most critical environmental issue in Southeast Asia. This is particularly true for the mountainous regions of northern Thailand, where agriculture has transformed from subsistence systems to market-oriented crop production. These areas are sources of agrochemicals leaching to water bodies by variable flow paths. In order to understand this critical process the hydrological characteristics of watersheds and the dynamics of pesticides in the stream must be investigated.

The presented dissertation attempts to reveal the underlying hydrological characteristics and transport patterns of agrochemicals of a mountainous, tropical catchment with intense agricultural land use. Therefore i) spatio-temporal rainfall distribution within the catchment, ii) runoff generation processes and iii) the dynamics of agrochemicals during single events were investigated within this study. All results will be implemented in a hydrological model, which focuses on transport of solutes within the observed catchment.

The study site, the Mae Sa watershed in Northern Thailand, was equipped with 12 rain gauges and 2 weather stations. Discharge data was recorded at three stations within the catchment: Headwater (28 km²), Mae Sa Noi (7 km²) and Outlet (77 km²). Each discharge gauge included an automatic water sampler to collect water samples from the stream for pesticide analysis.

To identify whether rainfall amount differs between the rainfall stations and which amount of rain gauges in the catchment is needed to maintain the annual rainfall mean, an ANOVA was applied and tests with regard to 5% and 10% deviation from the true annual mean were computed. The stations were not significantly different, which also was pointed out during the tests on the annual mean. There, the reduction of one station in turn, resulted in only one station (R02) causing a crossing of the 5% and 10% deviation limit. Random reduction of stations suggests a number of at least 9 stations to remain within 10% deviation from the annual mean. Furthermore, the spatio-temporal variability of rainfall was assessed with Generalized Additive Mixed Models (GAMMs). Time, elevation, slope and aspect were included in the analysis and models were applied with different time indices (days, months, years). The outcome showed a clear bimodal temporal distribution of rainfall with peaks around May and September. Slope had a statistically significant effect on the distribution of rainfall: stations with higher slope received more rainfall within all indices. Elevation showed an influence as well, but its effect was not statistically significant and the trend was also not persistent.

To identify the dominant runoff components in a subbasin of the Mae Sa watershed, water samples were collected with high temporal resolution during four single events. Electrical conductivity, major ions (Cl^-, Na^+, Mg^{2+}, K^+, etc.) and silica concentration served as tracers to separate storm flow into stream flow, shallow subsurface flow and surface runoff. Prior to this, the tracers had to be evaluated in terms of their suitability for this tropical subcatchment, and only silica and electrical conductivity were applicable for the hydrograph separation. Potassium was identified as an indicator for surface runoff, other major ions were either too low or the concentrations among the components were not distinguishable. The hydrograph separation revealed that all events were dominated by groundwater, followed by shallow subsurface flow and surface runoff.

The dynamics of seven selected pesticides (dichlorvos, atrazine, dimethoate, chlorothalonil, chlorpyrifos, (α, β) endosulfan, cypermethrin) were monitored with high temporal resolution on single events to compare the behavior at different scales and to pinpoint potential transport pathways. Time series analysis was used to identify correlations between runoff, rainfall and peak concentrations of the monitored compounds. The most significant occurrence of pesticides was observed along the rising limb of the hydrograph (e.g. atrazine and dimethoate) and along the recession limb (e.g. chlorothalonil and chlorpyrifos). A loss pattern (e.g. cypermethrin), which seemed to be independent from rainfall, was also detected. The early occurrence of pesticides along the hydrograph is explained by their high mobility. This suggests that a transport by fast flow components, such as surface runoff or shallow subsurface flow, is most likely. Although the losses were more pronounced at the headwater gauge, both scales revealed a comparable behavior.

The final part of this work was a calibration of the SWAT model for the Mae Sa watershed. Data from the previous investigations within this thesis were included in the model setup and theories were tested. With the help of a Nash-Sutcliffe Model Efficiency

Likelihood Match (ANSELM) the calibration of the water balance was successful (NSE: 0.77-0.87) and the single flow components were reproduced in a reasonable manner. The reasonability of the simulated flow components was backed up with results from the hydrograph separation. Although the calibration was only based on five out of 14 rain gauges, the remaining gauges were used to fill gaps, which initially decreased the input uncertainty of rainfall data.

The dissertation delivers a valuable data set from the Mae Sa watershed, which characterizes a region that is under environmental pressure and serves as a comparative study for research approaches in similar regions. The study also provides an important baseline for future projects focusing on long-term simulations of pesticide behavior, land use change and its effects on water balance and quality.

10 Zusammenfassung

Die Tropen zählen zu den von steigendem Bevölkerungswachstum, und dem damit einhergehenden erhöhten Bedarf an Lebensmitteln bewirkten Landnutzungsänderungen, am stärksten beeinflußten Gebieten. Da in tropischen Gebieten die höchsten Niederschlagsmengen fallen und die Quellgebiete einige der größten Flüsse der Welt liegen, wird ihnen eine große Bedeutung für den globalen Wasserhaushalt zugesprochen. Mit der Intensivierung der Landwirtschaft geht eine erhöhte Nutzung von Agrochemikalien einher, welche in die Gewässer gelangen können und diese stark verschmutzen und belasten.

In Südostasien wurden solche Gewässerverschmutzungen erst vor kurzem als die akuteste Umweltbelastung bestätigt. Dies ist insbesondere in Nordthailand zu beobachten, wo landwirtschaftliche Flächen heutzutage gewinnorientiert und ganzjährig bewirtschaftet werden. In solchen Regionen besteht erhöhte Gefahr des Eintrags von Agrochemikalien in die Gewässer auf unterschiedlichsten Fließwegen. Da die Transportwege von Agrochemikalien eng mit den Fließwegen von Wasser im Untergrund und auf der Oberfläche verbunden sind, ist es besonders wichtig, diese Fließwege zu identifizieren.

Das Ziel der vorliegenden Doktorarbeit ist es, das grundliegende hydrologische System zu charakterisieren und den Transport von Agrochemikalien in einem bergigen, tropischen Einzugsgebiet (EZG) mit intensiver Landwirtschaft nachzuvollziehen. Um dies zu erreichen gilt es, i) die räumliche und zeitliche Variabilität des Niederschlags zu untersuchen, ii) die abflussgenerierenden Prozesse zu identifizieren und iii) die Dynamik von Agrochemikalien während einzelner Abflussereignisse zu erfassen. Sämtliche Ergebnisse gehen in eine Modellierung der Wasserbilanz mit dem Modell SWAT ein und bilden die Basis für spätere Studien zum Stofftranport im Untersuchungsgebiet.

Die Niederschlagsverteilung wurde anhand von 12 Niederschlagstationen und zwei Wetterstationen erfasst. Abflussmengen wurden an drei Stationen gemessen, welche jeweils zwei Teileinzugsgebiete (Headwater: 28 km²; Mae Sa Noi: 7 km²) und den Gebietsauslass (Outlet: 77 km²) wiedergeben. Jede Abflussmessstation wurde zusätzlich mit einem automatischen Probennehmer ausgestattet, damit Wasserproben für die Pestizidanalytik entnommen werden konnten.

Um herauszufinden, ob die mittleren Jahresniederschlagsmengen an den Niederschlagsstationen signifikant voneinander unterscheidbar sind wurde eine ANOVA gerechnet. Es zeigte sich, dass die Stationsmittelwerte nicht signifikant voneinander unterscheidbar sind. Um die notwendige Anzahl von Stationen zum Erhalt des wahren Jahresmittelwertes innerhalb einer Abweichungsgrenze von ±5% und ±10% in solch einem Gebiet zu prüfen, wurde dieser auf zwei unterschiedliche Arten mit einer reduzierten Anzahl von Stationen neu berechnet. Im ersten Teil wurde der Zeitreihe jeweils eine Station (mit zurücklegen) pro Rechenvorgang entnommen. Bis auf eine Station (R02) zeigte keine einen Effekt auf den Jahresmittelwert, der eine Abweichung um 5% oder 10% bewirkte. Dies deckt sich mit den Ergebnissen der ANOVA. Im weiteren Verlauf wurden in jedem Rechenschritt zufällig ausgewählte Stationen entfernt, bis der Mittelwert außerhalb des definierten Bereiches lag. Daraus ergab sich, dass mindestens 9 Stationen mit in die Berechnungen einbezogen werden sollten. Das räumlich-zeitliche Muster der Niederschlagsverteilung wurde mittels Generalized Additive Mixed Models (GAMMs) untersucht. Die über verschiedene Zeitschritte in die Modelle eingehenden Variablen sind Zeit, Höhe, Hangneigung und Ausrichtung. Eine eindeutig zweigipflige Verteilung des Niederschlags mit Maxima um Mai und September konnte festgestellt werden. Die Hangneigung wurde als statistisch signifikante Variable mit dem stärksten Einfluss auf die Niederschlagsmenge bestimmt - je stärker die Hangneigung umso höher der Niederschlag. Die Höhe wies ebenfalls einen geringen Einfluss auf die Niederschlagsmenge auf, der Trend war jedoch weder durchgehend vorhanden noch statistisch signifikant.

Anhand einer tracerbasierten Ganglinienseparation (GLS) wurden die Anteile von grundwasserbürtigem Abfluss, oberflächennahem Zwischenabfluss und Oberflächenabfluss am Gesamtabfluss von vier Einzelereignissen im Mae Sa Noi (MSN) Teileinzugsgebiet (TEZG) untersucht. Die eingesetzten Tracer (Hauptionen, Silikat und elektrische Leitfähigkeit) wurden vorab auf ihre Anwendbarkeit in MSN geprüft. Elektrische Leitfähigkeit und Silikat erwiesen sich als brauchbare Tracer und wurden zur GLS eingesetzt. Neben Kalium (K^+), welches als Indikator für Oberflächenabfluss identifiziert wurde, wiesen die verbleibenden Ionen generell zu geringe Konzentrationen auf oder waren unterhalb der Komponenten nicht unterscheidbar. Mit durchschnittlich 62% dominierte der grundwasserbürtige Abflussanteil alle Ereignisse, gefolgt vom oberflächennahen Zwischenabfluss (23%) und dem Oberflächenabfluss (6%).

Um die Dynamik von Agrochemikalien im Einzugsgebiet zu untersuchen, wurden 7 ausgewählte Pestizide (Atrazin, Dimethoat, Dichlorvos, Chlorothalonil, Chlorpyrifos, (α, β) Endosulfan, Cypermethrin) über den Verlauf von einzelnen Ereignissen im oberen

(Headwater) und unteren Teil (Outlet) des EZG beobachtet. Anhand der Messungen konnten die Austragsmuster auf verschiedenen Skalen verifiziert und auf Vergleichbarkeit hin untersucht werden. Mittels Zeitreihenanalyse wurden die Zusammenhänge der Austragscharakteristika mit Niederschlag, Abfluss und maximaler Konzentration bestimmt. Pestizide mit hoher Löslichkeit (z. B. Atrazin und Dimethoat) wurden im Verlauf der ansteigenden und abfallenden Ganglinie gemessen, während jene mit geringerer Löslichkeit (z. B. Chlorothalonil und Chlorpyrifos) verzögert im Gewässer auftraten. Ein weiteres, ereignisunabhängiges Austragsmuster mit schwankender, geringer Hintergrundkonzentration wurde ebenfalls identifiziert (z B. Cypermethrin). Obwohl die Austragsmuster im oberen TEZG wesentlich markanter waren als jene im unteren, konnte ein ähnliches Verhalten belegt werden.

Diese Arbeit wurde mit der Kalibrierung des hydrologischen Teil des Modells SWAT abgerundet. Die Eignung des Modells für tropische Quelleinzugsgebiete in den Bergen wurden durch die hohen Gütekriterien (NSE = 0.77 – 0.87) bewiesen. Außerdem konnte nicht nur die Wasserbilanz zufriedenstellend reproduziert werden, sondern auch die Aufteilung des Gesamtabfluss in die einzelnen Komponenten. Die Plausibiltät dieser Komponenten wurde mit den Ergebnissen aus der Ganglinienseparation bekräftigt. Zusätzlich konnte das Modell mit qualitativ hochwertigen Niederschlagsdaten aufgesetzt werden, da mögliche Datenlücken in den 5 verwendeten Stationen mit Daten von nicht verwendeten Nachbarstationen gefüllt wurden. Somit konnten von vornherein Unsicherheiten in den Eingabedaten reduziert werden.

Diese Arbeit liefert einen wertvollen Datensatz für das Mae Sa Einzugsgebiet, welches für die südostasiatische Bergregion als repräsentativ betrachtet werden kann. Die Arbeit ermöglicht eine solide Grundlage für die Modellierung der Wasserbilanz und liefert weitere Daten und Erkenntnisse, welche zukünftige Simulationen der Pestiziddynamik und Szenarien zu Auswirkung von Landnutzungsänderung auf Wasserhaushalt und –qualität im Mae Sa Einzugsgebiet unterstützen.

11 References

Abbaspour, K., Johnson, C. and Genuchten, M. v., 2004: Estimating uncertain flow and transport parameter using a sequential uncertainty fitting procedure. Vadose Zone, 3: 1340-1352.

Aiemsupasit, N., 2005: Pesticides in Thailand: A survey on Environmental Perspectives. Ministry of Public Health, Department of Health, Bangkok.

Ajami, N. K., Gupta, H., Wagener, T. and Sorooshian, S., 2004: Calibration of a semi-distributed hydrologic model for streamflow estimation along a river system. Journal of Hydrology, 298: 112-135.

Alansi, A. W., Amin, M. S. M., Halim, G. A., Shafri, H. Z. M. and Aimrun, W., 2009: Validation of SWAT model for stream flow simulation and forecasting in Upper Bernam humid tropical river basin, Malaysia. Hydrology and Earth System Sciences, HESSD 6: 7581-7609.

Alibuyog, N., Ella, V., Reyes, M., Srinivasan, G., Heatwole, C. and Dillaha, T., 2009: Predicting the effects of land use on runoff and sediment yield in selected sub-watersheds of the Manupali River using the ArcSWAT model. World Association of Soil and Water Conservation,

Allamano, P., Claps, P., Laio, F. and Thea, C., 2009: A data-based assessment of the dependence of short-durtaion precipitation on elevation. Physics and Chemistry of the Earth, 34: 635-641.

Anyusheva, M., Lamers, M., Schwadorf, K. and Streck, T., 2012: Analysis of pesticides in surface water in remote areas in Vietnam: Coping with matrix effects and test of long-term stability. International Journal of Environmental Analytical Chemistry, 92: 797-809.

Appelo, C. A. J. and Postma, D., 2005: Geochemistry, Groundwater and Pollution. Taylor & Francis; 2nd edition, Leiden.

Arnold, J. G. and Allan, P. M., 1999: Automated methods for estimating baseflow and ground water recharge from streamflow records. Journal of the American Water Resources Association, 35: 411-424.

Arnold, J. G., Allen, P. M., Muttiah, R. and Bernhardt, G., 1995: Automated base flow separation and recession analysis techniques. Ground Water, 33: 1010-1018.

Arnold, J. G., Srinivasan, R., Muttiah, R. S. and Williams, J. R., 1998: Large area hydrologic modeling and assessment. Part I: Model development. Journal of the American Water Resources Association, 34: 73-89.

Bard, Y., 1974: Parameter Estimation. Academic Press, New York.

Bárdossy, A. and Das, T., 2008: Influence of rainfall observation network on model calibration and application. Hydrology and Earth System Sciences, 12: 77-89.

Bates, B. C. and Campbell, E. P., 2001: Markov Chain Monte Carlo scheme for parameter estimation and inference in conceptual rainfall-runoff modelling. Water Resources Research, 37: 9367-947.

Bazemore, D. E., Eshleman, K. N. and Hollenbeck, K. J., 1994: The role of soil water in storm-flow generation in a forested headwater catchment: synthesis of natural tracers and hydrometric evidence. Journal of Hydrology, 162: 47-75.

Beasley, D. B., Huggins, L. F. and Monke, E. J., 1980: ANSWERS: A model for watershed planning. Transactions of the American Society of Agricultural Engineers, 23: 938-944.

Beven, K., 2006: A manifesto for the equifinality thesis. Journal of Hydrology, 320: 18-36.

Beven, K. and Binley, A., 1992: The future of distributed models - model calibration and uncertainty prediction. Hydrological Processes, 6: 279-298.

Beven, K. and Freer, J., 2001: Equifinality, data assimilation, and uncertainty estimation in mechanistic modelling of complex environmental systems using the GLUE methodology. Journal of Hydrology, 149: 11-29.

Beven, K. J., 2002: The Primer - Rainfall-Runoff Modelling. Wiley, New York.

Bicknell, B. R., Imhoff, J. C., Jr., J. L. K., Jr., A. S. D. and Johanson, R. C., 1993: Hydrologic Simulation Program - FORTRAN (HSPF) User's Manual for Release 10. Athens, Ga.: U.S. EPA Environmental Research Lab, Report No. EPA/600/R-93-174.:

Bieger, K., Hörmann, G. and Fohrer, N., 2012: Simulation of stream flow and sediment with the SWAT model in a data scarce catchment in the Trhee Gorges Region, China. Journal of Environmental Quality, DOI 10.2134/jeq2011.0383.

Bingner, R. L. and Theurer, F. D., 2001: AnnAGNPS: estimating sediment yield by particle size for sheet & rill erosion. In Proceedings of the Sediment: Monitoring, Modelling and Managing., 7th Federal Interagency Sedimentation Conference, Reno, NV: Vol. 1, pp. I1-I7.

Bitew, M. M. and Gebremichael, M., 2010: Spatial variability of daily summer rainfall at a local-scale in a mountainous terrain and humid tropical region. Atmospheric Research, 98: 347-352.

Blocken, B., Poesen, J. and Carmeliet, J., 2006: Impact of wind on the spatial distribution of rain over micro.scale topography - numerical modelling and experimental verification. Hydrological Processes, 20: 345-368.

Boithias, L., Sauvage, S., Taghavi, L., Merlina, G., Probst, J.-L. and Perez, J. M. S., 2011: Occurence of metolachlor and trifluralin losses in the Save river agricultural catchment during floods. Journal of Hazardous Materials, 196: 210-219.

Bonell, M., 1993: Progress in the understanding of runoff generation dynamics in forests. Journal of Hydrology, 150: 217-275.

Bonell, M. and Bruijnzeel, L. A., 2004: Forest, Water and People in the Humid Tropics: Past, Present and Future Hydrological Research for Integrated Land and Water Management. I. H. Series, Cambridge University Press, Cambridge.

Bonell, M. and Gilmour, D. A., 1978: The Development of overland flow in a tropical rain forest catchment. Journal of Hydrology, 39: 365-382.

Boochabun, K., Tych, W., Chappell, N. A., Carling, P. A., Lorsirirat, K. and Obsaeng, S. P., 2004: Statistical Modelling of Rainfall and River Flow in Thailand. Journal Geological Society of India, 64: 503-515.

Borah, D. K. and Bera, M., 2004: Watershed-scale hydrologic and nonpoint-source pollution models: Review of applications. Transactions of the American Society of Agricultural Engineers, 47: 789-803.

Bouraoui, F. and Dillaha, T., 1996: ANSWERS-2000: Runoff and sediment transport model. Journal of Environmental Engineering and Science, 122: 493-502.

Bouraoui, F. and Dillaha, T., 2000: ANSWERS-2000: Nonpoint-source nutrient planning model. Journal of Environmental Engineering and Science, 126: 1045-1055.

Bouwmann, B. M. A., Castaneda, A. R. and Bhuiyan, S. I., 2002: Nitrate and pesticide contamination of groundwater under rice-based systems: past and current evidence from the Philippines. Agriculture Ecosystems & Environment, 92: 185-199.

Bremer, H., 1999: Die Tropen. Geographische Synthese einer fremden Welt im Umbruch. Bontraeger, Stuttgart.

Brown, C. D., Hodgkinson, R. A., Rose, D. A., Syers, K. and Wilcockson, S. J., 1995: Movement of pesticides to surface waters from a heavy clay soil. Pesticide Science, 43: 131-140.

Bruijnzeel, L. A., 2004: Hydrological functions of tropical forests: not seeing the soil for the trees? Agriculture Ecosystems & Environment, 104: 185-228.

Bruun, T. B., Neergaard, A. d., Larence, D. and Ziegler, A. D., 2009: Environmental consequences of the demis in swidden cultivation in Southeast Asia: Carbon storage and soil quality. Human Ecology, 249: 11-29.

Burns, D. A., McDonnell, J. J., Hooper, R. P., Peters, N. E., Freer, J. E., Kendall, C. and Beven, K., 2000: Quantifying contributions to storm runoff through end-member mixing analysis and hydrologic measurements at the Panola Mountain Research Watershed (Georgia, USA). Hydrological Processes, 15: 1903-1924.

Buytaert, W., Celleri, R., Willems, P., Bièvre, B. D. and Wyseure, G., 2006: Spatial and temporal rainfall variability in mountainous areas: A case study from the south Ecuadorian Andes. Journal of Hydrology, 329: 413-421.

Campling, P., Gobin, A. and Feyen, F., 2001: Temporal and spatial rainfall analysis across a humid tropical catchment. Hydrological Processes, 15: 359-375.

Castillo, L. E., Ruepert, C. and Solis, E., 2000: Pesticide residues in the aquatic environment of banana plantation areas in the north Atlantic zone of Costa Rica. Environmental Toxicology and Chemistry, 19: 1942-1950.

Chapell, N., 2010: Soil pipe distribution and hydrological functioning within the humid tropics: a synthesis. Hydrological Processes, 24: 1567-1581.

Chapell, N. A. and Lancaster, J. W., 2007: Comparison of methodological uncertainty within permeability measurements. Hydrological Processes, 21: 2504-2514.

Chaplot, V., Saleh, A. and Jaynes, D. B., 2005: Effect of the accuracy of spatial rainfall information on the modeling of water, sediment, and NO_3-N loads at the watershed level. Journal of Hydrology, 312: 223-234.

Chaubey, I., Haan, C. T., Grunwald, S. and Salisbury, J. M., 1999: Uncertainty in the model parameters due to spatial variability of rainfall. Journal of Hydrology, 220: 48-61.

Chaves, J., Neill, C., Germer, S., Neto, S. G., Krusche, A. and Elsenbeer, H., 2008: Land management impacts on runoff sources in small Amazon watersheds. Hydrological Processes, 22: 1766-1775.

Christophersen, N., Neal, C., Hooper, R. P., Vogt, R. D. and Andersen, S., 1990: Modelling streamwater chemistry as a mixture of soilwater end-members - a step towards second-generation acidification models. Journal of Hydrology, 116: 307-320.

Chuan, G. K., 2003: Hydrological studies and water resource concerns in Southeast Asia. Singapore Journal of Tropical Geography, 24: 86-110.

Ciglasch, H., 2006: Insecticide dynamics in the soil environment of a tropical lychee plantation - A case study from northern Thailand. Universität Berlin,

Ciglasch, H., Amelung, W., Totrakool, S. and Kaupenjohann, M., 2005: Water flow patterns and pesticide fluxes in an upland soil in northern Thailand. European Journal of Soil Science, 56: 765-777.

Cobley, L. S. and Steele, W. M., 1984: An introduction to the Botany of Tropical Crops. Longman, New York.

Dairaku, K., Emori, S. and Oki, T., 2004: Rainfall Amount, Intensity, Duration and Frequency Relationships in the Mae Chaem Watershed in Southeast Asia. Journal of Hydrometeorology, 5: 458-470.

Dairaku, K., Kuraji, K., Suzuki, M., Tangtham, N., Jirasuktaveekul, W. and Punyatrong, K., 2000: The Effect of Rainfall Duration and Intensity on Orographic Rainfall Enhancement in a Mountainous Area: A case study in the Mae Chaem Watershed, Thailand. Journal of Japan Society of Hydrology and Water Resources, 13: 57-68.

Delang, C. O., 2002: Deforestation in Northern Thailand: The result of Hmong farming practices or thai development strategies? Society and Natural Resources, 15: 483-501.

Doherty, J. and Johnston, J. M., 2003: Methodologies for calibration and predictive analysis of a watershed model. Journal of American Water Resources Association, 39: 251-265.

Duan, Q. Y., Gupta, V. K. and Sorooshian, S., 1993: Shuffled complex evolution approach for effective and efficient global minimization. Journal of Optimization Theory and Applications, 76: 501-521.

Duan, Q. Y., Sorooshian, S. and Ibbitt, R. P., 1988: A maxiumum likelihood criterion for use with data collected at unequal time intervals. Water Resources Research, 24: 1163-1173.

Duffner, A., 2010: Hydrograph separation and mapping of the saturated hydraulic conductivity for identifying pesticide transport pathways from a sloped litchi orchard to an adjacent stream. Master Thesis, University of Hohenheim.

Duffner, A., Ingwersen, J., Hugenschmidt, C. and Streck, T., 2012: Pesticide transport pathways from a sloped litchi orchard to an adjacent tropical stream as identified by hydrograph separation. Journal of Environmental Quality, 41: 1315-1323.

Dykes, A. P., 2000: Climatic patterns in a tropical rainforest in Brunei. The Geographical Journal, 166: 63-80.

Dykes, A. P. and Thornes, J. B., 2000: Hillslope hydrology in tropical rainforest steeplands in Brunei. Hydrological Processes, 14: 215-235.

Elfman, L., Tooke, N. E. and Patring, J. D. M., 2011: Detection of pesticides used ion rice cultivation in streams on the island of Leyte in the Philippines. Agricultural Water Management, 101: 81-87.

Elsenbeer, H., 2001: Hydrologic flowpaths in tropical rainforest soilscapes - a review. Hydrological Processes, 15: 1751-1759.

Elsenbeer, H. and Lack, A., 1996: Hydrometric and hydrochemical evidence for fast flowpaths at La Cuence, Western Amazonia. Journal of Hydrology, 180: 237-250.

Elsenbeer, H., Lorieri, D. and Bonell, M., 1995: Mixing model approaches to estimate storm flow sources in an overland flow dominated tropical rain forest catchment. Water Resources Research, 31: 2267-2278.

Elsenbeer, H. and Vertessy, R. A., 2000: Stormflow generation and flowpath characteristics in an Amazonian rainforest catchment. Hydrological Processes, 14: 2367-2381.

Elsenbeer, H., West, A. and Bonell, M., 1994: Hydrologic pathways and stormflow hydrochemistry at South Creek, northeast Queensland. Journal of Hydrology, 162: 1-21.

EXTOXNET, 1996: Pesticide Information Profile. Oregon State University, page cited April 2007: URL: http://extoxnet.orst.edu/pips/ghindex.html.

FAO, 2006: Global Forest Resources Assessment 2005 - Progress towards sustainable forest management. FAO Forestry Paper, Food and Agricultural Organisation of the United Nations, Rome.

FAO, 2010: Growth of Agricultural Production 1999-2009. FAO Statistic Devision, Food and Agricultural Organisation of the United Nations, Rome.

Fekete, B. M. and Vörösmarty, C. J., 2002: High-resolution field of global runoff combining observed river discharge and simulated water balances. Global Biogeochemical Cycles, 16: 15.1-15.10.

Flury, M., 1996: Experimental evidence of transport of pesticides through field soils - a review. Journal of Environmental Quality, 25: 25-45.

Footprint, 2011: The Footprint Pesticide Properties Database (PPDP); Agriculture and Environmental Research Unit (AERU). University of Hertfordshire, accessed April 2011: http://sitem.herts.ac.uk/aeru/footprint/en/index.htm.

Fox, J. and Vogler, J. B., 2005: Land-use and land-cover change in montane mainland southeast asia. Environmental Management, 36: 394-403.

Fox, J., Krummel, J., Yarnasarn, S., Ekasingh, M. and Podger, N., 1995: Land use and landscape dynamics in northern Thailand: Assessing change in three upland watersheds. Ambio, 24: 328-334.

Frey, M., Schneider, M. K., Dietzel, A., Reichert, P. and Stamm, C., 2009: Predicting critical source areas for diffuse herbicide losses to surface waters: Role of connectivity and boundary conditions. Journal of Hydrology, 365: 23-36.

Gablani, S., Boni, G., Ferraris, F., Hardenberg, J. v. and Provenzale, A., 2007: Propagation of uncertainty from rainfall to runoff: A case study with a stochastic rainfall generator. Advances in Water Resources, 30: 2061-2071.

Gassman, P. W., Reyes, M. R., Green, C. H. and Arnold, J. G., 2007: The Soil and Water Assessment Tool: Historical development, applications and future research directions. American Society of Agricultural and Biological Engineers, 50: 1211-1250.

Genereux, D., 1998: Quantifying uncertainty in tracer-based hydrograph separations. Water Resources Research, 34: 915-919.

Giertz, S. and Diekkrüger, B., 2003: Analysis of the hydrological processes in a small headwater catchment in Benin (West Africa). Physics and Chemistry of the Earth, 28: 1333-1341.

Giertz, S., Diekkrüger, D. and Stemp, G., 2006: Physically-based modelling of hydrological processes in a tropical headwater catchment (West Africa) - process representation and multi-criteria validation. Hydrology and Earth System Sciences, 10: 829-847.

GISTDA, 2007: SPOT 5 image, SPOT-5 K-J: 256-312, Date 06-11-2006. Available from: http://www.gistda.or.th/Gistda/HtmlGistda/Html/index2.htm.

Godsey, S., Elsenbeer, H. and Stallard, R., 2004: Overland flow generation in two lithologically distinct rainforest catchments. Journal of Hydrology, 295: 276-290.

Godula, M., Hajslová, J. and Alterová, K., 1999: Pulsed splitless injection and the extent of martrix effects in the analysis of pesticides. Journal of High Resolution Chromatography, 22: 395-402.

Goller, R., Wilcke, W., Leng, M. J., Tobschall, H. J., Wagner, K., Valarezo, C. and Zech, W., 2005: Tracing water paths through small catchments under a tropical montane rain forest in south Ecuador by an oxygen isotope approach. Journal of Hydrology, 308: 67-80.

GPCC, 2003: Mean annual precipitation (1961-1990). Global Precipitation Climatology Centre.

Graiprab, P., Pongput, K., Tangtham, N. and Gassman, P. W., 2010: Hydrological evaluation and effect of climate change on the At Samat watershed, Northeastern regions, Thailand. International Agricultural Engineering Journal, 19: 12-22.

Green, C. H. and Griensven, A. v., 2008: Autocalibration in hydrologic modeling: Using SWAT2005 in small-scale watersheds. Environmental Modelling & Software, 23: 422-434.

Griensven, A. v. and Meixner, T., 2007: A global and efficient multi-objective auto-calibration and uncertainty estimation method for water quality catchment models. Journal of Hydroinformatics, 9: 277-291.

Griensven, A. v., Meixner, T., Grunwald, S., Bishop, T., Diluzio, A. and Srinivasan, R., 2006: A global sensitivity analysis tool for the parameters of multi-variable catchment models. Journal of Hydrology, 324: 10-23.

Gupta, H. V., Kling, H., Yilmaz, K. K. and Martinez, G. F., 2009: Decomposition of the mean squared error and NSE performance criteria: Implications for improving hydrological modelling. Journal of Hydrology, 377: 80-91.

Hewlett, J. D. and Hibbert, A. R., 1967: Factors affecting the response of small watersheds to precipitation in humid areas. W. E. S. a. H. W. Lull, Pergamon Press, New York.

Hodnett, M. G. and Tomasella, L., 2002: Marked differences between van Genuchten soil water-retention parameters for temperate and tropical soils: A new water-retention pedo-transfer function developed for tropical soils. Geoderma, 108: 155-180.

Hoeg, S., Uhlenbrook, S. and Leibundgut, C., 2000: Hydrograph separation in a mountainous catchment - combining hydrochemical and isotopic tracers. Hydrological Processes, 14: 1199-1216.

Holvoet, K., Griensven, A. v., Gevaert, V., Seuntjens, P. and Vanrolleghem, P. A., 2007: Modifications to the SWAT code for modelling direct pesticide losses. Environmental Modelling & Software, 23: 72-81.

Howard, P. H., 1991: Handbook of environmental fate and exposure data for organic chemicals. Volume III - Pesticides. Lewis Publishers, Chelsea.

Hoyos, C. D. and Webster, P. J., 2007: The role of intraseasonal variability in the natrue of asian monsoon precipitation. Journal of Climate, 20: 4402-4424.

Hugenschmidt, C., Ingwersen, J., Sangchan, W., Sukvanachaikul, Y., Uhlenbrook, S. and Streck, T., 2010: Hydrochemical analysis of stream water in a tropical, mountainous headwater catchment in Northern Thailand. Hydrology and Earth System Sciences Discussion, MS No. hess-2010-65:

Irwin, R. R., 1976: Replacing shifting agriculture through intensive settled agriculture, crop diversification and conservation farming. , UNDP/FAO, Working Paper 9, Food and Agricultural Organisation of the United Nations, Chiang Mai, Thailand.

Jaipieam, S., Visuthismajarn, P., Sutheravut, P., Siriwong, W., Thoumsang, S., Borjan, M. and Robson, M., 2009: Organophosphate pesticide residues in drinking water from artesion wells and health risk assessment of agricultural communities, Thailand. HERA, 15: 1304-1316.

Jantschke, C., 2002: Theoretische und empirische Ermittlung des Pflanzenwasserbedarfs von Lycheebäumen in Nordthailand. Universität Hohenheim, Stuttgart.

Joerin, C., Beven, K. J., Iorgulescu, I. and A.Musy, 2002: Uncertainty in hydrograph separations based on geochemical mixing models. Journal of Hydrology, 255: 90-106.

Johanson, R. C., Imhoff, J. C., Jr., J. L. K. and Donigian, A. S., 1984: Hydrological Simulation Program - FORTRAN (HSPF): Users Manual for Release 8.0. Environmental Research Laboratory, U. S. EPA, Athen, GA. 30613., EPA-600/3-84-066:

Juston, J. M., Kauffeldt, A., Montano, B. Q., Seibert, J., Beven, K. J. and Westerberg, I. K., 2013: Smiling in the rain: Seven reasons to be positive about uncertainty in hydrological modelling. Hydrological Processes, 27: 1117-1122.

Kahl, G., 2003: Untersuchungen zum lateralen Stofftransport im Boden an einem Hangstandort in einer Bergregion Nordthailands. Diplomarbeit, Technische Universität Braunschweig, Braunschweig.

Kahl, G., Ingwersen, J., Nutniyom, P., Totrakool, S., Pansombat, K., Thavornyutikarn, P. and Streck, T., 2007: Micro-Trench Experiments on Interflow and Lateral Pesticide Transport in a Sloped Soil in Northern Thailand. Journal of Environmental Quality, 36: 1205-1216.

Kahl, G., Nutniyom, P., Ingwersen, J., Totrakool, S., Pansombat, K., Thavornyutikarn, P. and Streck, T., 2010: Simulating Pesticide transport from a sloped tropical soil to an adjacent stream. Journal of Environmental Quality, 39: 353-363.

Kahl, G., Nutniyom, P., Ingwersen, J., Totrakool, S., Pansombat, K., Thayornyutikarn, P. and Streck, T., 2008: Loss of pesticides from a litchi orchard to an adjacent stream in Northern Thailand. European Journal of Soil Science, 59: 71-81.

Kannan, N., White, S. M., Worrall, F. and Whelan, M. J., 2007: Hydrological modelling of a small catchment using SWAT-2000-Ensuring correct flow partitioning for contaminant modelling. Journal of Hydrology, 334: 64-72.

Khoi, D. N. and Suetsugi, T., 2012: The responses of hydrological processes and sediment yield to land-use and climate change in the Be River catchment, Vietnam. Hydrological Processes, DOI: 10.1002/hyp.9620.

Kienzler, P. M. and Naef, F., 2008: Subsurface storm flow formation at different hillslopes and implications for the old water paradox. Hydrological Processes, 22: 104-116.

Kinner, D. A. and Stallard, R. F., 2004: Identifying Storm Flow Pathways in a Rainforest Catchment Using Hydrological and Geochemical Modelling. Hydrological Processes, 18: 2851-2875.

Kladivko, E. J., VanScoyoc, G. E., Monke, E. J., Oates, K. M. and Pask, W., 1991: Pesticide and nutrient movement into sub-surface tile drains on a silt loam soil in Indiana. J. Environ. Qual. 20, 264-270.

Kladivko, E., Brown, L. and Baker, J., 2001: Pesticide transport to subsurface tile drains in humid regions of North America. Critical Reviews in Environmental Science and Technology, 31: 1-62.

Kreuger, J., 1998: Pesticides in stream water within an agricultural catchment in southern Sweden, 1990-1996. Science of the Total Environment, 216: 227-251.

Kreuger, J. and Törnqvist, L., 1998: Multiple regression analysis of pesticide occurence in streamflow related to pesticide properties and quantities applied. Chemosphere, 37: 189-207.

Kruawal, K., Sacher, F., Werner, A., Müller, J. and Knepper, T. P., 2005: Chemical water quality in Thailand and its impact on the drinking water production in Thailand. Science of the Total Environment, 340: 57-70.

Kuczera, G. and Parent, E., 1998: Monte Carlo assessment of parameter uncertainty in conceptual catchment models: The Metropolis algorithm. Journal of Hydrology, 211: 69-85.

Kuntiyawichai, K., Schulz, B., Uhlenbrook, S., Suryadi, F. X. and Griensven, A. V., 2011: Comparison of flood management options for the Yang River Basin, Thailand. Irrigation and Drainage, 60: 526-543.

Kuraji, K., Goymo, M. and Punyatrong, K., 2009: Inter-annual and spatial variation of altitudinal increase of rainfall over Mount Inthanon and Mae Chaem Watershed, Northern Thailand. Hydrological Research Letters, 3: 18-21.

Kuraji, K., Punyatrong, K. and Suzuki, M., 2001: Altitudinal increase in rainfall in the Mae Chaem watershed, Northern Thailand. Hydrological Research Letters, 3: 18-21.

Ladouche, B., Probst, A., Viville, D., Idir, S., Babqué, D., Loubet, M., Probst, J.-L. and Bariac, T., 2001: Hydrograph separation using isotopic, chemical and hydrological approaches (Strengbach catchment , France). Journal of Hydrology, 242: 255-274.

Lamers, M., Anyusheva, M., La, N., Nguyen, V. V. and Streck, T., 2011: Pesticide pollution in surface- and groundwater by paddy rice cultivation: A case stud from Northern Vietnam. Clean - Soil, Air, Water, 39: 356-361.

Larose, M., Heathman, G. C., Norton, L. D. and Engel, B., 2007: Hydrologic and Antrazine Simulation of the Cedar Creek Watershed Using the SWAT Model. Journal of Environmental Quality, 36: 521-531.

Latrubesse, E. M., Stevaux, J. C. and Sinha, R., 2005: Tropical rivers. Geomorphology, 70: 187-206.

Laudon, H. and Slaymaker, O., 1997: Hydrograph separation using stable isotopes, silica and electrical conductivity: an alpine example. Journal of Hydrology, 201: 82-101.

Leu, C., Singer, H., Stamm, C., Müller, S. R. and Schwarzenbach, R. P., 2004: Simultaneous assessment of sources, processes and factors influencing herbicide losses to surface waters in a small agricultural catchment. Environmental Science & Technology, 38: 3827-3834.

Lewan, E., Kreuger, J. and Jarvis, N., 2009: Implications of precipitation patterns and antecedent soil water content for leaching of pesticides from arable land. Agricultural Water Management, 96: 1633-1640.

Lin, Z. and Radcliffe, D. E., 2006: Automatic calibration and predictive uncertainty analysis of a semidistributed watershed model. Vadose Zone, 5: 248-260.

Louchart, X., Coulouma, M. V. G. and Andrieux, P., 2004: Oryzalin fate and transport in runoff water in mediterranean vineyards. Chemosphere, 57: 921-930.

Marquínez, J., Lastra, J. and Garcia, P., 2003: Estimation models for precipitation in mountainous regions: The use of GIS and multivariate analysis. Journal of Hydrology, 270: 1-11.

Matsubayashi, U., Valesquez, G. T. and Takagi, F., 1993: Hydrograph separation and flow analysis by specific electrical conductance of water. Journal of Hydrology, 152: 179-199.

McCullagh, P. and Nelder, J. A., 1989: Generalized Linear Models. Second Edition, Chapman and Hall/CRC.

McDonnell, J. J., 1990: A rationale for old water discharge through macropores in a steep, humid catchment. Water Resources Research, 26: 2821-2832.

McGlynn, B. L. and McDonnell, J. J., 2003: Quantifying the relative contributions of riparian and hillslope zones to catchment runoff. Water Resources Research, 39: doi:10.1029/2003WR002091.

McGrath, G., Hinz, C. and Sivapalan, M., 2010: Asessing the impact of regional rainfall variability on rapid pesticide leaching potential. Journal of Contaminant Hydrology, 113: 56-65.

McGregor, G. R. and Nieuwolt, S., 1998: Tropical Climatology. Second Edition, Wiley, Chichester.

McMillan, H., Jackson, B., Clark, M., Kavetski, D. and Woods, R., 2011: Rainfall uncertainty in hydrological modelling: An evaluation of multiplicative error models. Journal of Hydrology, 400: 83-94.

McMillan, H., Krueger, T. and Freer, J., 2012: Benchmarking observational uncertainties for hydrology: rainfall, river discharge and water quality. Hydrological Processes, 26: 4087-4111.

Metropolis, N., Rosenbluth, A. W., Rosenbluth, M. N., Teller, E. and Teller, A. H., 1953: Equation of state calculations of fast computing machines. Journal of Chemical Physics, 21: 1087-1092.

Montanari, L., Sivapalan, M. and Montanari, A., 2008: Investigation of dominant hydrological processes in a tropical catchment in a monsoonal climate via the downward approach. Hydrology and Earth System Sciences, 10: 769-782.

Montgomery, D. R., Dietrich, W. E., Torres, R., Anderson, S. P., Heffner, J. T. and Loague, K., 1997: Piezometric response of a steep unchanneled valley to natural and applied rainfall. Water Resources Research, 33: 91-109.

Moriasi, D. N., Arnold, J. G., Liew, M. W. V., Bingner, R. L., Harmel, R. D. and Veith, T. L., 2007: Model evaluation guidelines for systematic quantification of accuracy in watershed simulations. 50: 885-900.

Moussa, R., Voltz, M. and Andrieux, P., 2003: Effects of the spatial organization of agricultural management on the hydrological behavioue of a farmed catchment during flood events. Hydrological Processes, 16: 393-412.

Mul, M., Savenije, H. H. G. and Uhlenbrook, S., 2009: Spatial rainfall variability and runoff response during an extreme event in a semi-arid catchment in the South Pare Mountains, Tanzanzia. Hydrology and Earth System Sciences, 13: 1659-1670.

Mul, M. L., Mutiibwa, R. K., Uhlenbrook, S. and Savenije, H. H. G., 2008: Hydrograph separation using hydrochemical tracers in the Mankanya catchment, Tanzania. Physics and Chemistry of the Earth, 33: 151-156.

Müller, K., Deurere, D., Hartmann, H., Bach, M., Spiteller, M. and Frede, H. G., 2003: Hydrological characterisation of pesticide loads using hydrograph separation at different scales in a german catchment. Journal of Hydrology, 273: 1-17.

Müller, K., M.Trovole, James, T. and Rahman, A., 2002: Herbicide runoff studies in an arable soil under simulated rainfall. New Zealand Plant Protection, 55: 172-176.

Müller, K., Stenger, R. and Rahman, A., 2006: Herbicide loss in surface runoff from a pastoral hillslope in the Pukemanga catchment (New Zealand): Role of pre-event soil water content. Agriculture Ecosystems & Environment, 112: 381-390.

Nash, J. E. and Sutcliffe, J. V., 1970: River flow forecasting through conceptual models Part 1 - A discussion of principles. Journal of Hydrology, 10: 282-290.

National Environmental Board, 1994: Notification of National Environmental Board, No. 8, B.E. Royal Thai Government Gazette, Bangkok, Thailand.

Ndomba, P., Mtalo, F. and Killingtveit, A., 2008: SWAT model application in a data scarce tropical complex catchment in Tanzania. Physics and Chemistry of the Earth, 33: 626-632.

Negishi, J. N., Noguchi, S., Sidle, R. C., Ziegler, A. D. and Nik, A. R., 2007: Stormflow generation involving pipe flow in a zero-order basin of Peninsular Malaysia. Hydrological Processes, 21: 789-806.

Neitsch, S. L., Arnold, J. G., Kiniry, J. R. and Williams, J. R., 2011: Soil and Water Assessment Tool - Theoretical Documentation, Version 2009. S. a. W. R. L. o. A. R. S. Grassland, Texas Water Resources Institute Technical Report No. 406.

Neitsch, S. L., Arnold, J. G. and Srinivasan, R., 2002: Pesticide fate and transport predicted by the Soil and Water Assessment Tool (SWAT): Atrazine, Metolachlor and Trifluralin an the Sugar Creek Watershed. BRC Report 2002-2003, Blackland Research and Extension Center, Temple, Texas,

Ng, H. Y. F. and Clegg, S. B., 1997: Atrazine and metolachlor losses in runoff events from an agricultural watershed: the importance of runoff components. The Science of the Total Environment, 193: 215-228.

Noguchi, S., Nik, A. R., Sammori, T., Tani, M. and Tsubayama, Y., 1996: Rainfall characteristic of tropical rain forest and temperate forest: Comparison between Bukit Tarek in Peninsular Malaysia and Hitachi Ohta in Japan. Journal of Tropical Forest Science, 9: 206220.

Oerke, E. C. and Dehne, G. W., 2004: Safeguarding production - losses in major crops and the role of crop protection. Crop Protection, 23: 275-286.

Ogunkoya, O. O. and Jenkins, A., 1993: Analysis of storm hydrograph and flow pathways using a three-component hydrograph separation model. Journal of Hydrology, 142: 71-88.

Oliver, D. P., Kookana, R. S., Anderson, J. S., Cox, J., Waller, N. and Smith, L., 2011: The off-site transport of pesticide loads from two land uses in relation to hydrological events in the Mt. Lofty Ranges, South Australia. Agricultural Water Management, PAN, 2008: Pesticide Database North America. Pesticide Action Network, accessed April 2008, http://pesticideinfo.org.

Panuwet, P., Prapamontol, T., Chantara, S., Thavornyutikarn, P., Montesano, M. A., Whitehead, R. D. and Barr, D. B., 2008: Concentrations of urinary pesticide metabolites in small-scale farmers in Chiang Mai Province, Thailand. Sience of the Total Environment, 407: 655-668.

Panuwet, P., Siriwong, W., Prapamantol, T., Ryan, P. B., Fiedler, N., Robson, M. G. and Barr, D. B., 2012: Agricultural pesticide management in Thailand: status and population health risk. Environmentl Science and Policy, 17: 72-81.

Park, J. H., Inam, E., Abdullah, M. H., Agustiyani, D., Duan, L., Huong, T. T., Kim, K. W., Kim, S. D., Nguyen, M. H., Pekthong, T., Sao, V., Sarjiya, A., Savathvong, S., Stthiannopkao, S., Syers, J. K. and Wirojanagud, W., 2011: Implications of rainfall variability for seasonality and climate-induced risks concerning surface water quality in East Asia. Journal of Hydrology, 400: 323-332.

Peters, N. E. and Ratcliffe, E., 1998: Tracing Hydrologic pathways using chloride at the Panola Mountain Research Watershed, Georgia, USA. Water, Air and Soil Pollution, 105: 263-275.

Phomcha, P., Wirojanagud, P., Vangpaisal, T. and Thaveevouthi, T., 2011: Predicting sediment discharge in an agruicultural watershed: A case study of the Lam Sonthi watershed, Thailand. Science Asia, 37: 43-50.

Pinheiro, J. C. and Bates, D. M., 2004: Mixed-Effect Models in S and S-Plus. Springer, New York.

Polidoro, B. A., Morra, M. J., Ruepert, C. and Castillo, L. E., 2009: Pesticide sequestration in passive samplers (SPMDs): Considerations for deployment time, biofouling and stream flow in a tropical watershed. Journal of Environmental Monitoring, 11: 1866-1874.

R, 2009: R: A language and environment for statistical computing. R Foundation for Statistical Computing, ISBN 3-900051-07-0, http://www.R-project.org, Vienna, Austria.

Reichenberger, S., Amelung, W., Laabs, V., Pinto, A., Totsche, K. U. and Zech, W., 2002: Pesticide displacement along preferential flow pathways in a Brazilian Oxisol. Geoderma, 63: 63-86.

Reinert, K. H., Giddings, J. A. and Judd, L., 2002: Effect analysis of time-varying or repeated exposures in aquatic ecological risk assessment of agrochemicals. Environmental Toxicology and Chemistry, 21: 1977-1992.

Reungsang, P., Kanwar, R. S. and Srisuk, K., 2010: Applpication of SWAT Model simulating stream flow for the Chi River Subbasin II in Northeast Thailand. Trends Research in Science and Technology, 2: 23-28.

Ribolzi, O., Andrieux, P., Valles, V., Bouzigues, R., Bariac, T. and Voltz, M., 2000: Contribution of groundwater and overland flows to storm flow generation in a cultivated Mediterranean catchment. Quantification by natural chemical tracing. Journal of Hydrology, 233: 241-257.

Riise, G., Lundekvam, H., Wu, Q. L., Haugen, L. E. and Mulder, J., 2004: Loss of pesticide from agricultural field in SE Norway - runoff through surface and drainage water. Environmental Geochemistry and Health, 26: 269-276.

Rodgers, P., Soulsby, C., Waldron, S. and Tetzlaff, D., 2005: Using stable isotope tracers to assess hydrological flow paths, residence times and landscape influences in a nested mesoscale catchment. Hydrology and Earth System Sciences, 9: 139-155.

Rossi, C. G., Srinivasan, R., Jirayoot, K., Duc, T. L., Souvannabouth, P., Binh, N. and Gassman, P. W., 2009: Hydrologic evaluation of the lower Mekong River Basin with the Soil and Water Assessment Tool. International Agricultural Engineering Journal, 18: 1-13.

Sangchan, W., Bannwarth, M. A., Ingwersen, J., Hugenschmidt, C., Schwadorf, K., Thavornyutikarn, P., Pansombat, K. and Streck, T., 2013: Monitoring and risk assessment of pesticides in a tropical river of an agricultural watershed in Northern Thailand. Environmental Monitoring and Assessment, submitted.

Sangchan, W., Hugenschmidt, C., Ingwersen, J., Schwadorf, K., Thavornyutikarn, P., Pansombat, K., Sukvanachaikul, Y. and Streck, T., 2012: Short-term dynamics of pesticide concentrations and loads in a river of an agricultural watershed in the outer tropics. Agriculture Ecosystems & Environment, 158: 1-12.

Scanlon, T. M., Raffensperger, J. P. and Hornberger, G. M., 2001: Modeling transport of dissolved silica in a forested headwater catchment: Implications for defining the hydrochemical response of observed flow pathways. Water Resources Research, 37: 1071-1082.

Schellekens, J., Scatena, G. N., Bruijnzeel, L. A., Dijk, A. I. J. M. v., Groen, M. M. A. and Hogezand, R. J. P. v., 2004: Stormflow generation in a small rainforest catchment in the Luquillo Experimental Forest, Puerto Rico. Hydrological Processes, 18: 505-530.

Scherrer, S. and Naef, F., 2003: A decision scheme to indicate dominant hydrological flow processes on temperate grassland. Hydrological Processes, 17: 391-401.

Schmitter, P., Dercon, G., Hilger, T., Hertel, M., Treffner, J., Lam, N., Vien, T. D. and Cadisch, G., 2011: Linking spatio-temporal varitaion of crop response with sediment deposition along paddy rice terraces. Agriculture, Ecosystems and Environment, 140: 34-45.

Schreinemachers, P., Berger, T., Sirijinda, A. and Praneetvatakul, S., 2009: The diffusion of greenhouse agriculture in northern Thailand: Combining econometrics and agent-based modeling. Canadian Journal of Agricultural Economics.

Schreinemachers, P. and Sirijinda, A., 2010: Pesticide use data for the Mae Sa watershed, Thailand. Report within the SFB 564: Sustainable Land Use and Rural Development in Mountainous Regions of Southeast Asia, University of Hohenheim, Germany.

Schreinemachers, P. and Sirijinda, A., 2008: Pesticide use data for the Mae Sa watershed, Thailand. Report within the SFB 564: Sustainable Land Use and Rural Development in Mountainous Regions of Southeast Asia, University of Hohenheim, Germany.

Schreinemachers, P., Sringarm, S. and Sirjinda, A., 2011: The role of synthetic pesticides in the intensification of highland agriculture in Thailand. Crop Protecion, 30: 1430-1437.

Schriever, C. A., Ohe, P. C. v. d. and Lies, M., 2007: Estimating pesticide runoff on small streams. Chemosphere, 68: 2162-2171.

Schuler, U., 2008: Towards regionalisation of soils in Northern Thailand and consequences for mapping approaches and upscaling procedures. P. Thesis, University of Hohenheim,

Schuol, J., Abbaspour, K., Yang, H., Srinivasan, R. and Zehnder, A., 2008: Modeling blue and green water availability in Africa. Water Resources Research, 44:1-18.

Setegn, S. G., Srinivasan, R., Melesse, A. M. and Dargahi, B., 2010: SWAT model application and prediction uncertainty analysis in the Lake Tana Basin, Ethiopia. Hydrological Processes, 24: 357-367.

Shanley, J. B., Kendall, C., Smith, T. E., Wolock, D. M. and McDonnell, J. J., 2002: Controls on old and new water contributions to stream flow at some nested catchments in Vermont, USA. Hydrological Processes, 16: 589-609.

Shaw, E. M., 1988: Hydrology in Practice - Second Edition. Van Nostrand Reinhold (International) Co. Ltd, London.

Shen, Z. Y., Chen, L. and Chen, T., 2012: Analysis of parameter uncertainty in hydrological and sediment modeling using GLUE method: A case study of SWAT model applied to Three Gorges Reservoir Region, China. Hydrology and Earth System Sciences, 16: 121-132.

Singh, C. V., 2006: Pattern characteristics of Indian monsoon rainfall using principal component analysis. Atmospheric Research, 79: 317-326.

Singh, P. and Kumar, N., 1997: Effect of orography on precipitation in the western Himalayn region. Journal of Hydrology, 199: 183 - 206.

Singh, P., Ramasastri, K. S. and Kumar, N., 1995: Topographical influence on precipitation distribution in different ranges of western Himalayas. Nord. Hydrol. 26, 259 - 284.

Singh, V. P. and Frevert, D. K., 2006: Watershed models. Taylor and Francis, Boca Raton.

Siriwong, W., Thirakhupt, K., Sitticharoenchai, D., Borjan, M. and Robson, M., 2008: Organochlorine pesticide residu in plankton, Rangsit agriculture area, Central Thailand. Bulletin of Environmental Contamination and Toxicology, 81: 608-612.

Sklash, M. G. and Farvolden, R. N., 1979: The role of groundwater in storm runoff. Journal of Hydrology, 43: 45-65.

Spohrer, K., Herrmann, L., Ingwersen, J. and Stahr, K., 2005: Applicability of uni- and bimodal retention functions for water flow modelling in a tropical acrisol. Vadose Zone, 5: 48-58.

Spohrer, K., Jantschke, C., Herrmann, L., Engelhardt, M., Pinmanee, S. and Stahr, K., 2006: Lychee tree parameters for water balance modelling. Plant and Soil, 284: 59-72.

Strauch, M., Bernhofer, C., Koide, S., Volk, M., Lorenz, C. and Makeschin, F., 2012: Using precipitation data ensemble for uncertainty analysis in SWAT streamflow simulation. Journal of Hydrology, 414-415: 413-424.

Stuetz, W., Prapamontol, T., Erhardt, J. G. and Classen, H. G., 2001: Organochloric pesticide residues in human milk of a Hmong hill tribe living in Northern Thailand. Science of the Total Environment, 273: 53-60.

Sun, X., Mein, R. G., Keenan, T. D. and Elliot, J. F., 2000: Flood estimation using radar and raingauge data. Journal of Hydrology, 239: 4-18.

Syed, K. H., Goodrich, D. C., Meyers, D. E. and Sorooshian, S., 2003: Spatial characteristics of thunderstorm rainfall fields and their relation to runoff. Journal of Hydrology, 271: 1-21.

Taneepanichskul, N., Siriwong, W., Siripattanakul, S. and Robson, G. M., 2010: Risk assessment of chorpyrifos (organophosphate pesticide) associated with dermal exposure in chilli-growing farmers at Ubonrachatani Province, Thailand. JHR, 24: 149-156.

TDIC, 1986: Data and information for weather modification in Thailand. Technical Data and Information Committee - Ministry of Agriculture and Cooperatives, Bangkok.

Tetzlaff, D. and Uhlenbrook, S., 2005: Significance of spatial variability in precipitation for process-oriented modelling: Results from two nested catchments using radar and ground station data. Hydrology and Earth System Sciences, 9: 29-41.

Thai Meteorological Department, 2011: accessed on November 2011: http://www.tmd.go.th/info/info.php?FileID=23.

Thanapakpawin, P., Richey, J., Thomas, D., Rodda, S., Campbell, B. and Lodgson, M., 2006: Effects of landuse change on the hydrologic regome of the Mae Chaem river basin, NW Thailand. Journal of Hydrology, 334: 215-230.

Thirakhupt, K., Sitthicharoenchai, D., Keithmaleesatti, S. and Siriwong, W., 2006: Organochlorine pesticides and their usages in Thailand: A review. Journal of Scientific Research, 31: 1-15.

Tripathi, M. P., Panda, R. K. and Raghuwanshi, N. S., 2003: Identification and prioritisation of critical sub-watersheds for soil conservation management using the SWAT model. Biosystems Engineering, 85: 365-379.

Tromp-van Meerveld, H. J. and McDonnel, J. J., 2006: Threshold relations in subsurface stormflow: 2. The fill and spill hypothesis. Water Resources Research, 42: 11.

Uhlenbrook, S., 2003: An empirical approach for delineating spatial units with the same dominating runoff generation processes. Physics and Chemistry of the Earth, 28: 297-303.

Uhlenbrook, S., Didszun, J. and Wenninger, J., 2008: Source areas and mixing of runoff components at the hillslope scale - a multi-technical approach. Hydrological Science Journal - Journal des Sciences Hydrologiques, 53: 741-753.

Uhlenbrook, S., Frey, M., Leibundgut, C. and Maloszewski, P., 2002: Hydrograph separations in a mesoscale mountainous basin at event and seasonal timescales. Water Resources Research, 38: 1096-1110.

Uhlenbrook, S. and Hoeg, S., 2003: Quantifiying uncertainties in tracer-based hydrograph separations: a case study for two-, three and five component hydrograph separations in a mountainous catchment. Hydrological Processes, 17: 431-453.

Uhlig, H., 1984: Spontaneous and planned settlement in Southeast Asia. Institute of Asian Affairs. Hamburg.

Ullrich, A. and Volk, M., 2009: Application of the Soil and Water Assessment Tool (SWAT) to predict the impact of alternative management practiceson water quality and quantity. Agricultural Water Management, 96: 1207-1217.

Ulrich, U., Schulz, F., Hugenschmidt, C. and Fohrer, N., 2012: Vergleichende Messungen zu Herbizidausträgen auf drei unterschiedlichen Größenskalen. Hydrologie und Wasserwirtschaft, 56: 215 - 228.

Walker, A., 2002: Working Paper No. 37: Forests and Water in Northern Thailand. Resource Management in Asia-Pacific Program, RMAP Working Paper - Resource Management in Asia-Pacific, Australian National University, Canberra.

Walsh, S. J., Entwisle, B., Rindfuss, R. R. and Page, P. H., 2006: Spatial simulation modeling of land use/land cover change scenarios in northeast Thailand: A cellular automata approach. Journal of Land Use Science, 1: 5-28.

Walter-Echols, G. and Yongfan, P., 2005: In: Regional overview and analysis of country reports: Proceedings of Asia Regional Workshop on Implementation, Monitoring and Observance International Code of Conduct on the Distribution and Use of Pesticides. FAO, Regional Office for Asia and the Pacific, Bangkok.,

Wauchope, R. D., William, R. G. and Marti, L. R., 1990: Runoff of sulfometuron-methyl and cyanazine from small plots: Effects of formulation and grass cover. Journal of Environmental Quality, 14: 132-136.

Weischet, W., 1991: Einführung in die Allgemeine Klimatologie - Physikalische und meteorologische Grundlagen. B. G. Teubner, Stuttgart.

Wels, C., Cornett, R. J. and Lazerte, B. D., 1991: Hydrograph separation: A compariosn of geochemical and isotopic tracers. Journal of Hydrology, 122: 253-274.

Wickel, A. J., Giesen, N. C. v. d. and Sá, T. D. d. A., 2008: Stormflow generation in two headwater catchments in eastern Amazonia, Brazil. Hydrological Processes, 22: 3285-3293.

Wilk, J. and Andersson, L., 2000: GIS-supported modelling of areal rainfall in a mountainous river basin with monsoon climate in southern India. Hydrological Science Journal - Journal des Sciences Hydrologiques, 45: 185 - 202.

Williams, A. G., Dowd, J. F. and Meyles, E. W., 2002: A new interpretation of kinematic stormflow generation. Hydrological Processes, 16: 2791-2803.

Wohlfahrt, J., Colin, F., Assaghir, Z. and Bockstaller, C., 2010: Assessing the impact of the spatial arrangement of agricultural practices on pesticide runoff in small catchments: Combining hydrological modeling and supervised learning. Ecological Indicators, 10: 826-839.

Wood, S. N., 2006: Generalized Additive Models. An Introduction with R. C. Hall/CRC, Boca Raton, London, New York.

Woods, R., Grayson, R., Western, A., Duncan, M., Wilson, D., Young, R., Ibbitt, R., Henderson, R. and McMahon, T., 2000: Experimental design in initial results from the Mahurangi River Variability Experiment: MARVEX, in: Land Surface Hydrology, Meteorology and Climate: Observations and Modeling, edited by: Lakshmi, V., Albertson, J. D., Schaake, J. Journal of Water Science and Application, 201-213.

Wulfmeyer, V., Behrendt, A., Kottmeier, C., Corsmeier, U., Barthlott, C., Craig, G. C., Hagen, M., Althausen, D., Aoshima, F., Arpagaus, M., Bauer, H.-S., Bennett, L., Blyth, A., Brandau, C., Champollion, C., Crewell, S., Dick, G., Di Girolamo, P., Dorninger, M., Dufournet, Y., Eigenmann, R., Engelmann, R., Flamant, C., Foken, T., Gorgas, T., M. Grzeschik, M., J. Handwerker, J., C. Hauck, C., H. Höller, H., Junkermann, W., Kalthoff, N., Kiemle, C., Klink, S., König, M., Krauss, L., N. Long, C. N., Madonna, F., Mobbs, S., Neininger, B., Pal, S., Peters, G., Pigeon, G., Richard, E., Rotach, M. W., Russchenberg, H., Schwitalla, T., Smith, V., Steinacker, R., Trentmann, J., Turner, D. D., van Baelen, J., Vogt, S., Volkert, H., Weckherth, T., Wernli, H., Wiesner, A. and Wirth, M., 2011: The Convective and Orographically-induced Precipitation Study (COPS): The scientific strategy, the field phase and research highlights. Quarterly Journal of the Royal Meteorological Society, 137: 3-30.

Yang, J., Reichert, P., Abbaspour, K. C., Xia, J. and Yang, H., 2008: Comparing uncertainty analysis techniques for a SWAT application to the Chaohe Basin in China. Journal of Hydrology, 358: 1-23.

Young, R. A., Onstad, C. A., Bosch, D. D. and Anderson, W. P., 1987: ANGPS: Agricultural Non-Point Source pollution model: A large watershed analysis tool. USDA, ARS Conservation Research Report No. 35.

Ziegler, A. D., Brenner, S., Tantasarin, C., Jachowski, N. R., Wood, S. H., Sutherland, R. A., Lu, X. X., Giambelluca, T. W. and Nullet, M. A., 2013: Sediment load estimation using automated turbidity-based sediment monitoring in the Mae Sa catchment in northern Thailand. Submitted to River Research and Applications.

Ziegler, A. D., Bruun, T. B., Guardiola-Claramonte, M., Giambelluca, T. W., Lawrence, D. and Lam, N. T., 2009: Environmental consequences of the demise in swidden cultivation in montane mainland Southeast Asia: Hydrology and geomorphology. Human Ecology, 37: 361-373.

Ziegler, A. D., Giambelluca, T. W., Sutherland, R. A., Nullet, M. A., Yarnasarn, S., Pinthong, J., Preechapanya, P. and Jaiaree, S., 2004: Toward understanding the cumulative impacts of roads in unpkand agricultural watersheds of northern Thailand. Agriculture Ecosystems & Environment, 104: 145-158.

Ziegler, A. D., Negishi, J. N., Sidle, R. C., Gomi, T., Noguchi, S. and Nik, A. R., 2007: Persistence of road runoff generation in a logged catchment in Peninsula Malaysia. Earth Surface Processes and Landforms, 32: 1947-1970.

Ziegler, A. D., Sutherland, R. A. and Giambelluca, T. W., 2000: Runoff generation and sediment production on unpaved roads, foothpaths and agricultural land surfaces in Northern Thailand. Earth Surface Processes and Landforms, 25: 519-534.

Zuur, A. F., Ieno, E. N., Walker, N., Saveliev, P. and Smith, G. M., 2009: Mixed Effects Models and Extensions in Ecology with R. Springer, New York.